NASA TECHNICAL NOTE

NASA TN D-7034

NASA TN D-7034

WIND-TUNNEL INVESTIGATION OF A FOUR-ENGINE EXTERNALLY BLOWING JET-FLAP STOL AIRPLANE MODEL

by Raymond D. Vogler

Langley Research Center
Hampton, Va. 23365

NATIONAL AERONAUTICS AND SPACE ADMINISTRATION • WASHINGTON, D. C. • DECEMBER 1970

1. Report No.	2. Government Accession No.	3. Recipient's Catalog No.
NASA TN D-7034		

4. Title and Subtitle	5. Report Date
WIND-TUNNEL INVESTIGATION OF A FOUR-ENGINE EXTERNALLY BLOWING JET-FLAP STOL AIRPLANE MODEL	December 1970
	6. Performing Organization Code
7. Author(s)	8. Performing Organization Report No.
Raymond D. Vogler	L-7546
	10. Work Unit No.
9. Performing Organization Name and Address	721-01-11-01
NASA Langley Research Center Hampton, Va. 23365	11. Contract or Grant No.
	13. Type of Report and Period Covered
12. Sponsoring Agency Name and Address	Technical Note
National Aeronautics and Space Administration Washington, D.C. 20546	14. Sponsoring Agency Code

15. Supplementary Notes

16. Abstract

Data were obtained at low speeds over a moving ground plane through a model angle-of-attack range. The scope of the investigation included effects of model height, wing vertical location, blowing-momentum coefficient, combinations of flap-segment deflections, vertical-tail location, and ground-plane movement.

17. Key Words (Suggested by Author(s))	18. Distribution Statement
STOL model High lift Ground effects Ejector engines	Unclassified – Unlimited STAR Category 02

19. Security Classif. (of this report)	20. Security Classif. (of this page)	21. No. of Pages	22. Price*
Unclassified	Unclassified	85	$3.00

*For sale by the National Technical Information Service, Springfield, Virginia 22151

WIND-TUNNEL INVESTIGATION OF A FOUR-ENGINE EXTERNALLY BLOWING JET-FLAP STOL AIRPLANE MODEL

By Raymond D. Vogler
Langley Research Center

SUMMARY

An investigation was made to determine the low-speed longitudinal aerodynamic characteristics of a model of a four-engine externally blowing jet-flap STOL airplane. Fan-jet engine momentum was obtained with compressed air. The swept-wing model had leading-edge slats on the wing and tail and full-span, double-slotted, 38-percent-wing-chord flaps. Data were obtained in and out of ground effect over a moving ground plane at various model heights, flap deflections, and momentum coefficients for high-wing and low-wing configurations.

With the full-span flaps deflected 60°, corresponding to a landing condition, the lift coefficients of the high-wing configuration exceeded those of the low-wing configuration by 5 percent or more in or out of ground effect. Reducing the deflection of the inboard 50-percent-span segment of the flap to 30°, corresponding to a take-off or climb condition, reduced the lift by 30 percent, but eliminated almost all the loss in lift caused by ground proximity which was as much as 20 percent of the out-of-ground-effect lift for the flap deflections of 60°. Results over the moving and the fixed ground plane show few differences for the high-wing configuration except for small increments of forces and moments at the higher blowing-momentum coefficients.

INTRODUCTION

Successful development of short take-off and landing (STOL) aircraft opens the possibility of urban location of comparatively small commercial airports. Small airports may be used by aircraft that can land and take off at low speeds. The necessary lift at low speeds may be attained by increasing the circulation over the wings. This may be accomplished by blowing high-velocity air from within the wing rearward over the flaps or, as in this investigation, by allowing the efflux from fan-jet engines to impinge on a high-lift flap system. While earlier investigations have shown the feasibility of the externally blowing jet flap, data were not available for the high thrust coefficients and large flap chords necessary for the STOL airplane. Moreover, previous investigations (refs. 1 and 2) have shown that lift losses in ground effect occur if the jet impinges against the

ground. Reference 2 also indicated that for some lift and model height combinations, data obtained over a moving ground plane are more valid than those obtained over a stationary one.

The purposes of this investigation were to determine the low-speed longitudinal aerodynamic characteristics of the model using externally blowing jet flaps and to determine the effect of model height above a moving ground plane on these aerodynamic characteristics. The study was a joint effort by NASA and the Douglas Aircraft Division of McDonnell Douglas Corporation. The aircraft configuration used was a four-engine transport with the engines mounted on pylons under the wings. A two-part ejector, simulating a fan and gas generator, was used to provide the jet momentum. Tests were made in the 17-foot (5.18-meter) test section of the Langley 300-MPH 7- by 10-foot tunnel at a dynamic pressure of 10 lb/ft^2 (479 N/m^2) and a Reynolds number of 565 000 based on the mean aerodynamic chord.

SYMBOLS

The force and moment data are presented about the stability axes. The origin of the axes, longitudinally, is at a point in the vertical plane corresponding to the quarter-chord point of the mean aerodynamic chord. The vertical location of the origin is 1.17 in. (2.97 cm) above the fuselage center line for the high-wing configuration and 2.54 in. (6.45 cm) below the fuselage center line for the low-wing configuration. The units of measure used in this report are given both in the U.S. Customary Units and, parenthetically, in the International System of Units (SI). (See ref. 3.)

b wing span, ft (m)

C_D drag coefficient, $\frac{\text{Drag}}{q_\infty S}$

C_L lift coefficient, $\frac{\text{Lift}}{q_\infty S}$

$C_{L,\infty}$ lift coefficient out of ground effect

C_m pitching-moment coefficient, $\frac{\text{Pitching moment}}{q_\infty S\bar{c}}$

C_μ momentum coefficient, $\frac{\text{Static thrust}}{q_\infty S}$

c local chord, ft (m)

$\bar{c}$ wing mean aerodynamic chord, ft (m)

h distance from ground plane to quarter-chord point of mean aerodynamic chord of the wing, ft (m)

i_t incidence of horizontal tail with respect to fuselage, deg

q_∞ free-stream dynamic pressure, lb/ft^2 (N/m^2)

S wing area, ft^2 (m^2)

α fuselage angle of attack, deg

$\Delta C_L, \Delta C_D, \Delta C_m$ increments of lift, drag, and pitching-moment coefficients

δ_f flap deflection (deflection of three flap segments given in order from inboard to outboard on figures and in text), deg

δ_s slat deflection

δ_v vane deflection

MODEL AND APPARATUS

The model is a 0.05375-scale model of an externally blowing jet-flap STOL airplane. The fan-jet momentum was obtained with compressed air. A two-view drawing of the model is shown in figure 1; flap, vane, and slat details, in figure 2; and photographs of the model, in figure 3. Dimensional data of the model are given in table I.

The wing could be attached to the fuselage in either a high or low position. The wing had a leading-edge slat that extended from the fuselage to the wing tip. (See fig. 1.) The slat is a constant 15 percent of the wing chord to the outboard pylon. This percentage increases to 25 percent at the wing tip. The wing also had a double-slotted flap with a chord that is 38 percent of the wing chord (figs. 1 and 2(a)); this flap was divided into three segments. The segments extend from the fuselage to 0.50b/2, from 0.50b/2 to 0.75b/2, and from 0.75b/2 to the wing tip. The horizontal tail was an inverted airfoil with a leading-edge slat that was 15 percent of the airfoil chord. The horizontal tail could be installed in a high or a mid position on the vertical tail. Landing gear and gear pods were on the model and the landing gear was extended for all tests with the flaps deflected.

TABLE I.- MODEL GEOMETRY[a]

Item	Wing	Horizontal tail	Vertical tail
Area, ft^2 (m^2)	5.143 (0.4778)	1.733 (0.1610)	1.372 (0.1275)
Span, ft (m)	6.000 (1.8290)	2.940 (0.8961)	1.482 (0.4517)
Root chord (fuselage center line), ft (m)	1.319 (0.4020)	0.818 (0.2493)	1.219 (0.3716)
Tip chord, ft (m)	0.396 (0.1207)	0.360 (0.1097)	0.634 (0.1932)
Mean aerodynamic chord, ft (m)	0.940 (0.2865)	0.6185 (0.1885)	0.957 (0.2917)
Location of 0.25-mean-aerodynamic-chord point (distance from fuselage nose), ft (m)	2.2575 (0.6881)	5.1510 (1.570)	4.945 (1.506)
Aspect ratio	7.0	5.0	1.6
Taper ratio	0.3	0.44	0.52
Sweepback angle, c/4, deg	25.0	7.5	22.0
Dihedral angle, deg:			
High wing	0		
Low wing	4.0		
Horizontal tail		0	
Wing incidence angle, deg:			
At 0.11b/2	2.85		
At 0.95b/2	-2.20		
Horizontal tail height above fuselage center line, ft (m):			
High tail		1.8808 (0.5733)	
Mid tail		1.1698 (0.3566)	

[a]Fuselage length, 5.689 ft (1.734 m); maximum height, 0.792 ft (0.2414 m); maximum width, 0.867 ft (0.2642 m).

The nacelles are pylon mounted below the wing and simulate a high bypass-ratio fan-jet engine. The fan exhaust issues from an annular nozzle and the gas generator exhaust flows from a central nozzle at the rear of the nacelle. A two-part ejector is used to provide the efflux of the fan and gas generator. High-pressure air was brought to a plenum in the fuselage through a tube in the sting mount. The plenum consisted of two compartments, one of which furnished air to that part of the ejector simulating the fan and the other compartment furnished air for gas generator simulation. A valve between the compartments enabled the operator to vary the pressure in the compartments so as to produce a thrust ratio of approximately 3.4 between the fan and jet. Air from the plenum compartments was conducted to each ejector through tubes buried in the nose of the wing. The inboard ejectors were located at 0.26b/2 and the outboard at 0.44b/2.

The model was attached to a six-component strain-gage balance on the end of the mounting sting over a movable ground plane in the 17-foot (5.18-m) test section of the

Langley 300-MPH 7- by 10-foot tunnel. The moving ground plane was a fabric belt between two rollers driven by an electric motor.

TESTS

All data were obtained at a tunnel dynamic pressure of 10 lb/ft^2 (479 N/m^2) and a Reynolds number of 565 000 based on the mean aerodynamic chord. The angle-of-attack range was from -8^o to 28^o when the model was away from the ground plane. Near the ground plane, the model angle-of-attack range was restricted to prevent contact between model and ground plane. Data were obtained at ratios of model height to wing span of 1.24, 0.32, and 0.19 for the high-wing configuration and ratios of 1.24, 0.19, and 0.12 for the low-wing configuration. The horizontal tail was in a high position for the high-wing configuration and in a high and mid position on the vertical tail for the low-wing configuration. Tests at all model heights were run with tail off and with tail incidence of -10^o, and some tests out of ground effect were made with the tail incidence at 0^o.

The full-span flap, composed of three segments, was deflected by segment from inboard to outboard to get the following flap deflections: 30^o, 60^o, 0^o; 60^o, 60^o, 0^o; 60^o, 60^o, 60^o. The leading-edge slat was deflected 19^o with these flap deflections. Data for these three flap deflections were obtained at all model heights, and out-of-ground-effect data were also obtained with zero deflection (0^o, 0^o, 0^o) and slats retracted.

Tests were made for all flap deflections at the various model heights for momentum coefficients (or gross thrust coefficients) of 0, 1.0, 2.0, and 3.0. A relationship was established between ejector thrust and pressure in the fuselage plenum compartments by which any desired momentum coefficient could be attained by varying the pressure.

Except for the out-of-ground-effect data ($h/b = 1.24$) and a few runs close to the ground plane for comparative purposes, all data were obtained with the ground plane moving with approximately free-stream velocity.

RESULTS AND DISCUSSION

Presentation of Results

The basic wind-tunnel data figures showing the longitudinal aerodynamic characteristics of the model for various distances (heights) from the ground plane and for various power conditions and flap deflections are listed in table II. Additional figures showing more clearly some of the results of the investigation are listed in table III.

TABLE II.- BASIC DATA FIGURES

Figure	h/b	δ_f, deg	δ_s, deg	Tail position	i_t, deg
High-wing position					
4	1.24	0, 0, 0	0	High	Off, 0
5	1.24	30, 60, 0	19	High	Off, 0, -10
6, 7	0.32, 0.19	30, 60, 0	19	High	Off, -10
8, 9, 10	1.24, 0.32, 0.19	60, 60, 0	19	High	Off, -10
11, 12, 13	1.24, 0.32, 0.19	60, 60, 60	19	High	Off, -10
14	0.19	60, 60, 0	19	High	Off, -10
Low-wing position					
15, 16, 17	1.24, 0.19, 0.12	30, 60, 0	19	Mid	Off, -10
18	1.24	60, 60, 0	19	High, mid	Off, -10
19	0.19	60, 60, 0	19	Mid	Off, -10
20	0.12	60, 60, 0	19	High, mid	Off, -10
21, 22, 23	1.24, 0.19, 0.12	60, 60, 60	19	Mid	Off, -10

TABLE III.- SPECIAL FIGURES

Figure	Description	h/b	δ_f, deg
14	Effect of moving ground plane	0.19	60, 60, 0
24	Effect of tail incidence	1.24	30, 60, 0
25	Effect of ground proximity on lift characteristics	Range	Range
26, 27, 28	Incremental lift, drag, and pitching moments produced by flap	Range	Range
29	Comparison of lift characteristics of high- and low-wing configurations	1.24, 0.19	60, 60, 60
30	Ratio of lift coefficients in ground effect to those out of ground effect	Range	Range

High-Wing Configuration

Longitudinal aerodynamic characteristics.- The longitudinal aerodynamic characteristics of the high-wing configuration in the cruise condition are shown in figure 4. The model is stable and near trim at small positive angles of attack with a horizontal tail setting of 0°. At these angles of attack, power has little effect on lift coefficients and about 95 percent of the static engine thrust registers as propulsive force at the higher momentum coefficients. For the take-off condition ($\delta_f = 30^\circ, 60^\circ, 0^\circ$) shown in figure 5, deflecting the inboard flap 30° allows about two-thirds of the engine power to be used for propulsion while large increases in lift coefficient are obtained. As expected, the large-chord flaps produce large negative pitching moments (figs. 5, 6, and 7) in or out of ground effect. The horizontal tail deflected -10° is able to trim the model up to a lift coefficient of only about 2.5.

Deflecting the inboard flap segment an additional 30° provides a potential landing configuration ($\delta_f = 60^\circ, 60^\circ, 0^\circ$) and produces several significant results. The power-on maximum lift coefficients are increased but the largest increases are at low angles of attack where the lift coefficients are about doubled for both the in- and out-of-ground-effect conditions. (See figs. 8, 9, and 10.) The highly deflected inboard flap diverts the thrust downward and produces large increases in drag. Though the tail-off diving moments of the landing configuration (fig. 8(a)) are greater than those of the take-off configuration (fig. 5(a)), increased downwash from the extra flap deflection enables the tail at an incidence of -10° to trim the landing configuration at a lift coefficient of 4.0 (fig. 8(b)) as compared with a lift coefficient of about 2.5 for the take-off configuration (fig. 5(c)). In ground effect, the downwash is reduced and the tail moment is correspondingly reduced. (See figs. 9(b) and 10(b).)

Deflection of the full-span flaps ($\delta_f = 60^\circ, 60^\circ, 60^\circ$, figs. 11, 12, 13) gives 5 to 9 percent more lift at small angles of attack than does deflection of only the inboard segments. (Compare figs. 11(a) and 8(a).) Deflection of the full-span flaps also gives lower drag coefficients for a given lift coefficient than deflection of the partial-span flaps. This result is due to a more favorable span lift distribution.

Effect of moving ground plane.- The effect of the moving ground plane at the lowest ground height for the high-wing configuration is shown in figure 14. The effect is noticeable only at the higher lift coefficients corresponding to the higher momentum coefficients. The moving ground plane for the tail-on configuration results in an increase in lift, a reduction in drag, and a more positive moment. These increments are small and follow the same trends as found for a model using internal blowing over the flaps. (See ref. 1.)

Effect of tail incidence.- The effect of horizontal tail incidence on the longitudinal aerodynamic characteristics of the high-wing configuration out of ground effect with flaps deflected 30°, 60°, 0° is shown in figure 24. The -10° of tail deflection is sufficient to trim only about one-half of the diving moment at maximum lift and high momentum. For some conditions the model is neutrally stable with the tail off, and the addition of the tail gives a very stable model even after power has reduced by 60 percent the power-off stability. The pitching-moment curves indicate that power increases the favorable downwash by 5° to 10° for this flap deflection.

Effect of ground proximity.- The effect of ground proximity and the relative effectiveness of the various flap deflections for the high-wing model are shown in figure 25. The lift coefficients of the model with deflected full-span flaps are reduced by the presence of the ground plane by about 5 percent without blowing, but the percentage loss increases with blowing to a maximum of 13 percent at the highest angles of attack (8°) in ground effect investigated. At zero angle of attack, the maximum lift loss caused by ground effect is only about 10 percent. With the inboard segment of the flap deflected 30° instead of 60°, the lift loss caused by ground proximity is insignificant with or without blowing momentum. This flap configuration (30°, 60°, 0°) results in lift coefficients that are about 76 percent of the lift coefficients of the fully deflected (60°, 60°, 60°) full-span flap at high angles of attack out of ground effect and about 68 percent at $\alpha = 8^{\circ}$ in ground effect.

The increments of lift, drag, and pitching-moment coefficients produced by various flap deflections and the effect of model height on these increments for an angle-of-attack range are shown in figures 26, 27, and 28, respectively. The reductions in increments of lift due to the presence of the ground plane are about the same or slightly greater than the reductions shown in figure 25 for the complete wing. The ground plane also causes a reduction in drag (fig. 27) and a reduction in diving moments (fig. 28).

Low-Wing Configuration

The longitudinal aerodynamic characteristics of the low-wing configuration are given in figures 15 to 23. The large negative moments of the high-wing, tail-off configuration (fig. 5(a)) are greatly reduced (fig. 15(a)) by lowering the wing a distance approximately equal to the fuselage diameter. The new moment center was moved downward less than one-half of the distance the wing was moved. This new relation between moment center and engine-flap thrust axis results in reduced diving moments for the low-wing configuration. It also results in greatly reduced power effects on the pitching moments for the inboard flap deflection of 30°. As power is increased, the diving moments of the flaps are balanced by the nose-up moments of the thrust. When the flaps are deflected 60° (figs. 18(a) and 21(a)) the diving moments are almost as large as those

of the high-wing configuration (figs. 8(a) and 11(a)). At large flap deflections, the engine-flap thrust vector is more vertical and the pitching moments are less sensitive to vertical location of the moment center.

With the inboard flap deflected 30°, a horizontal-tail deflection of -10° is sufficient to trim the low-wing configuration at much higher lift coefficients (figs. 15, 16, and 17) than the high-wing configuration because the tail-off out-of-trim moments of the low-wing configuration are much smaller. With the inboard flap deflected 60°, the high-wing configuration (figs. 8(b), 10(b), 11(b), and 13(b)) is always trimmed at a higher lift coefficient than the low-wing configuration (figs. 18(b), 19(b), 21(b), and 22(b)) because the tail, on the high-wing configuration, is closer to the flaps and is therefore in a stronger downwash field. For the low-wing configuration, the trimming power of the horizontal tail in the mid position (figs. 18(c) and 20(c)) is somewhat greater than that of the tail in the high position (figs. 18(b) and 20(b)).

Comparisons

A comparison of the lift characteristics of the high-wing and the low-wing configurations in and out of ground effect is shown in figure 29. The high-wing configuration gives a higher lift coefficient through the angle-of-attack range in ground effect or out of ground effect. The greater lift of the high-wing configuration is probably due to the end-plate effect of the fuselage on the flaps. (See figs. 3(b) and 3(d).) The high-wing configuration as compared with the low-wing configuration has about 5 percent higher lift coefficients in or out of ground effect at low angles of attack and about 7 percent higher at high angles of attack out of ground effect.

The ratios of lift coefficients in ground effect to lift coefficients out of ground effect are shown in figure 30 for the various flap deflections for both the low- and high-wing configurations. With the flap deflected 60°, both the high- and the low-wing configurations show considerable loss in lift close to the ground. With the inboard flap deflected only 30°, only the low-wing configuration shows any significant loss and that is at the higher blowing momentums. Near the ground with the flaps fully deflected, the losses increase rapidly as the wing height is reduced. Losses for the low-wing configuration are as high as 20 percent at a distance of 0.12 wing span (13.4 ft (4.1 m) full scale), and losses are about 10 percent for the high-wing configuration at a distance of 0.19 (21.0 ft (6.4 m) full scale) wing span. The difference in these heights is about three-fourths the fuselage diameter so with the same landing gear the lift losses due to ground effect for the high-wing configuration would be less than half the losses for the low-wing configuration. This comparison plus the fact that the high-wing configuration has 5 percent greater lift coefficients (fig. 29) indicates that, based on lift characteristics, the high-wing configuration is more desirable.

SUMMARY OF RESULTS

A wind-tunnel investigation was made to determine the low-speed longitudinal aerodynamic characteristics of a model of a four-engine externally blowing jet-flap STOL airplane. The momentum of the simulated fan-jet engines was obtained with compressed air. The swept-wing model had leading-edge slats on the wing and tail and full-span, double-slotted, 38-percent-wing-chord flaps. Data were obtained in and out of ground effect over a moving ground plane at various model heights, flap deflections, and momentum coefficients for high-wing and low-wing configurations.

Some of the results are as follows:

1. With the full-span flaps deflected 60°, corresponding to a landing condition, the high-wing configuration had lift coefficients about 5 percent greater than the low-wing configuration at low angles of attack in or out of ground effect. Lift coefficients out of ground effect are reduced by the presence of the ground by as much as 20 percent at a distance of 0.12 wing span for the low-wing configuration and about half that percentage for the high-wing configuration at a distance of 0.19 wing span.

2. With flap-segment deflections of 30° inboard, 60° midboard, and 0° outboard, corresponding to a take-off or climb condition, lift coefficients out of ground effect are reduced to about 70 percent of those for full-span flap deflections of 60°, but losses caused by ground proximity are eliminated for the high-wing configuration and greatly reduced for the low-wing configuration.

3. Use of a moving ground plane as compared with a fixed one results in small increases in lift and pitching-moment coefficients and reduction in drag coefficients, only at high lift coefficients corresponding to high momentum coefficients.

4. For the low-wing configuration, lowering the horizontal tail from the high position to the mid position results in a slight improvement in the trim capability of the horizontal tail.

Langley Research Center,
National Aeronautics and Space Administration,
Hampton, Va., November 4, 1970.

REFERENCES

1. Vogler, Raymond D.: Investigation Over Moving Ground Plane of a Transport Airplane Model Using Blowing Over Flaps for Boundary-Layer Control. NASA TN D-4083, 1967.

2. Turner, Thomas R.: A Moving-Belt Ground Plane for Wind-Tunnel Ground Simulation and Results for two Jet-Flap Configurations. NASA TN D-4228, 1967.

3. Mechtly, E. A.: The International System of Units – Physical Constants and Conversion Factors (Revised). NASA SP-7012, 1969.

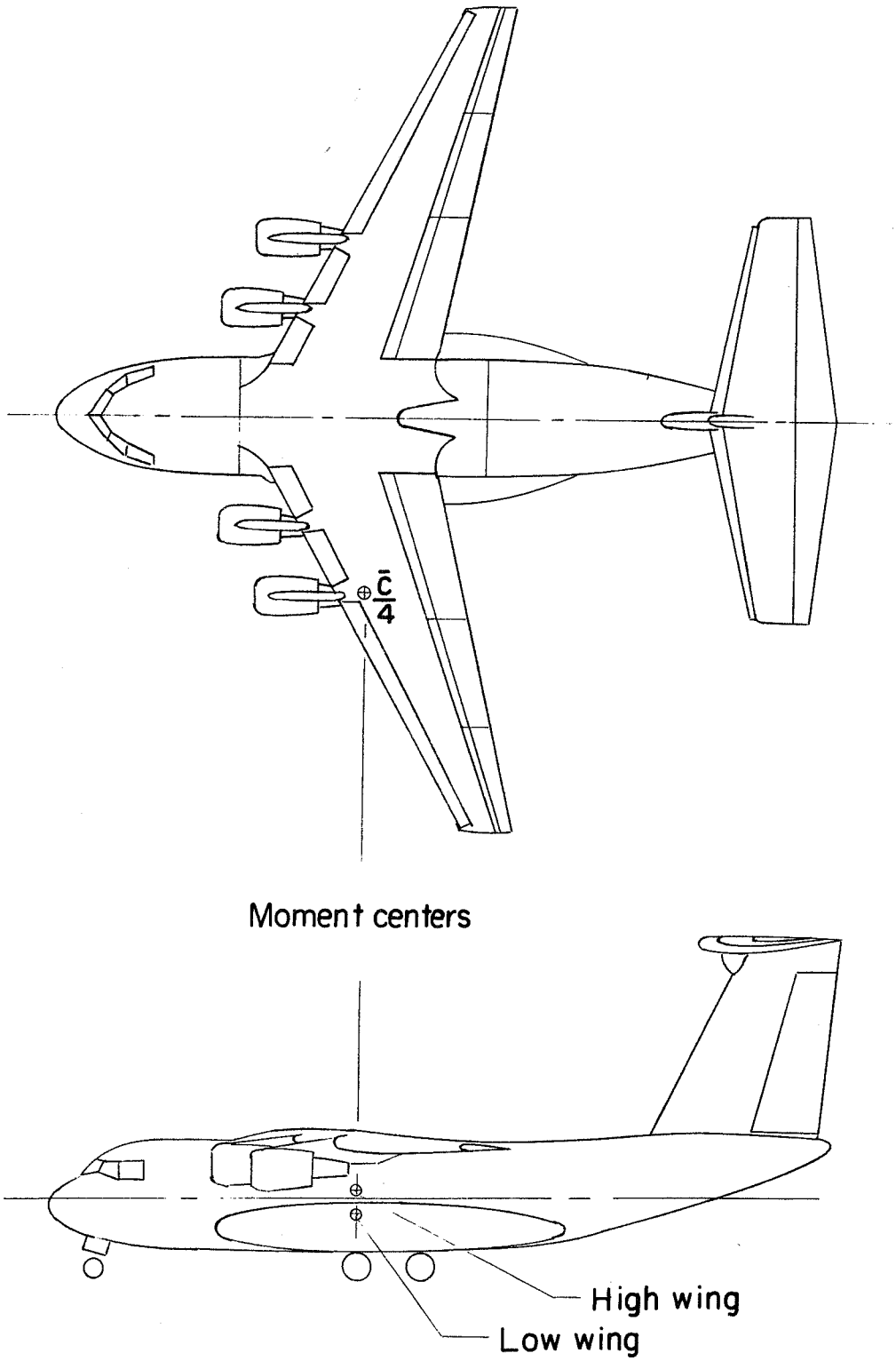

Figure 1.- Two-view drawing of the model.

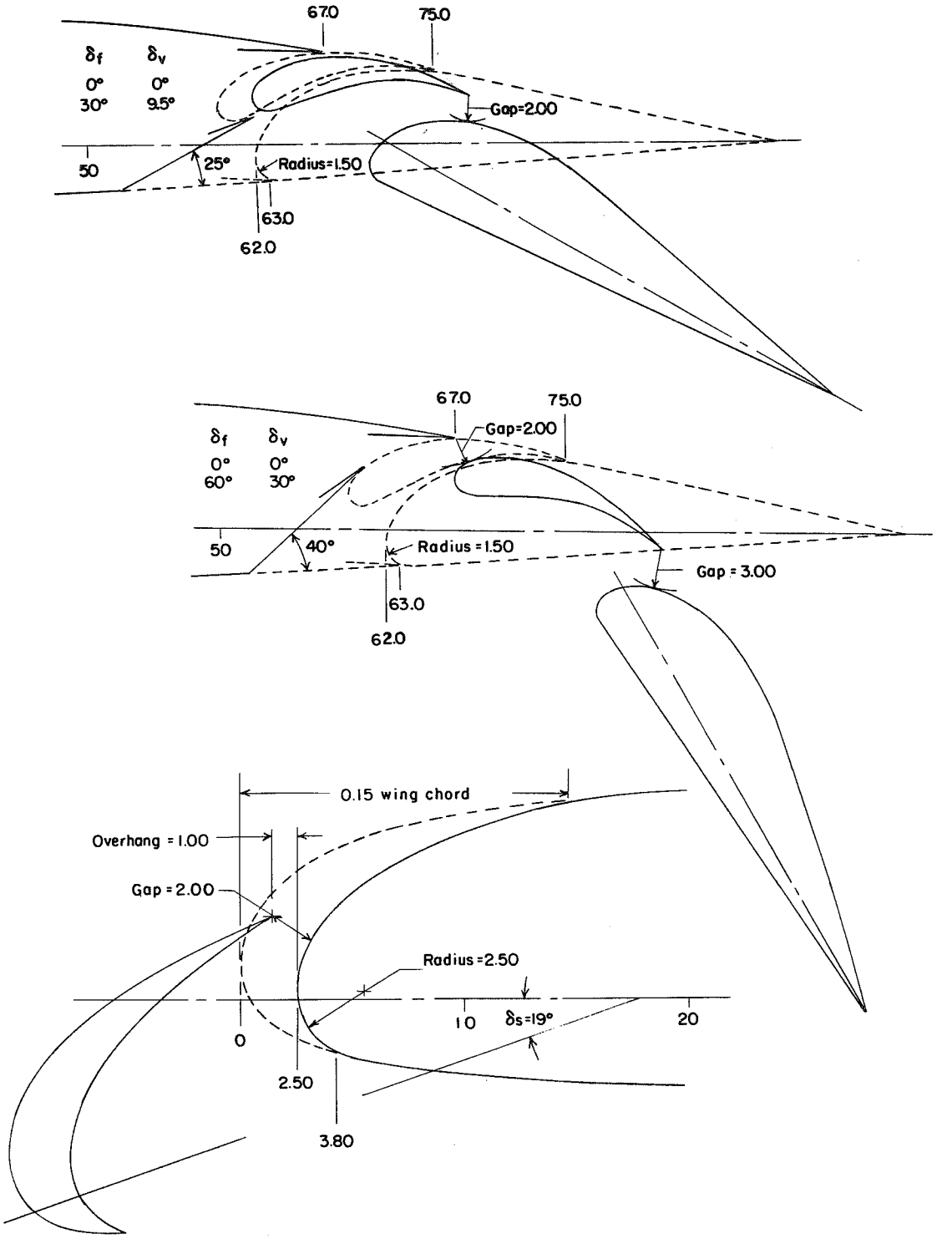

(a) Flap and slat.

Figure 2.- Details of flap, slat, and vane sections at 0.35 span. All dimensions are given in percent of wing chord unless otherwise noted.

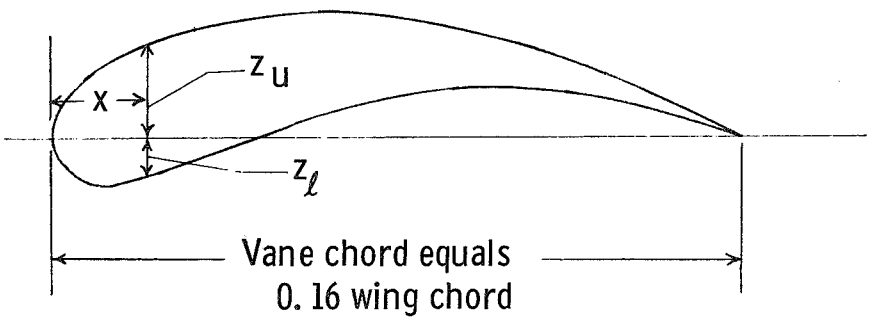

x, percent vane chord	z_u, percent vane chord	z_ℓ, percent vane chord
0	0	0
2.5	5.6	-5.4
5	8.1	-6.8
10	11.4	-6.9
15	13.7	-5.6
20	15.4	-3.9
25	16.6	-1.9
30	17.4	0.1
40	18.1	3.1
50	17.6	5.6
60	15.9	7.0
70	13.4	7.3
80	9.7	6.2
90	5.3	3.5
100	0	0

(b) Vane.

Figure 2.- Concluded.

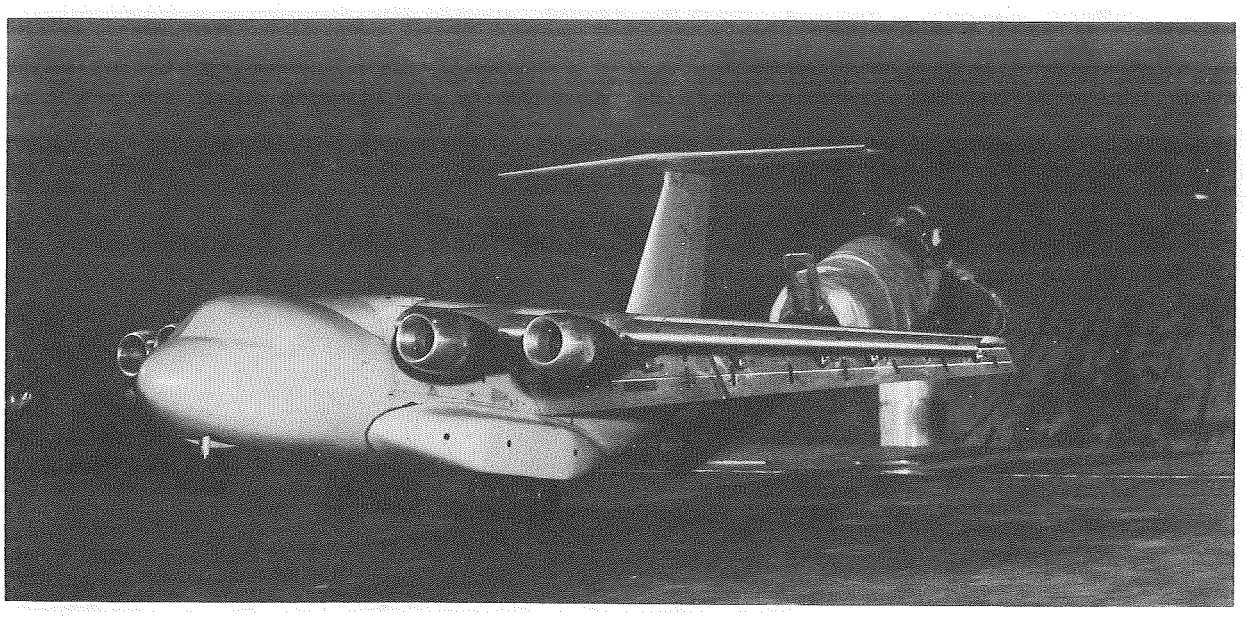

(a) Three-quarter front view of high-wing configuration. L-69-8655

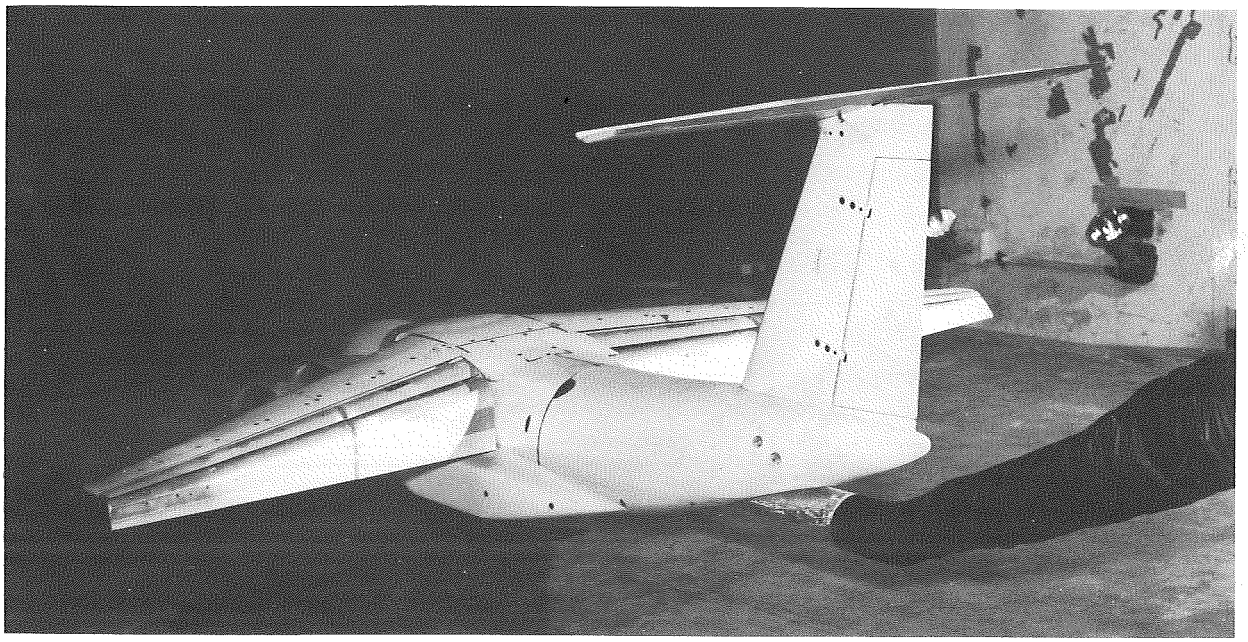

(b) Three-quarter rear view of high-wing configuration. L-69-8653

Figure 3.- Photograph of model near the ground plane.

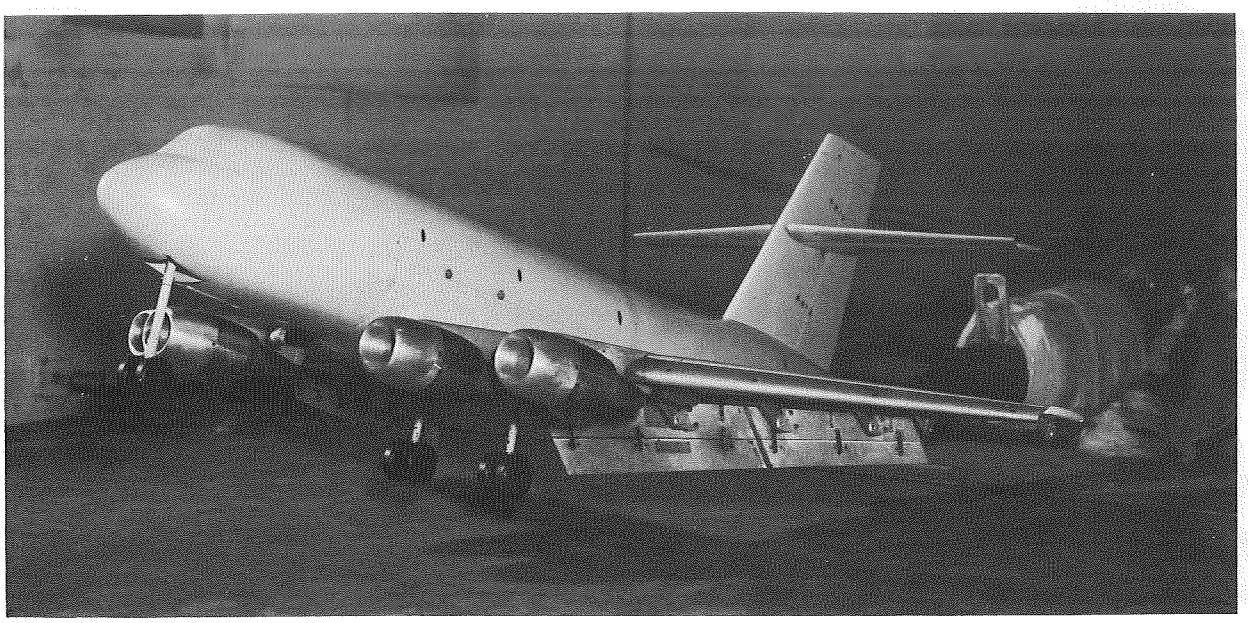

(c) Three-quarter front view of low-wing configuration. L-70-1049

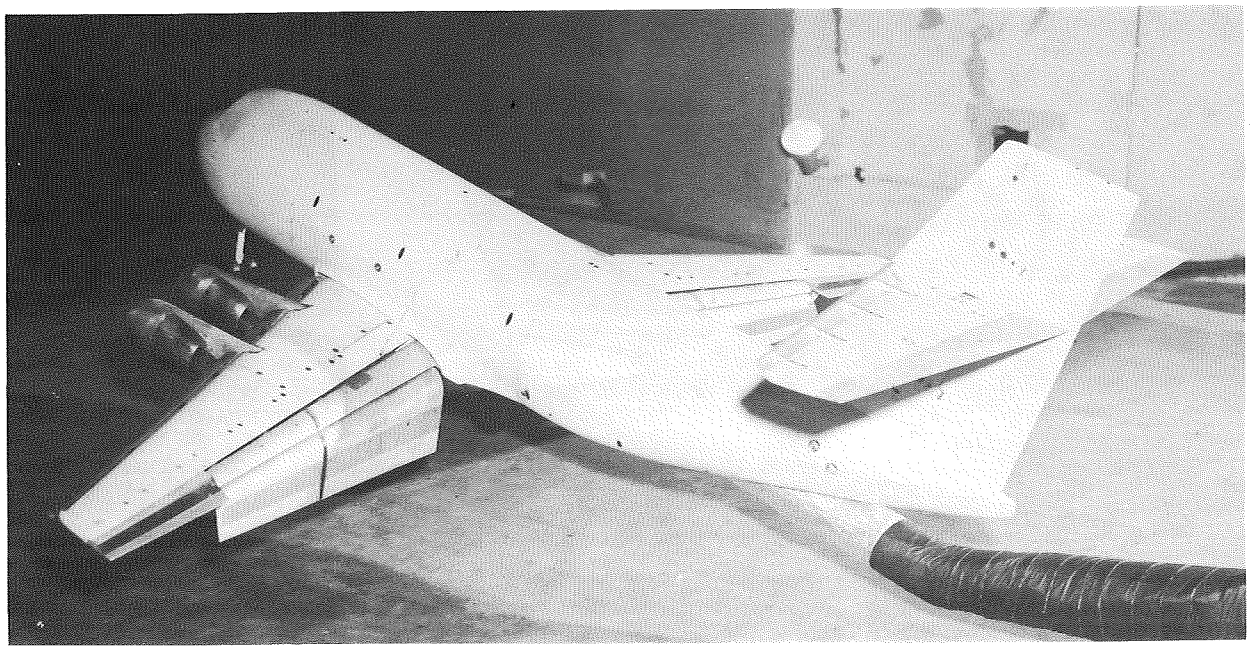

(d) Three-quarter rear view of low-wing configuration. L-70-1050

Figure 3.- Concluded.

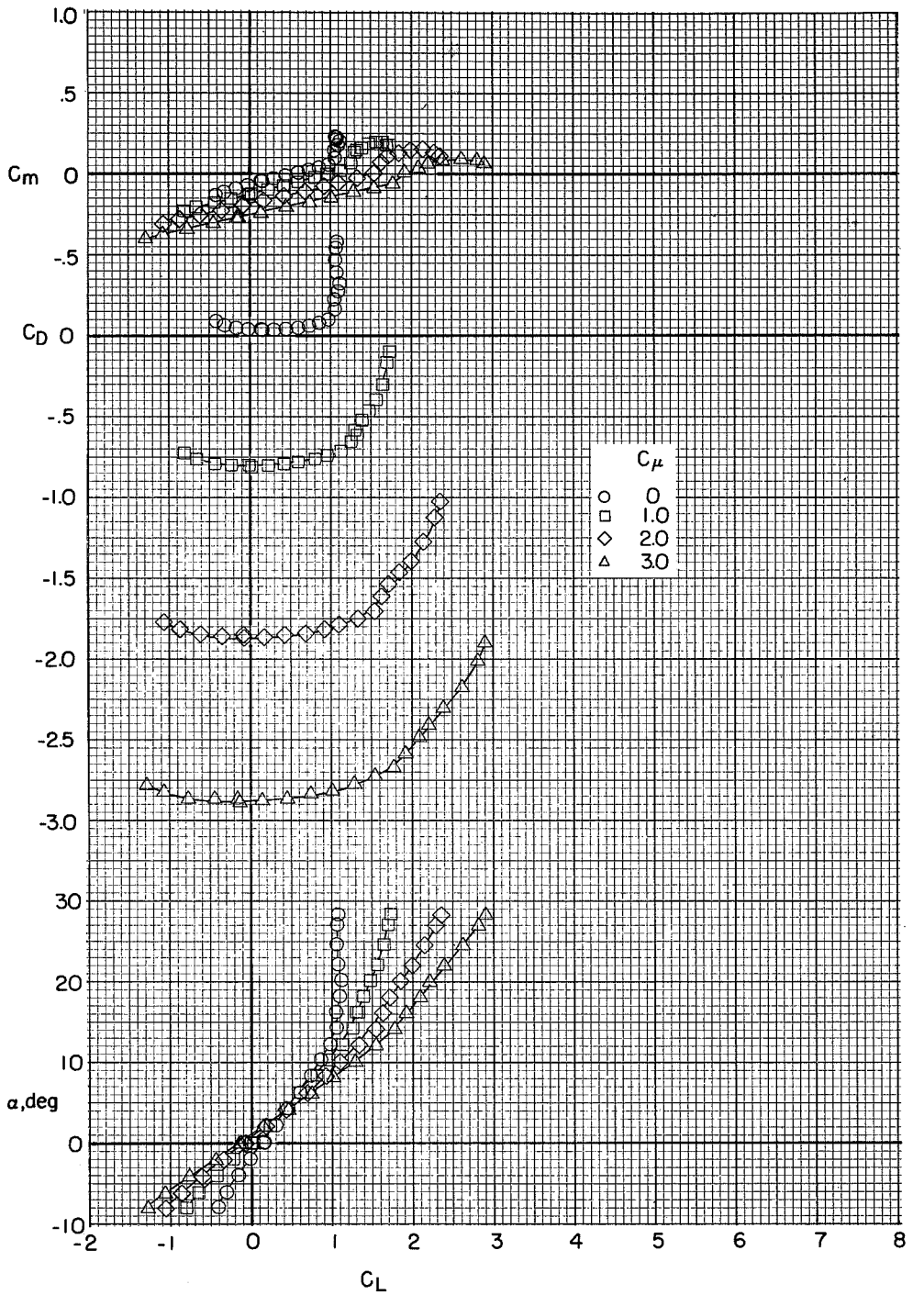

(a) Tail off.

Figure 4.- Longitudinal aerodynamic characteristics of the high-wing configuration out of ground effect with leading-edge slats retracted. h/b = 1.24; $\delta_f = 0^o, 0^o, 0^o$.

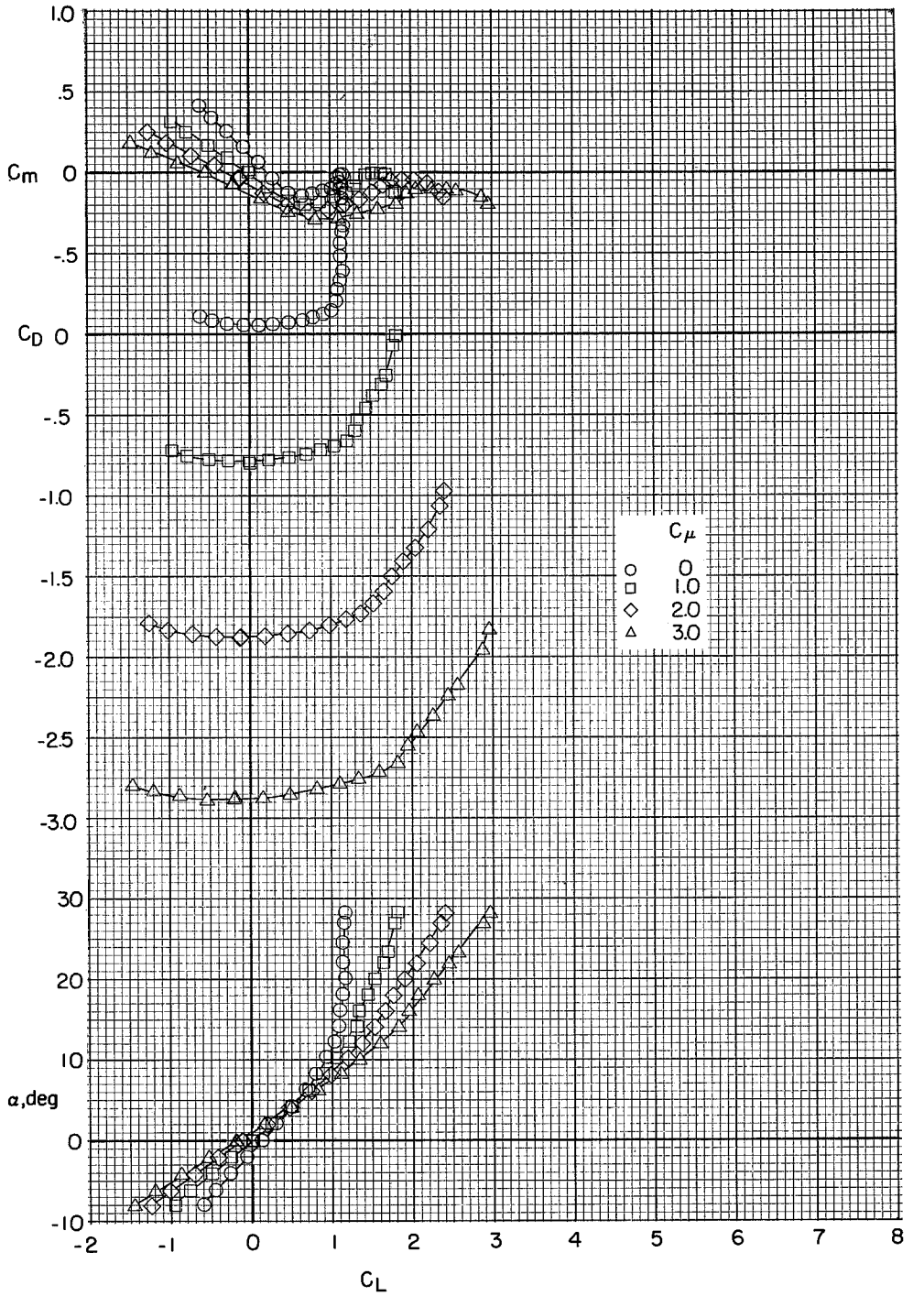

(b) Tail in high position. $i_t = 0^o$.

Figure 4.- Concluded.

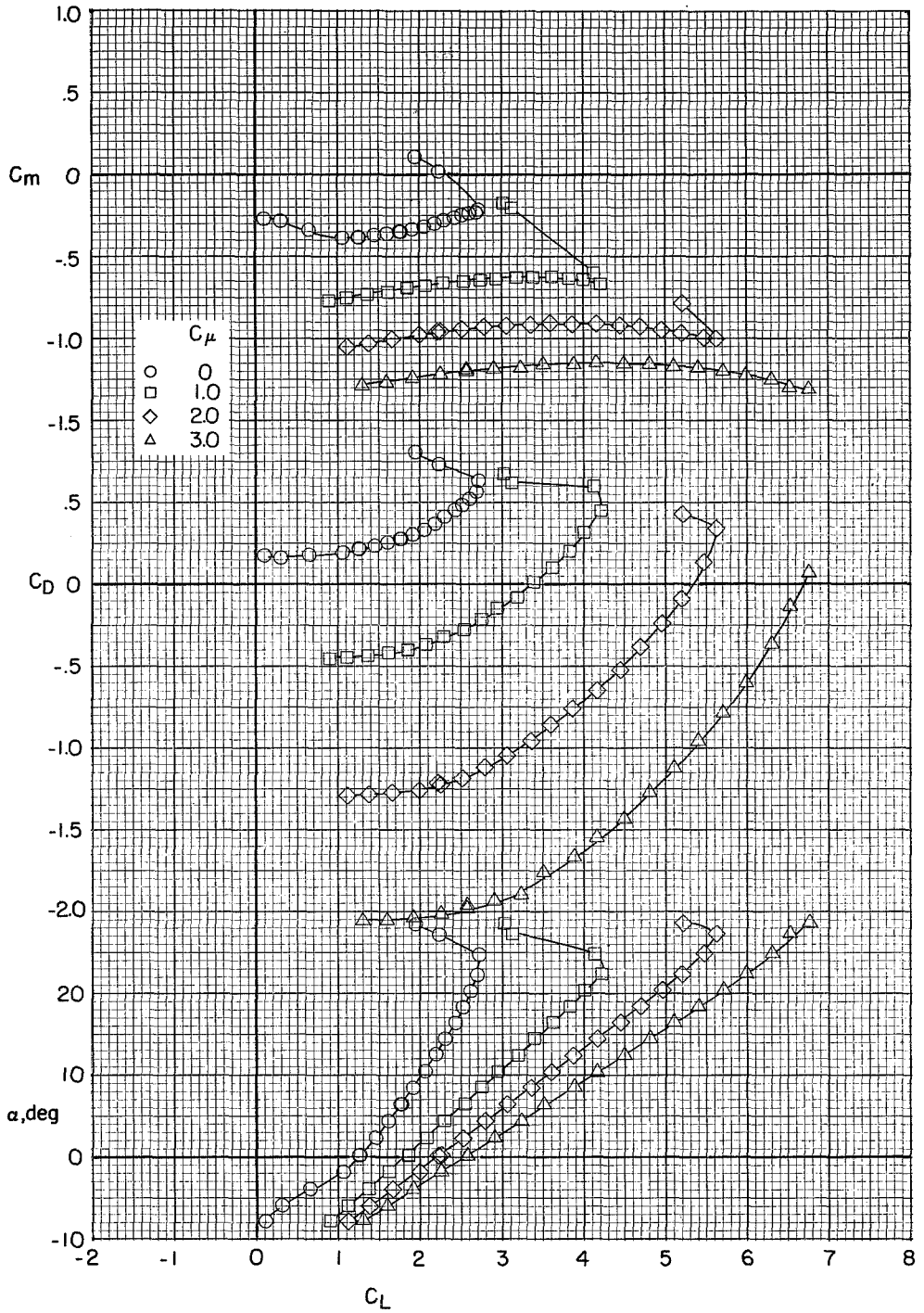

(a) Tail off.

Figure 5.- Longitudinal aerodynamic characteristics of the high-wing configuration out of ground effect. h/b = 1.24; $\delta_f = 30^o, 60^o, 0^o$.

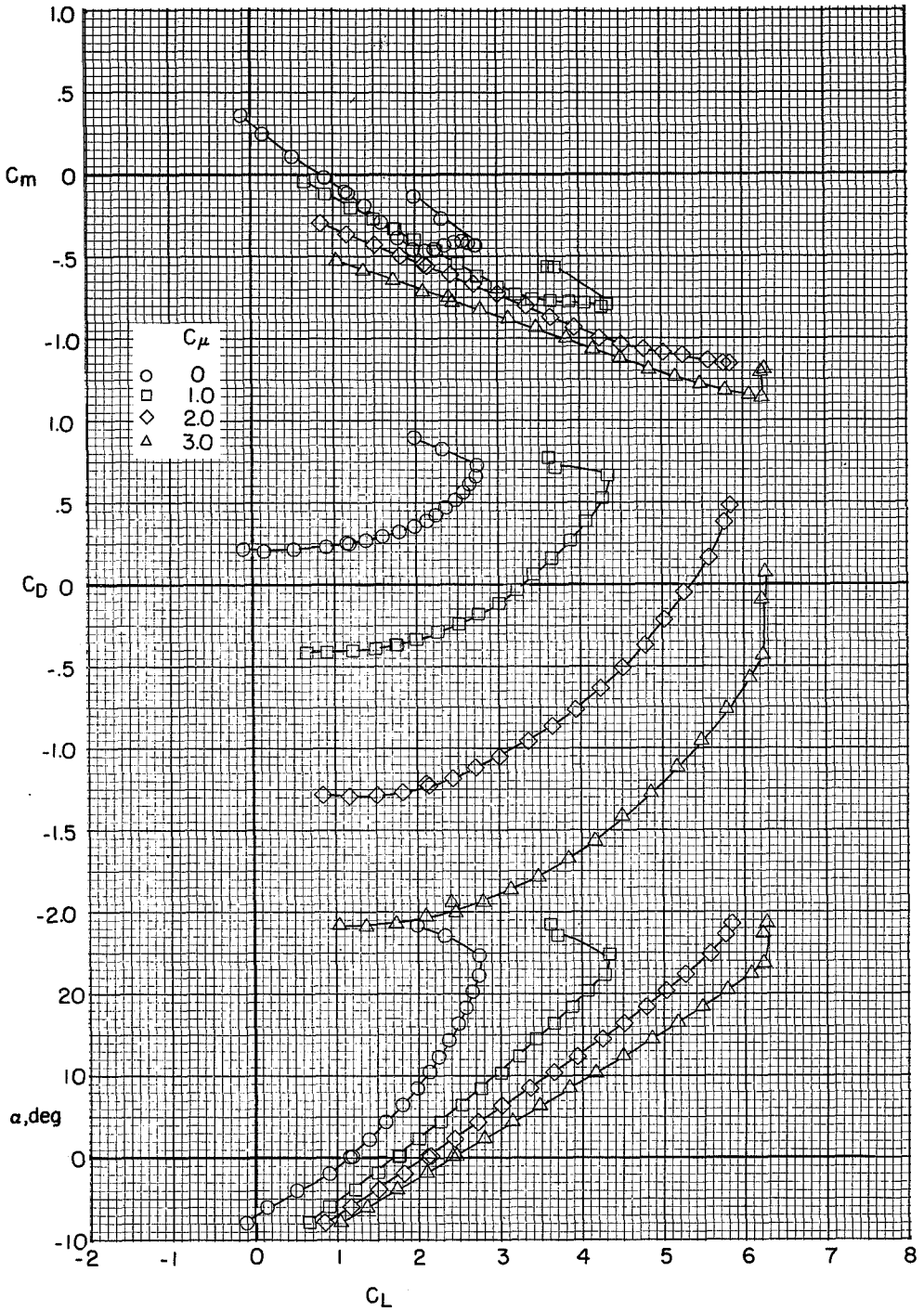

(b) Tail in high position; $i_t = 0^o$.

Figure 5.- Continued.

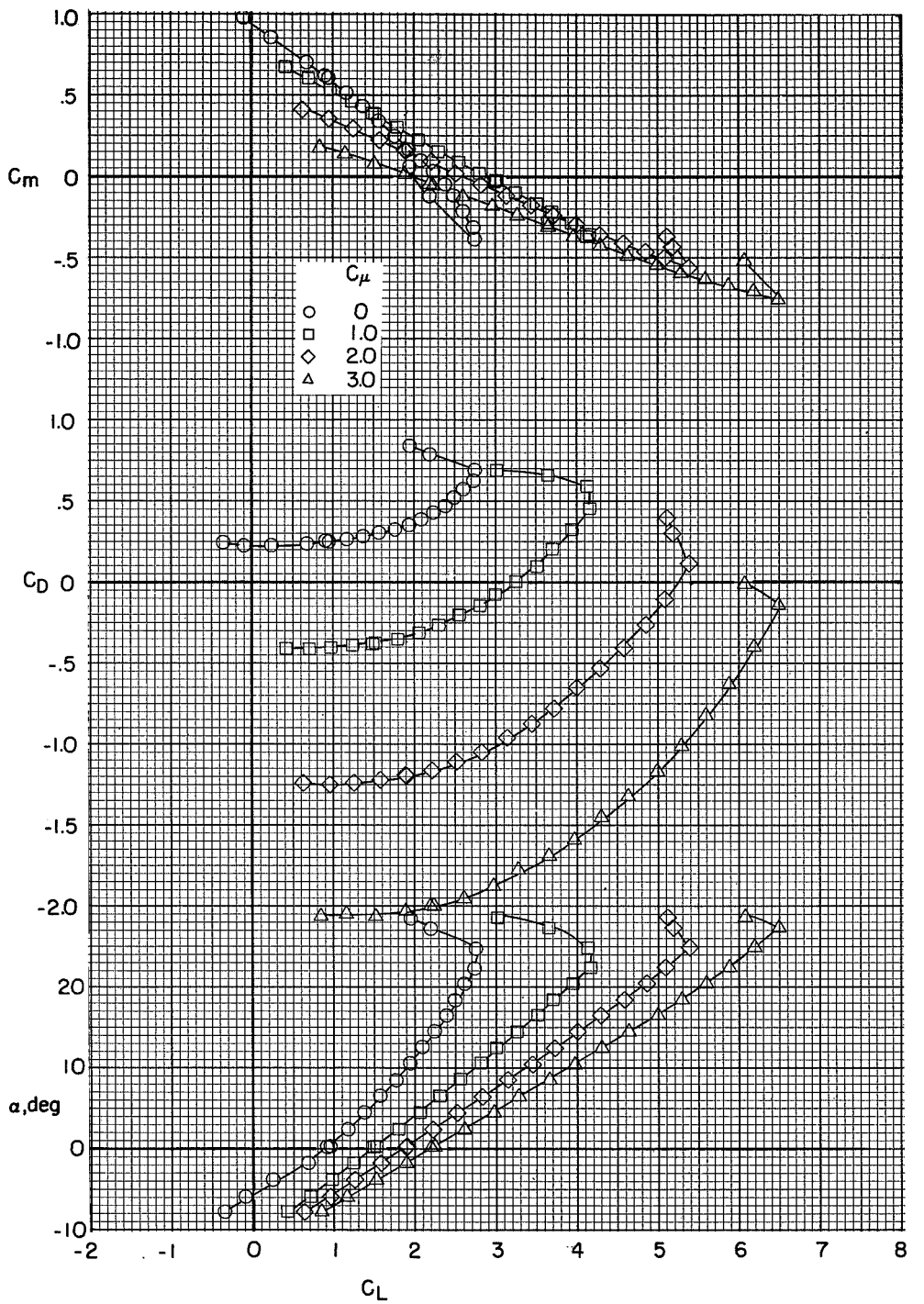

(c) Tail in high position; $i_t = -10^o$.

Figure 5.- Concluded.

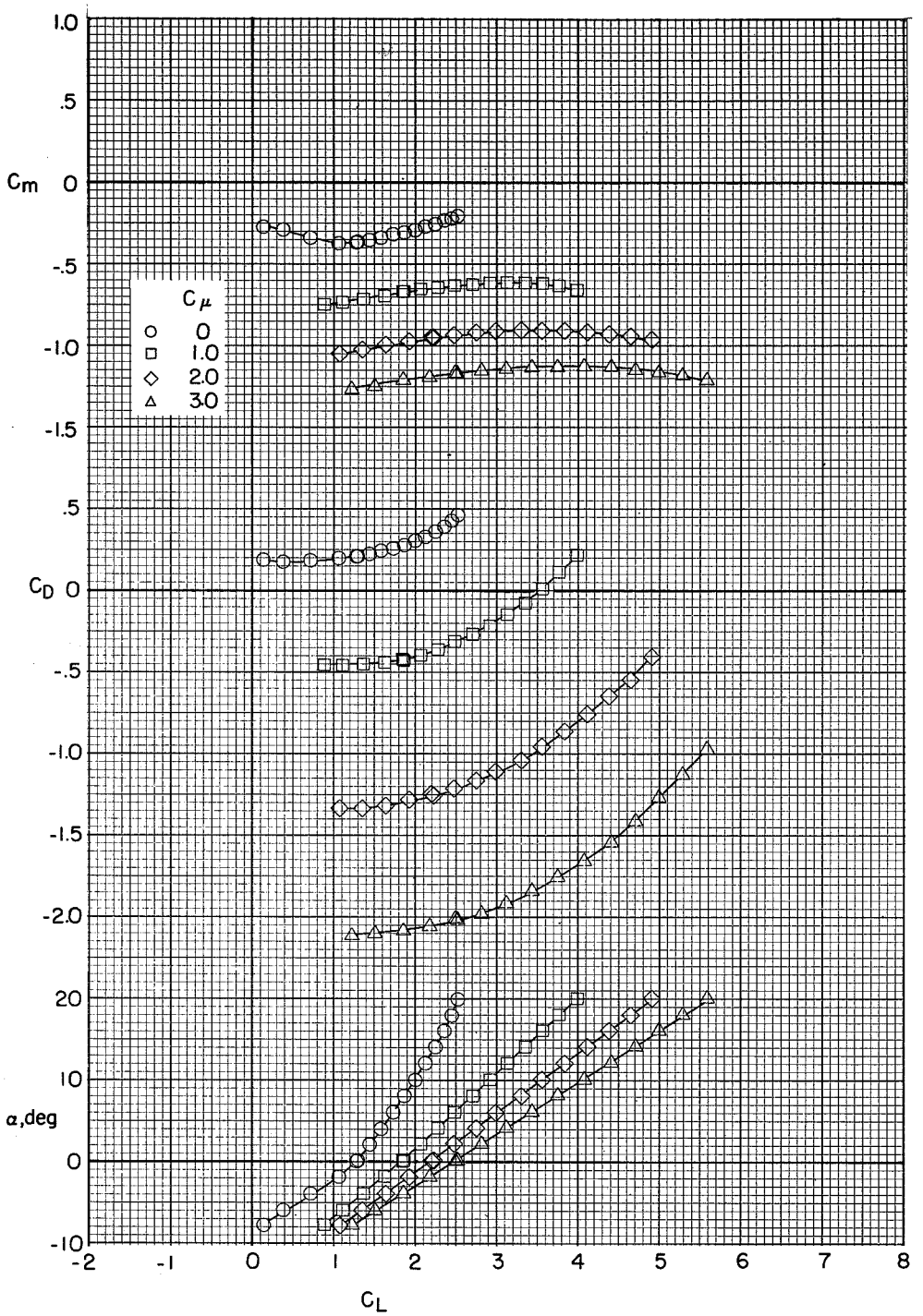

(a) Tail off.

Figure 6.- Longitudinal aerodynamic characteristics of the high-wing configuration in ground effect. h/b = 0.32; $\delta_f = 30^o, 60^o, 0^o$.

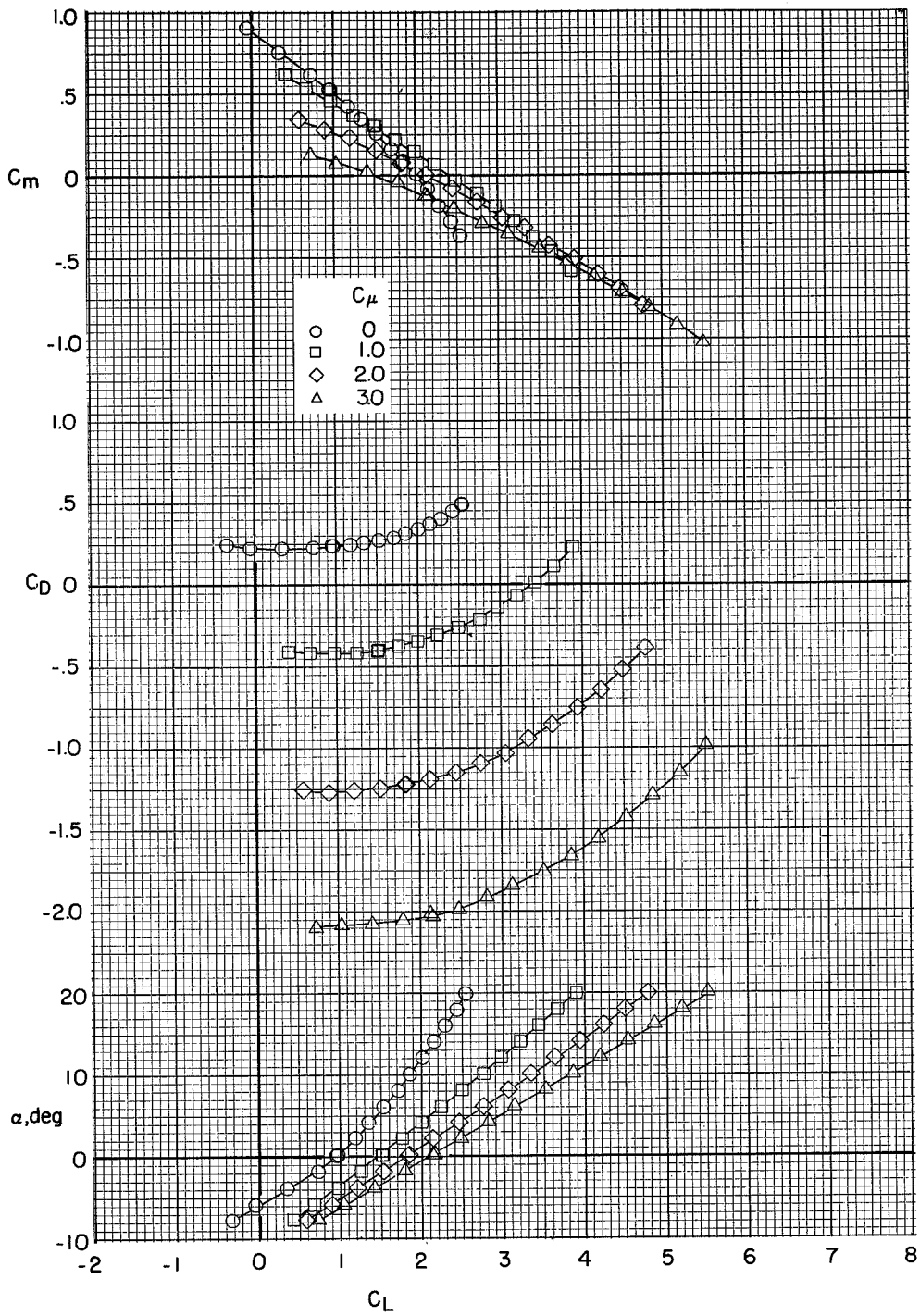

(b) Tail in high position; $i_t = -10^o$.

Figure 6.- Concluded.

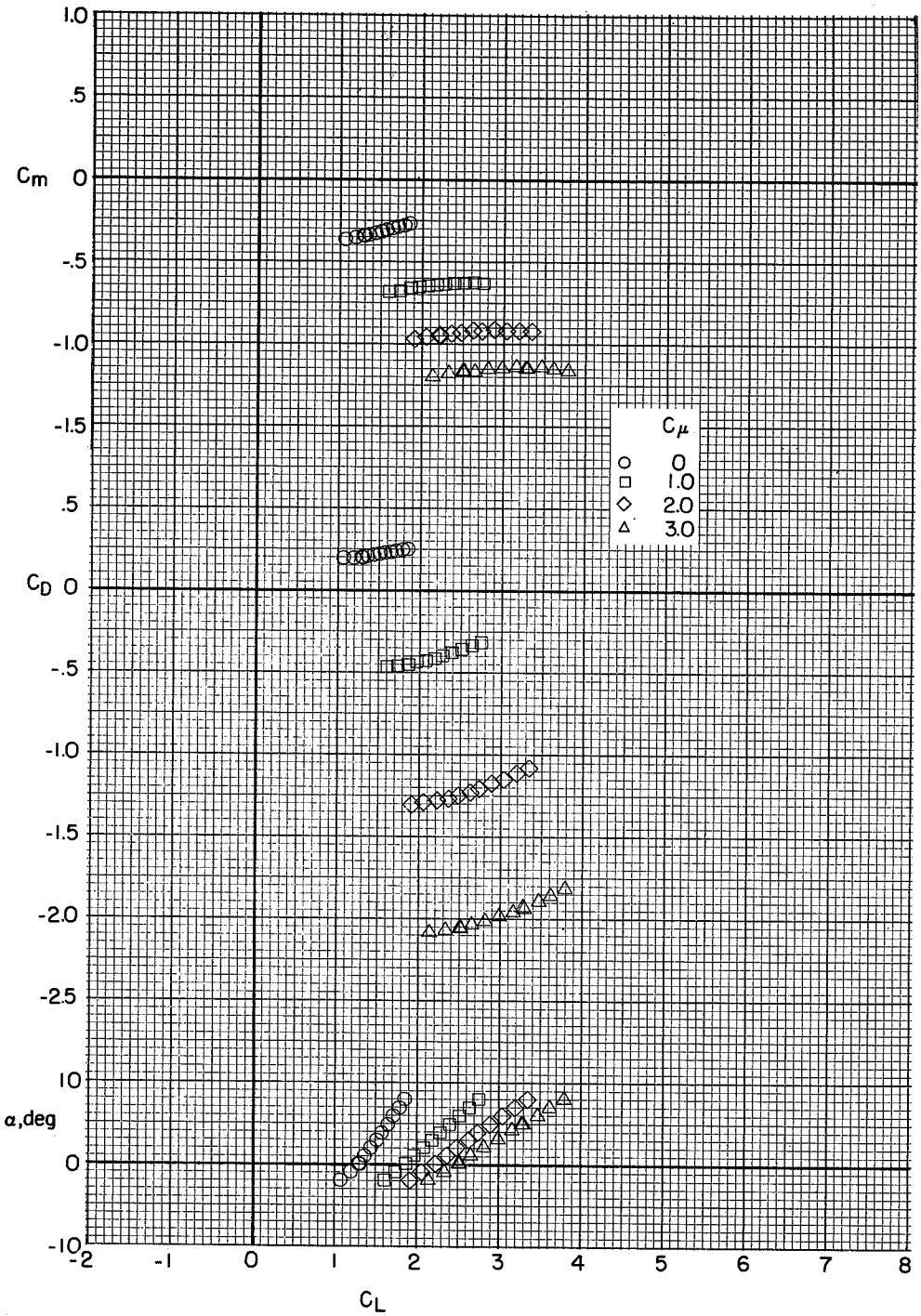

(a) Tail off.

Figure 7.- Longitudinal aerodynamic characteristics of the high-wing configuration in ground effect. h/b = 0.19; $\delta_f = 30^o, 60^o, 0^o$.

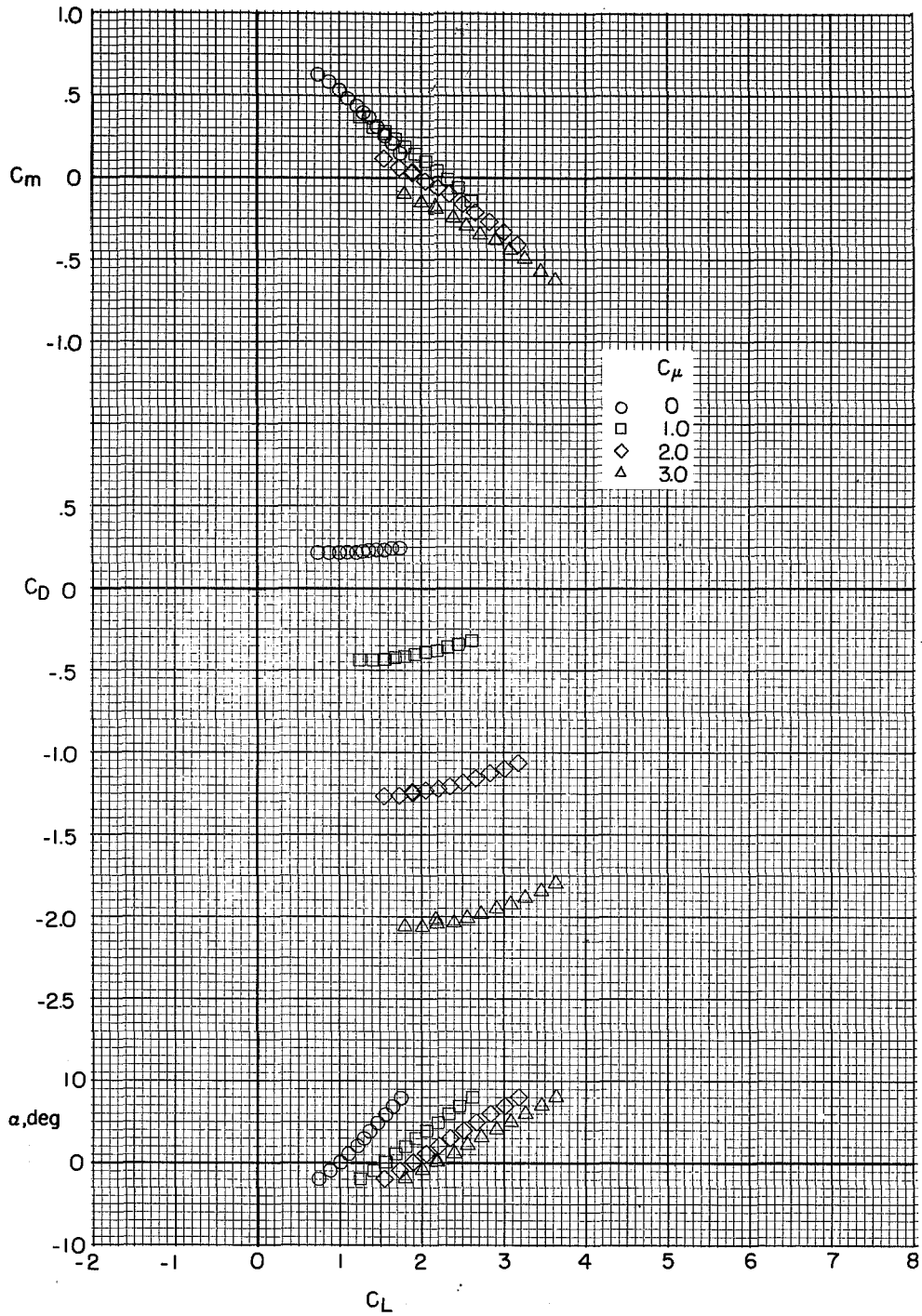

(b) Tail in high position; $i_t = -10^o$.

Figure 7.- Concluded.

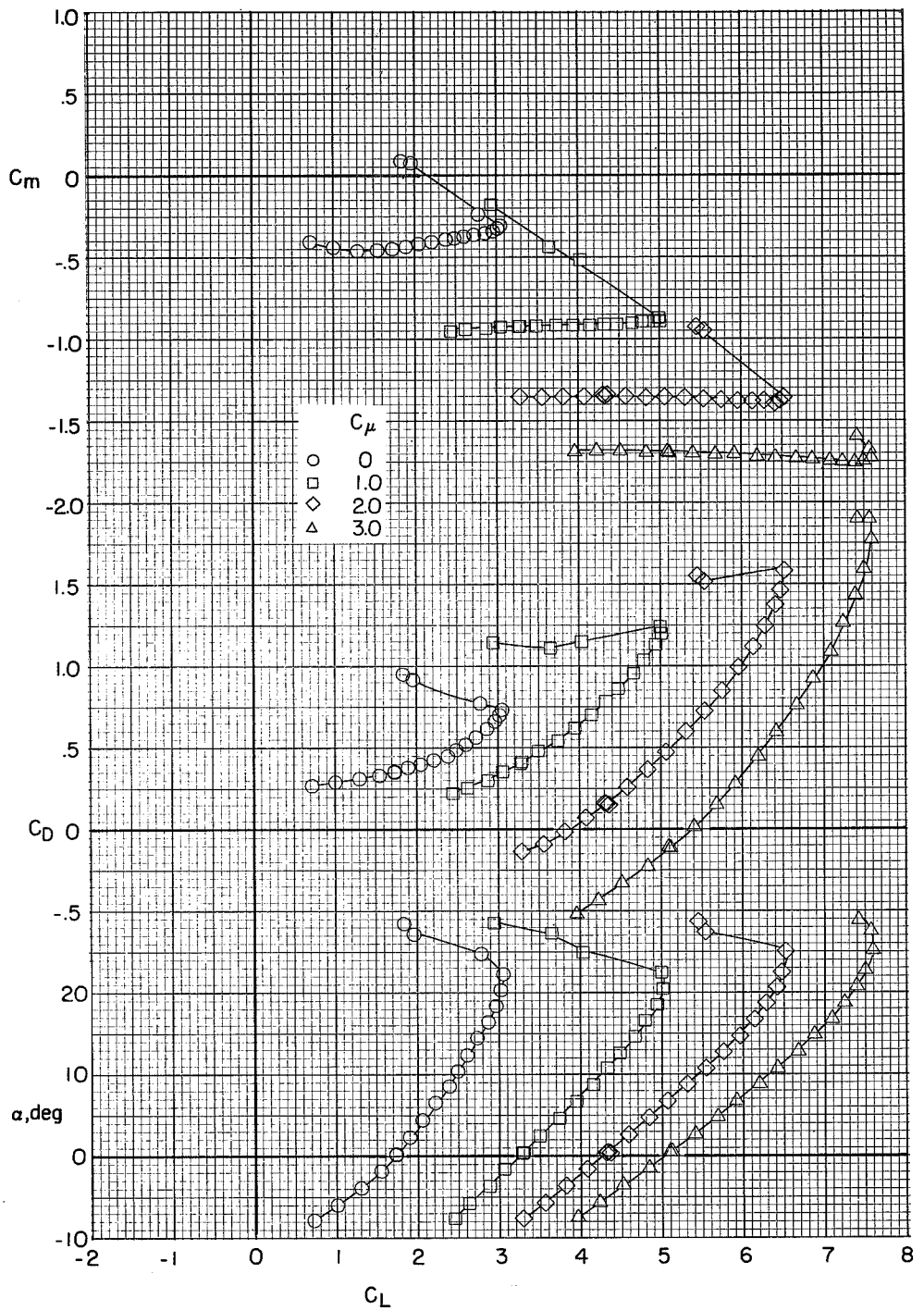

(a) Tail off.

Figure 8.- Longitudinal aerodynamic characteristics of the high-wing configuration out of ground effect. h/b = 1.24; $\delta_f = 60^o, 60^o, 0^o$.

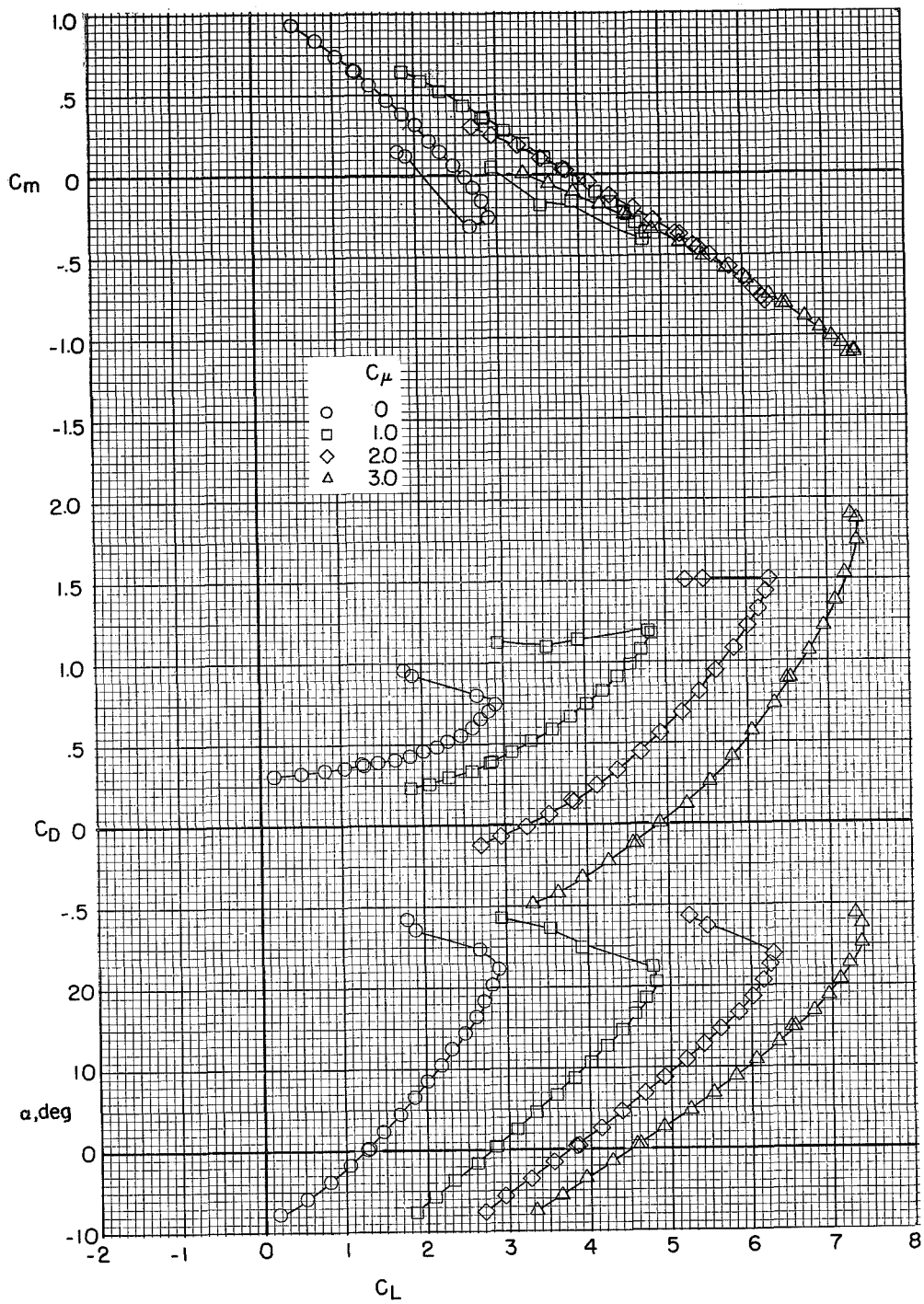

(b) Tail in high position; $i_t = -10^o$.

Figure 8.- Concluded.

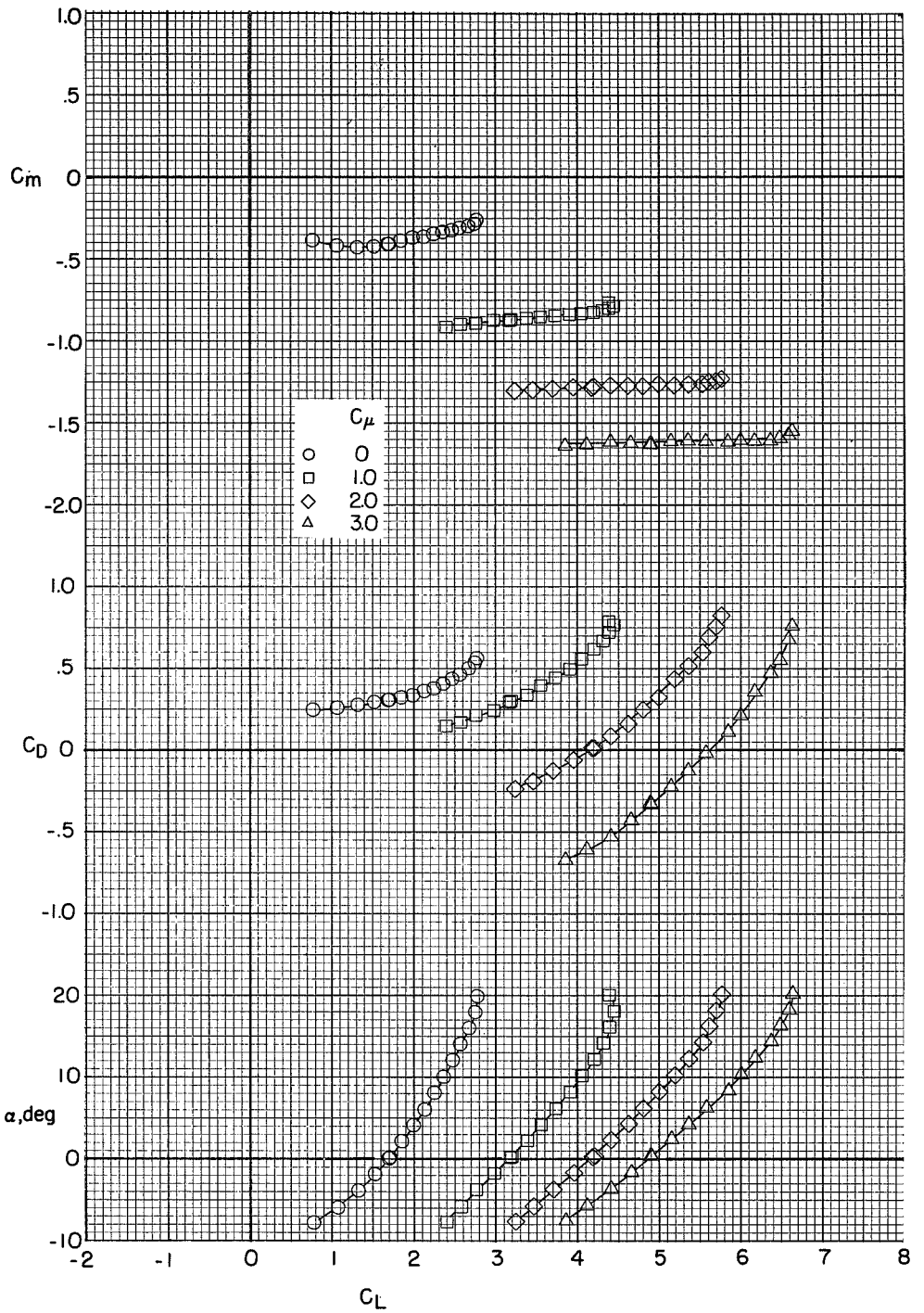

(a) Tail off.

Figure 9.- Longitudinal aerodynamic characteristics of the high-wing configuration in ground effect. $h/b = 0.32$; $\delta_f = 60^o, 60^o, 0^o$.

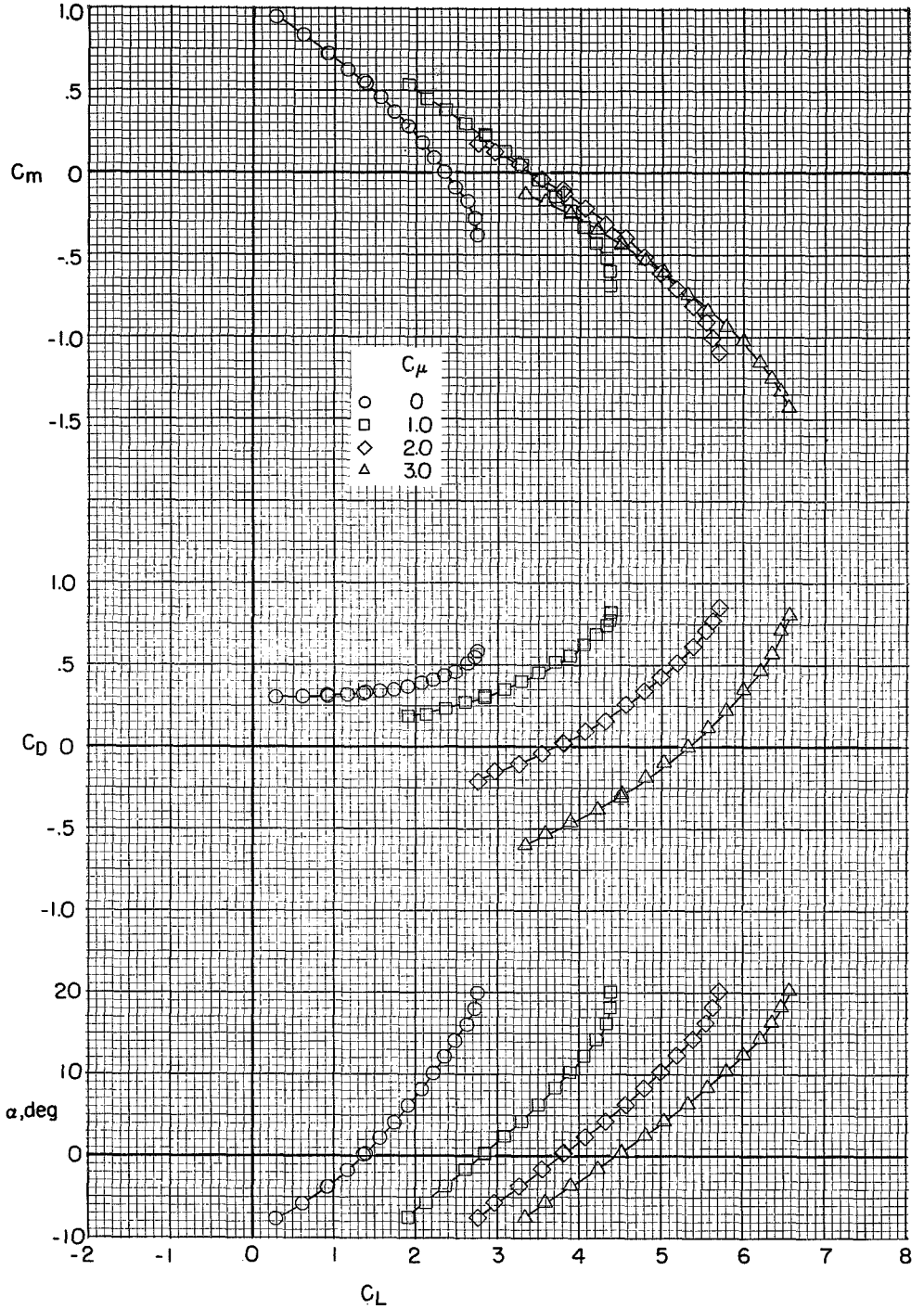

(b) Tail in high position; $i_t = -10^o$.

Figure 9.- Concluded.

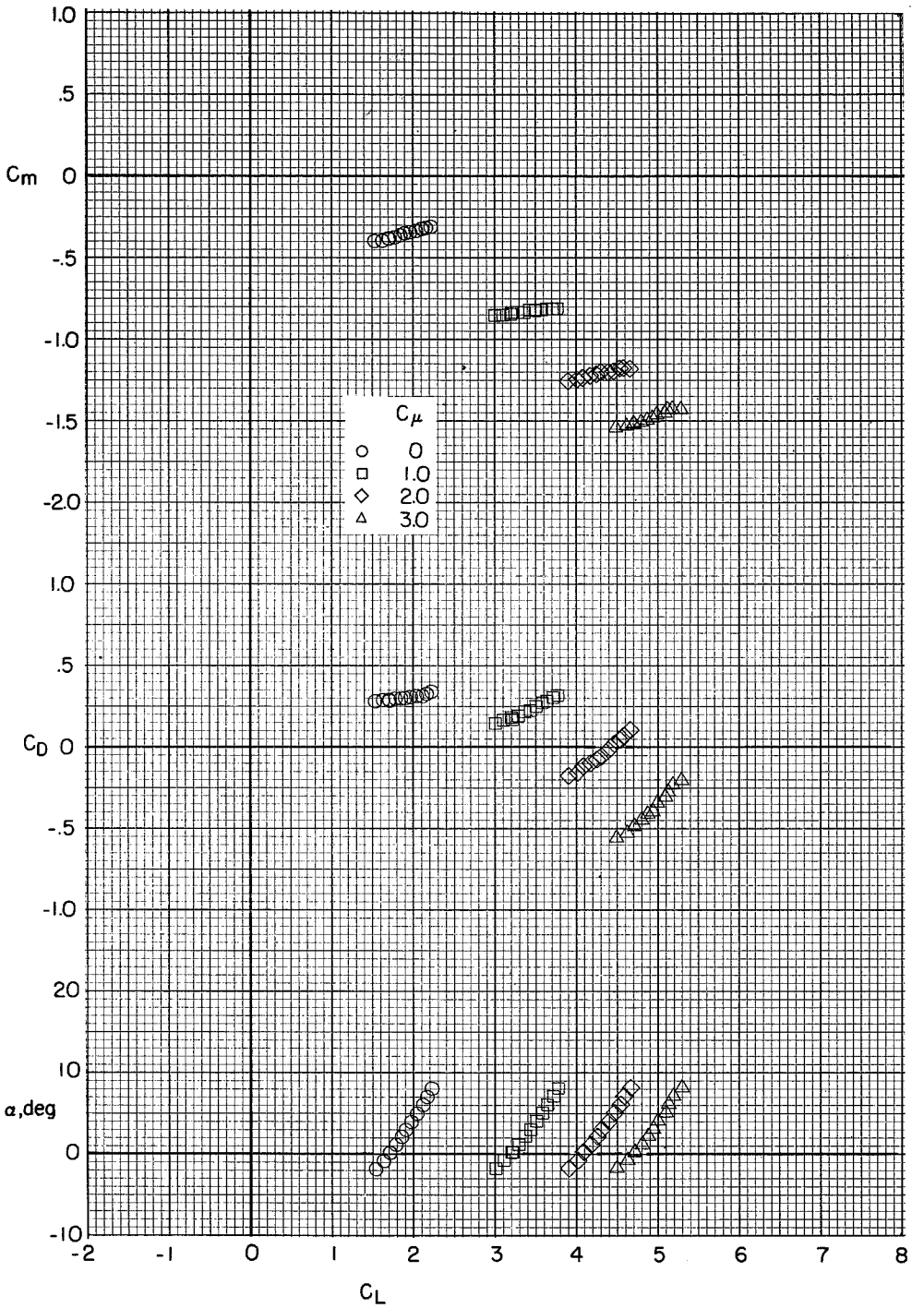

(a) Tail off.

Figure 10.- Longitudinal aerodynamic characteristics of the high-wing configuration in ground effect. h/b = 0.19; $\delta_f = 60^o, 60^o, 0^o$.

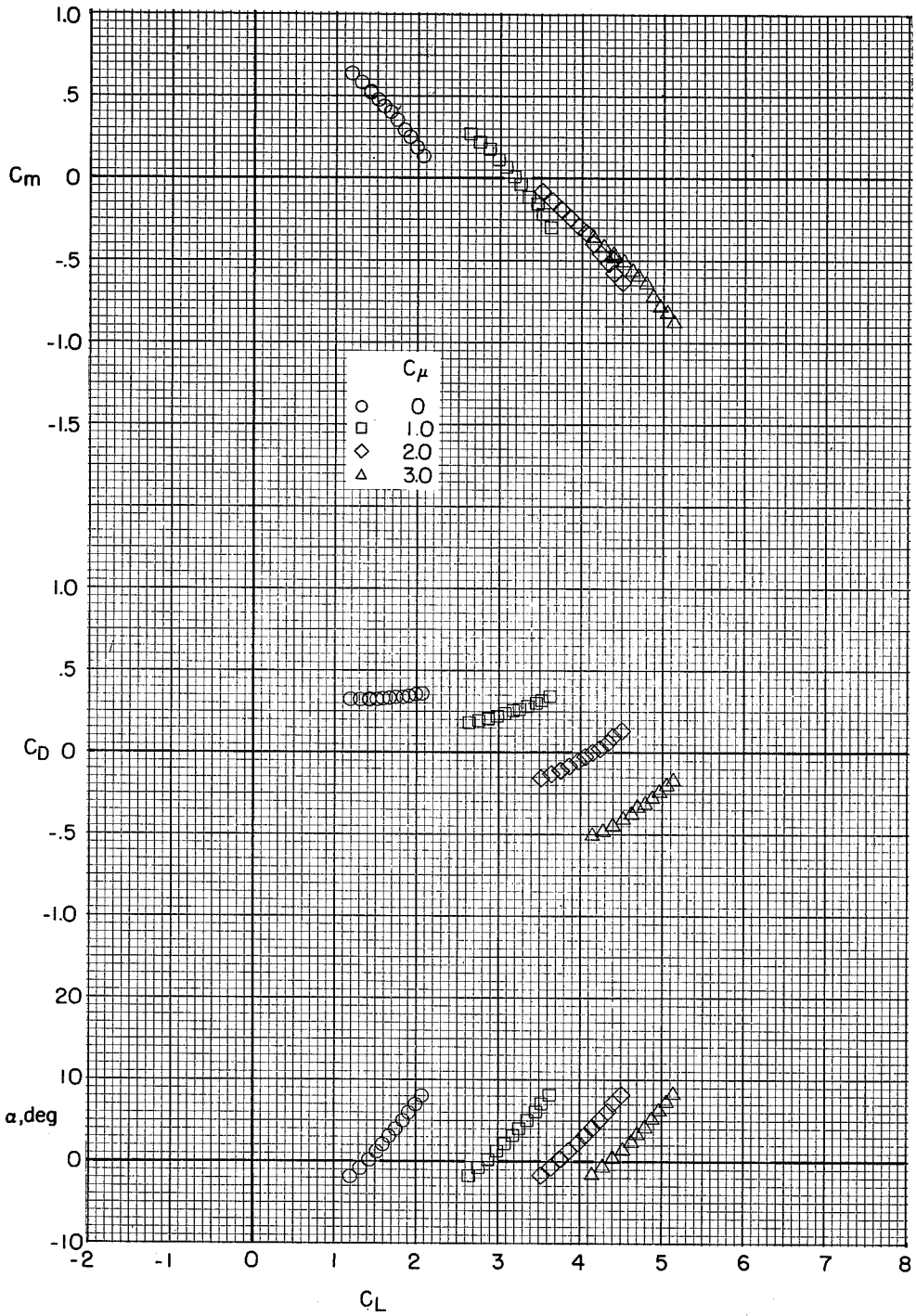

(b) Tail in high position; $i_t = -10^o$.

Figure 10.- Concluded.

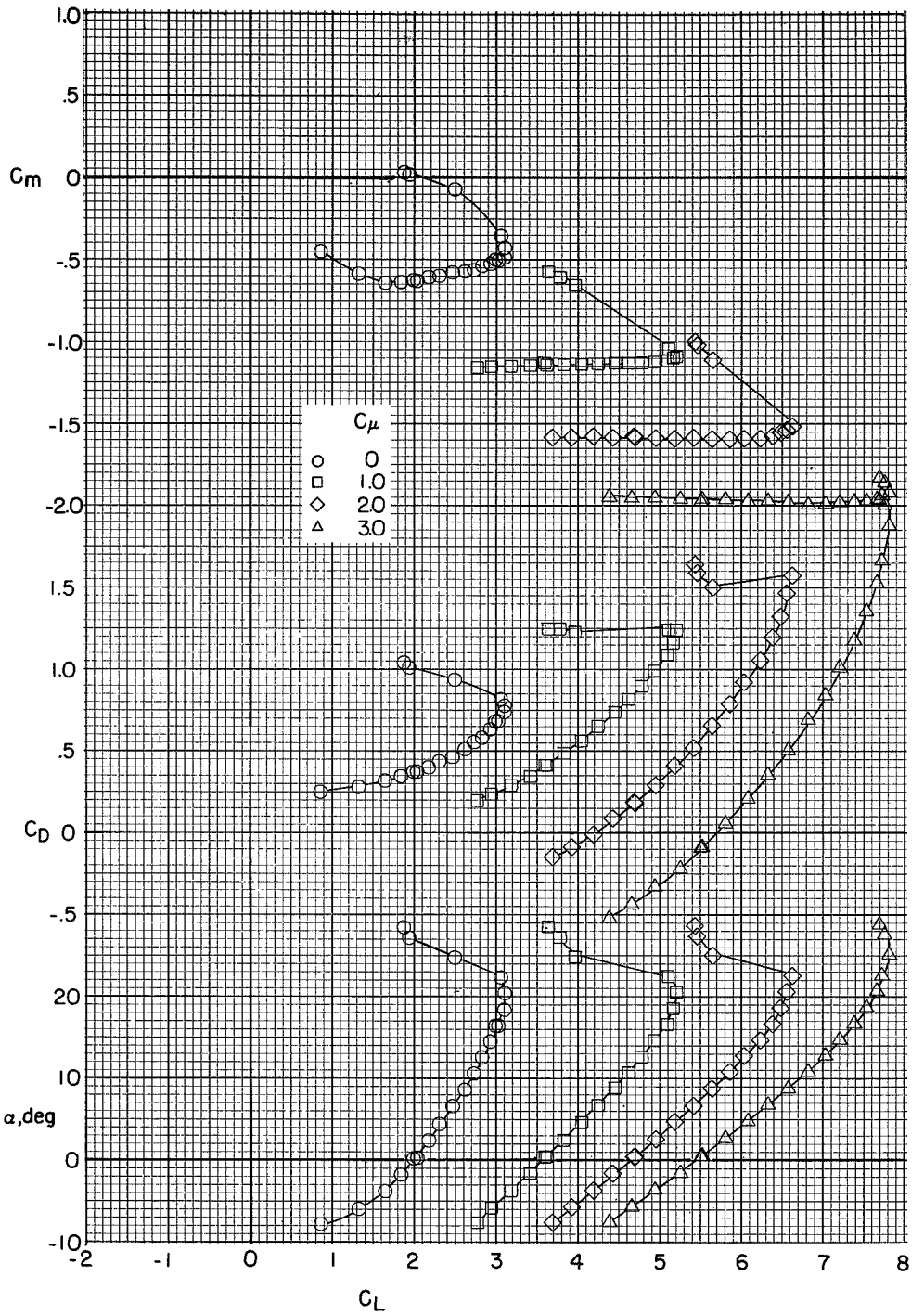

(a) Tail off.

Figure 11.- Longitudinal aerodynamic characteristics of the high-wing configuration out of ground effect. h/b = 1.24; $\delta_f = 60^o, 60^o, 60^o$.

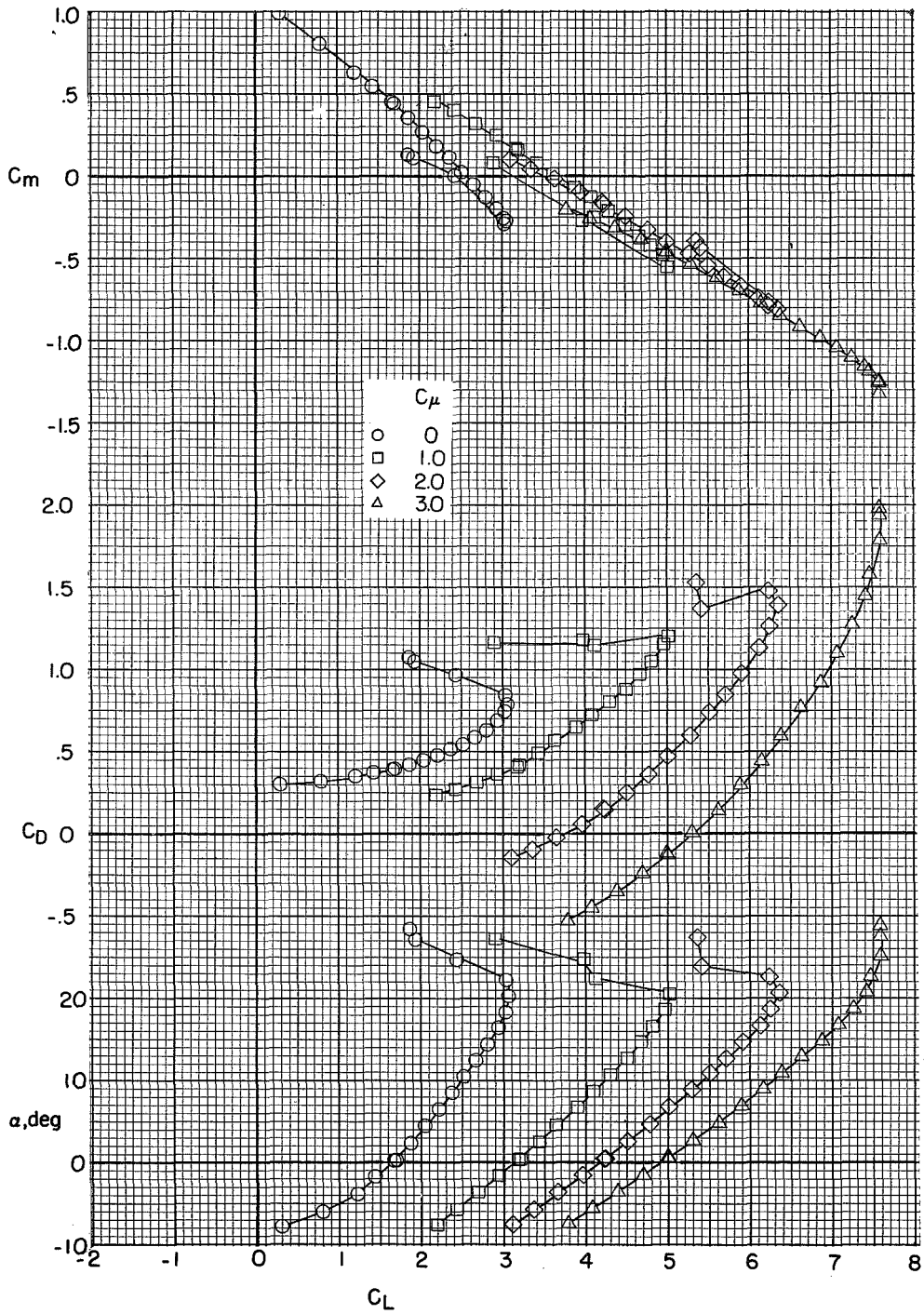

(b) Tail in high position; $i_t = -10^o$.

Figure 11.- Concluded.

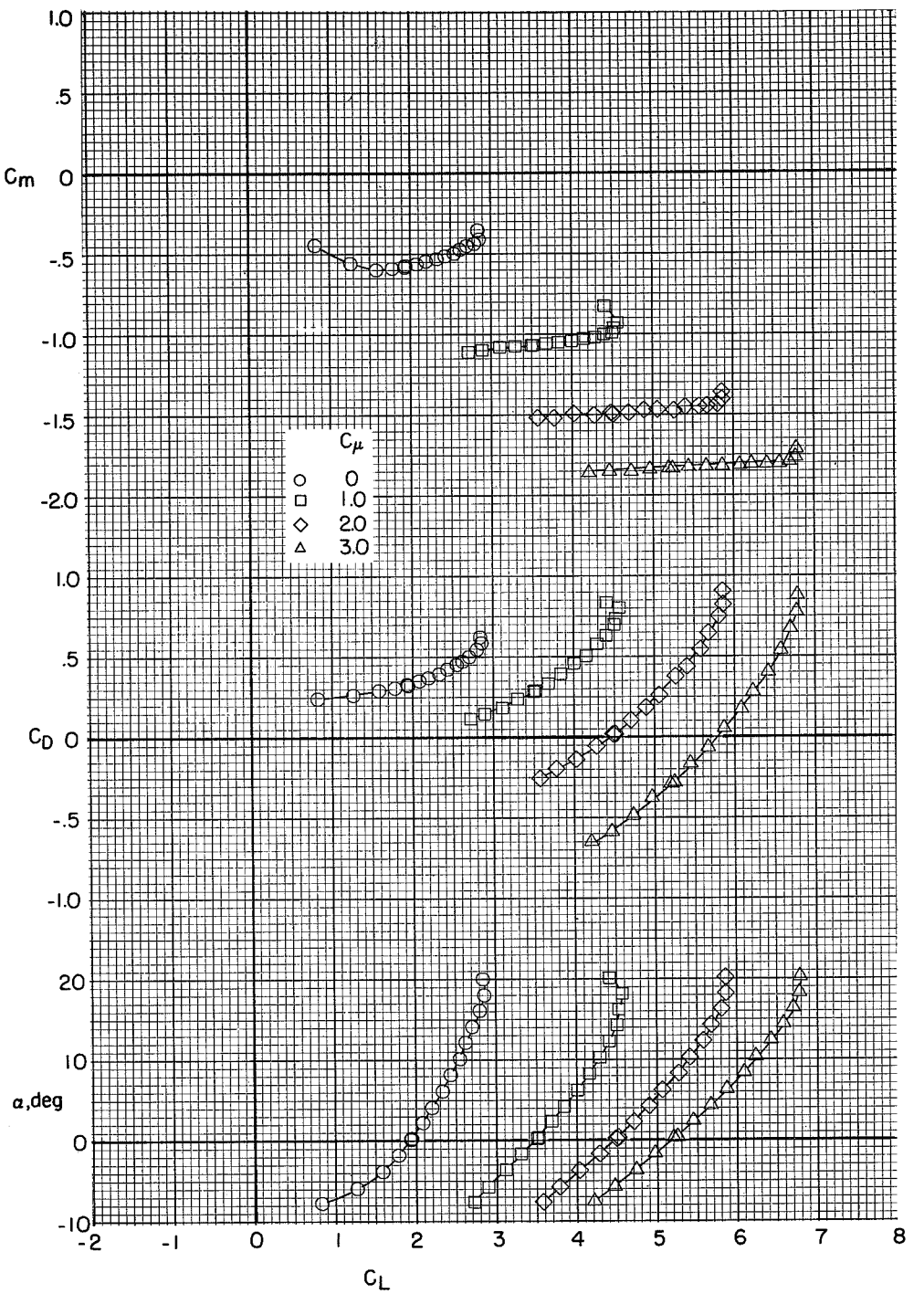

(a) Tail off.

Figure 12.- Longitudinal aerodynamic characteristics of the high-wing configuration in ground effect. h/d = 0.32; $\delta_f = 60^o, 60^o, 60^o$.

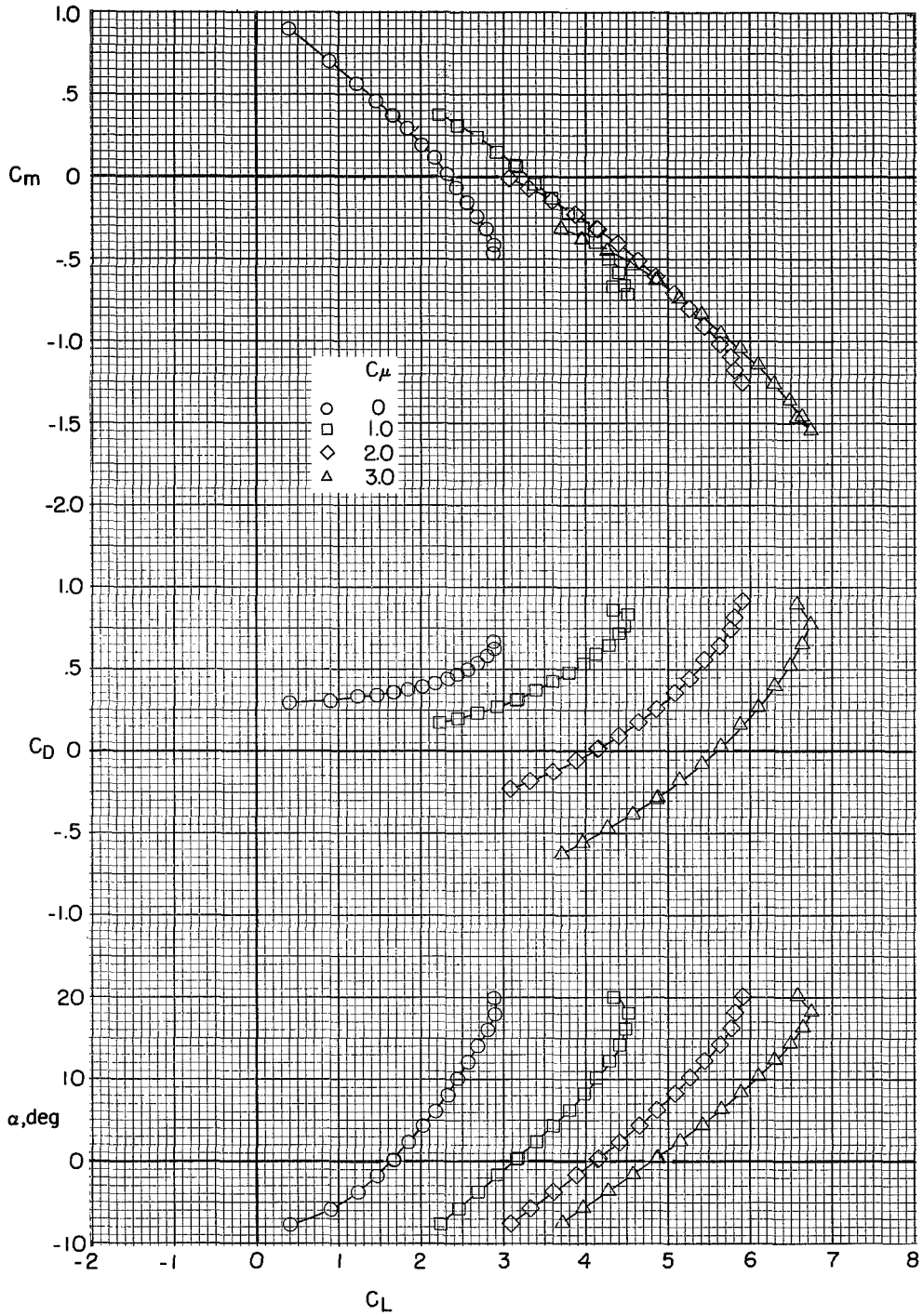

(b) Tail in high position; $i_t = -10^o$.

Figure 12.- Concluded.

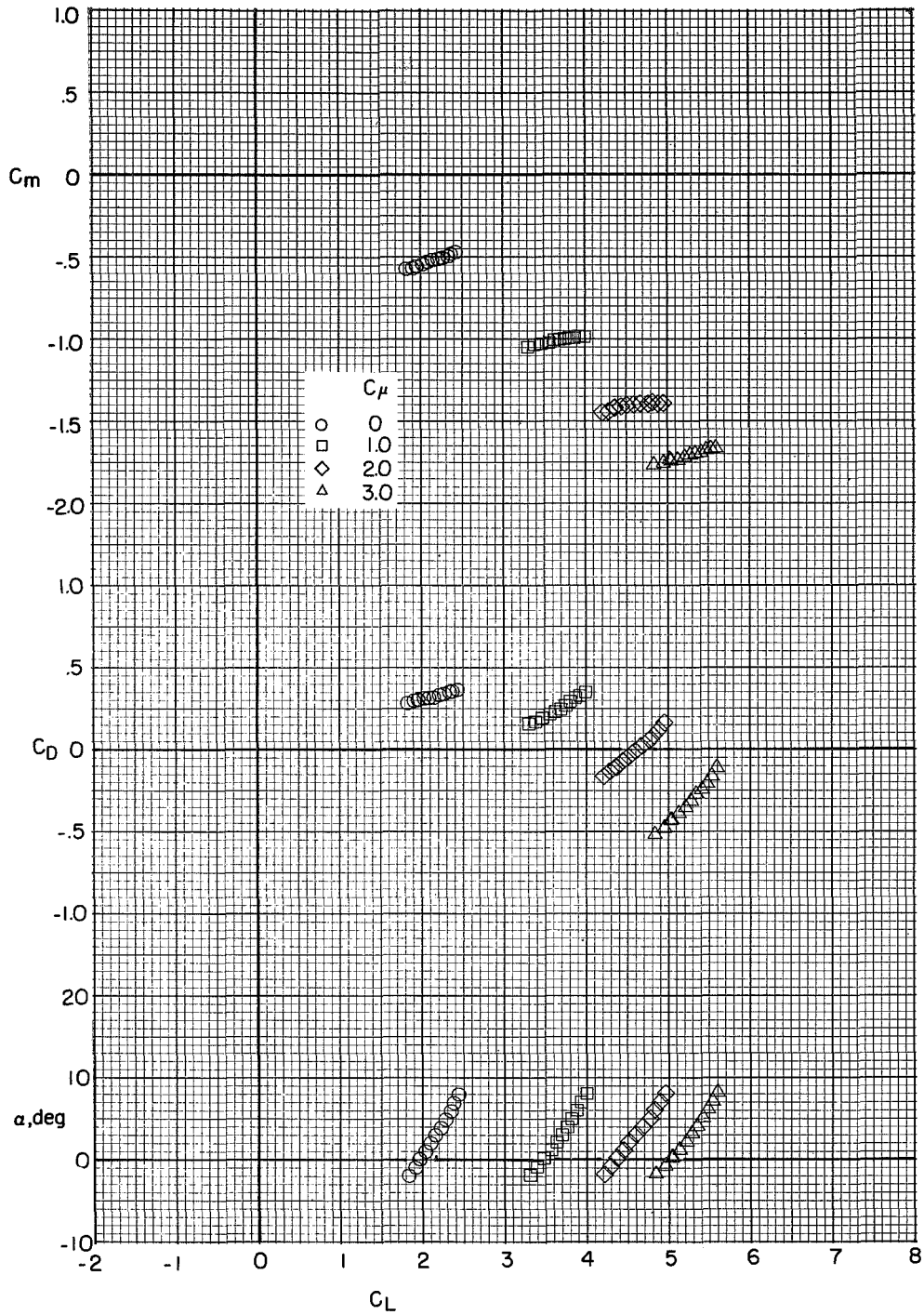

(a) Tail off.

Figure 13.- Longitudinal aerodynamic characteristics of the high-wing configuration in ground effect. h/b = 0.19; $\delta_f = 60^o, 60^o, 60^o$.

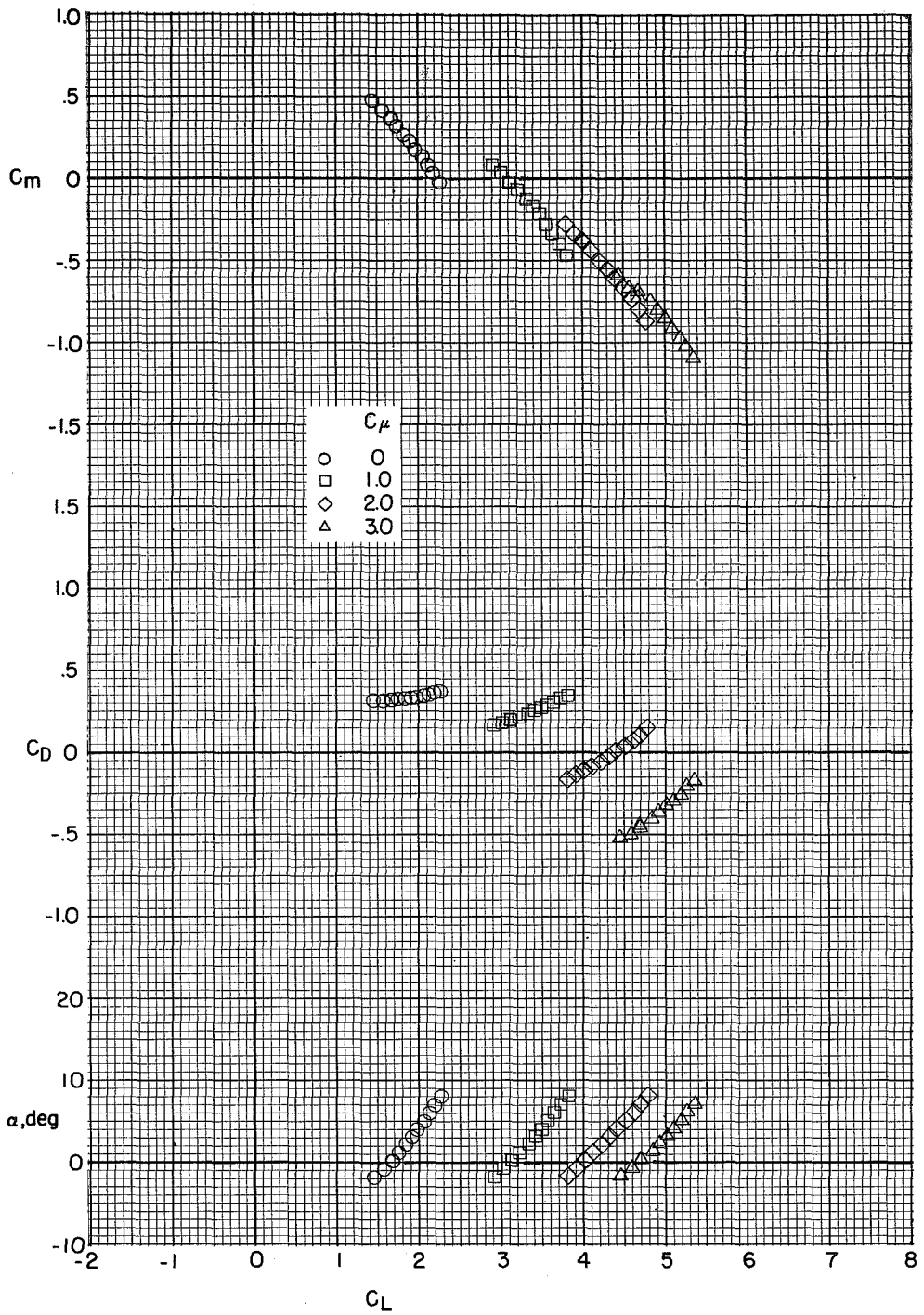

(b) Tail in high position; $i_t = -10^o$.

Figure 13.- Concluded.

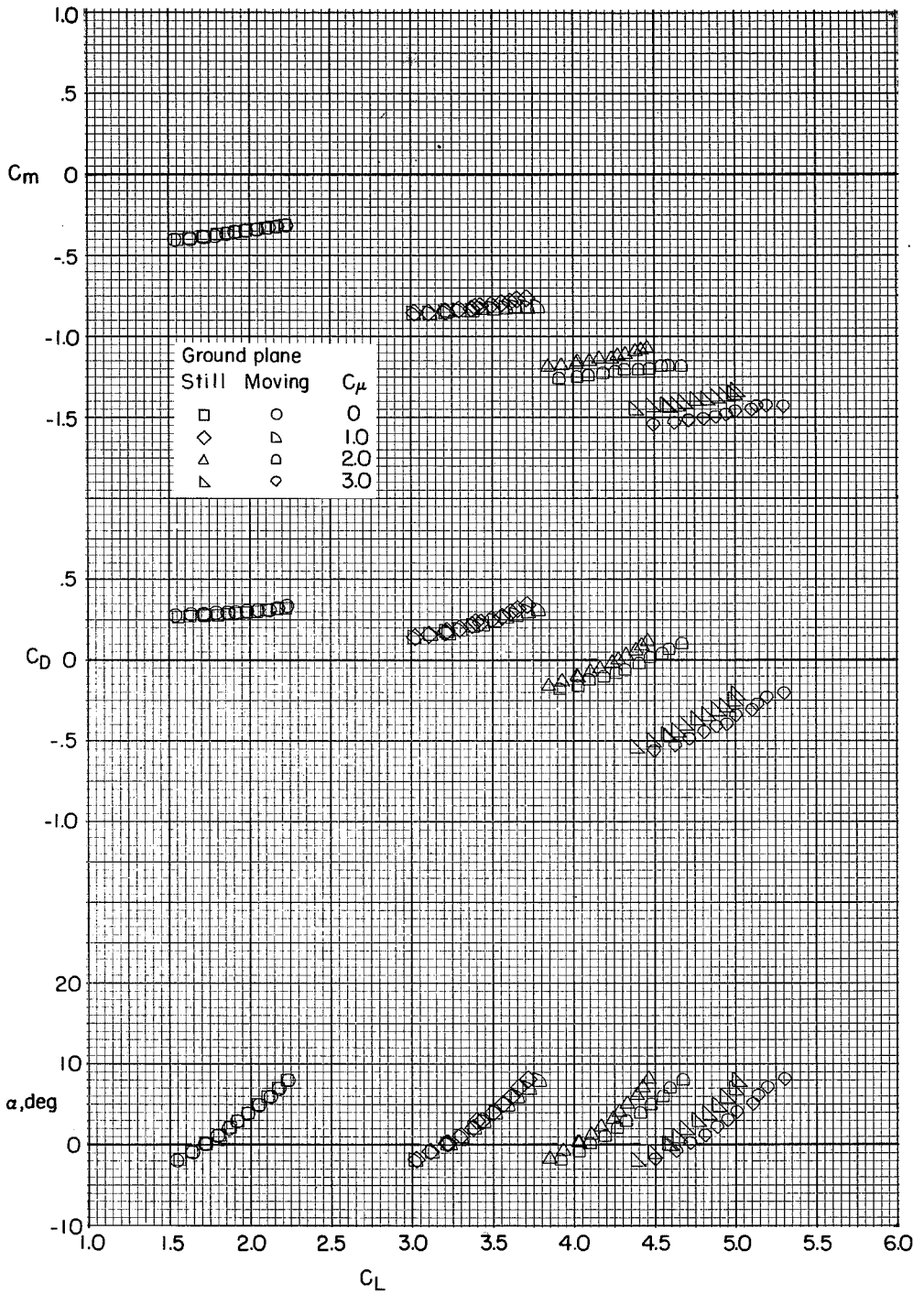

(a) Tail off.

Figure 14.- Comparison of the longitudinal aerodynamic characteristics of the high-wing configuration over still and over moving ground planes. h/b = 0.19; $\delta_f = 60^o, 60^o, 0^o$.

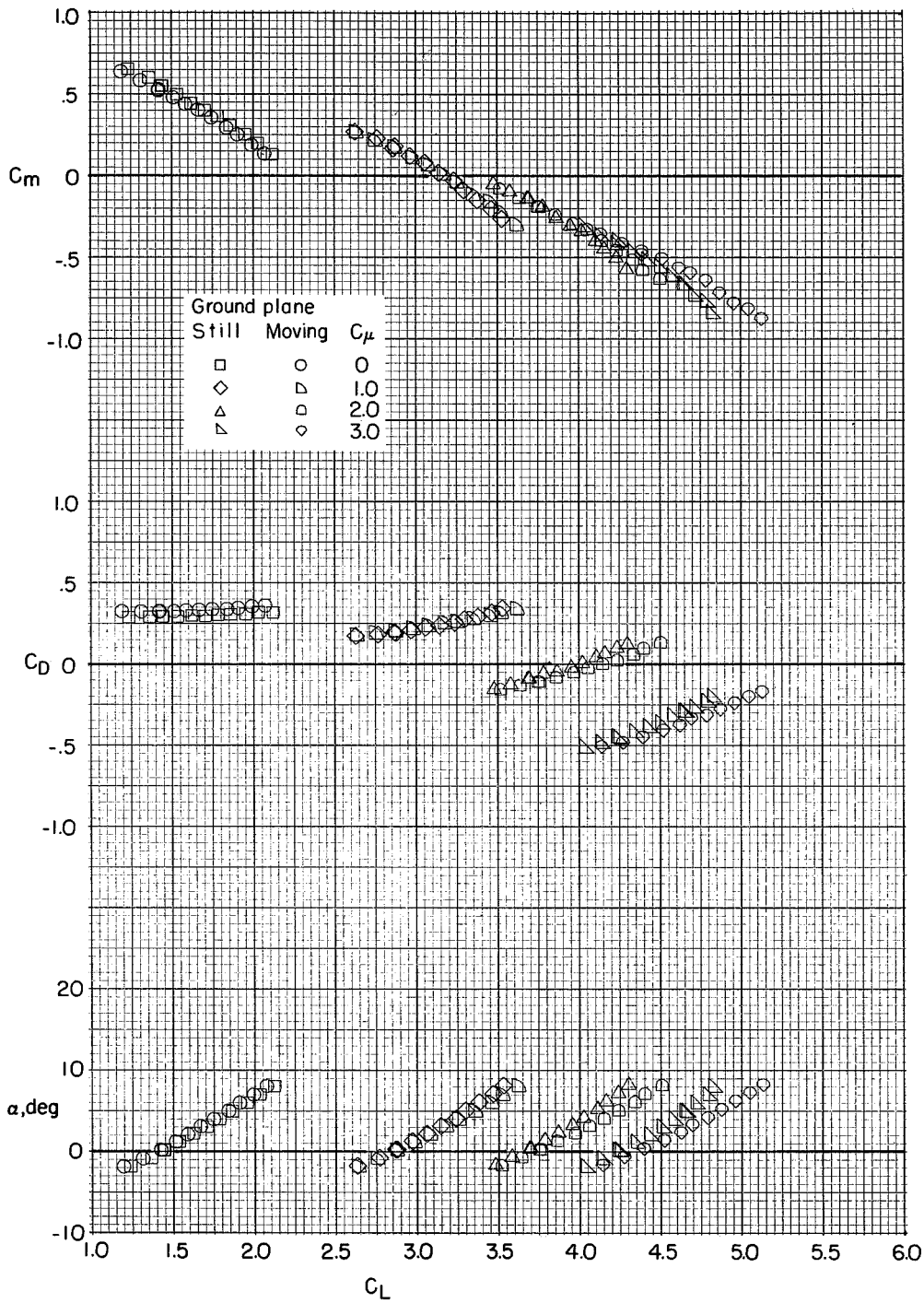

(b) Tail in high position; $i_t = -10^o$.

Figure 14.- Concluded.

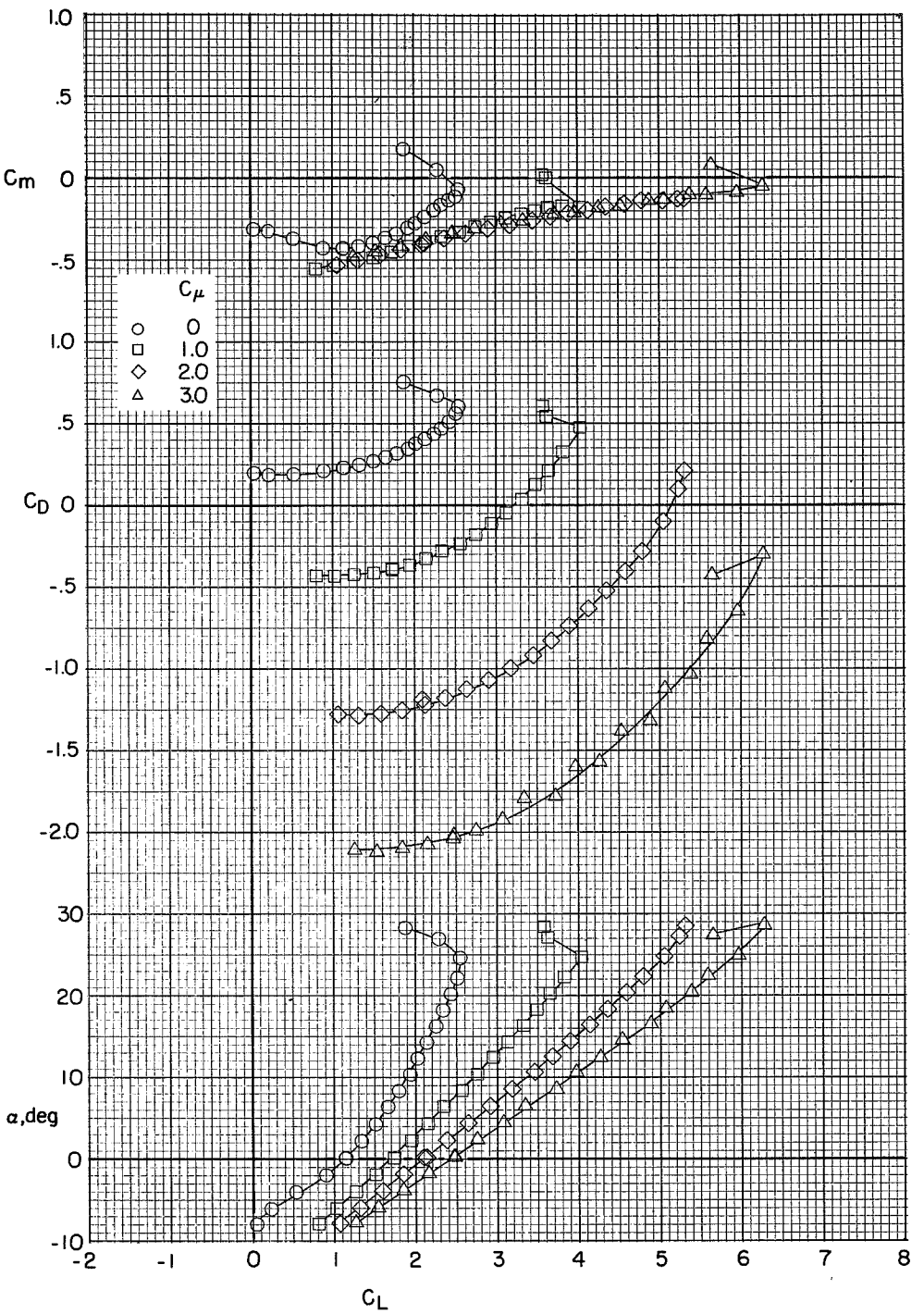

(a) Tail off.

Figure 15.- Longitudinal aerodynamic characteristics of the low-wing configuration out of ground effect. h/b = 1.24; $\delta_f = 30^o, 60^o, 0^o$.

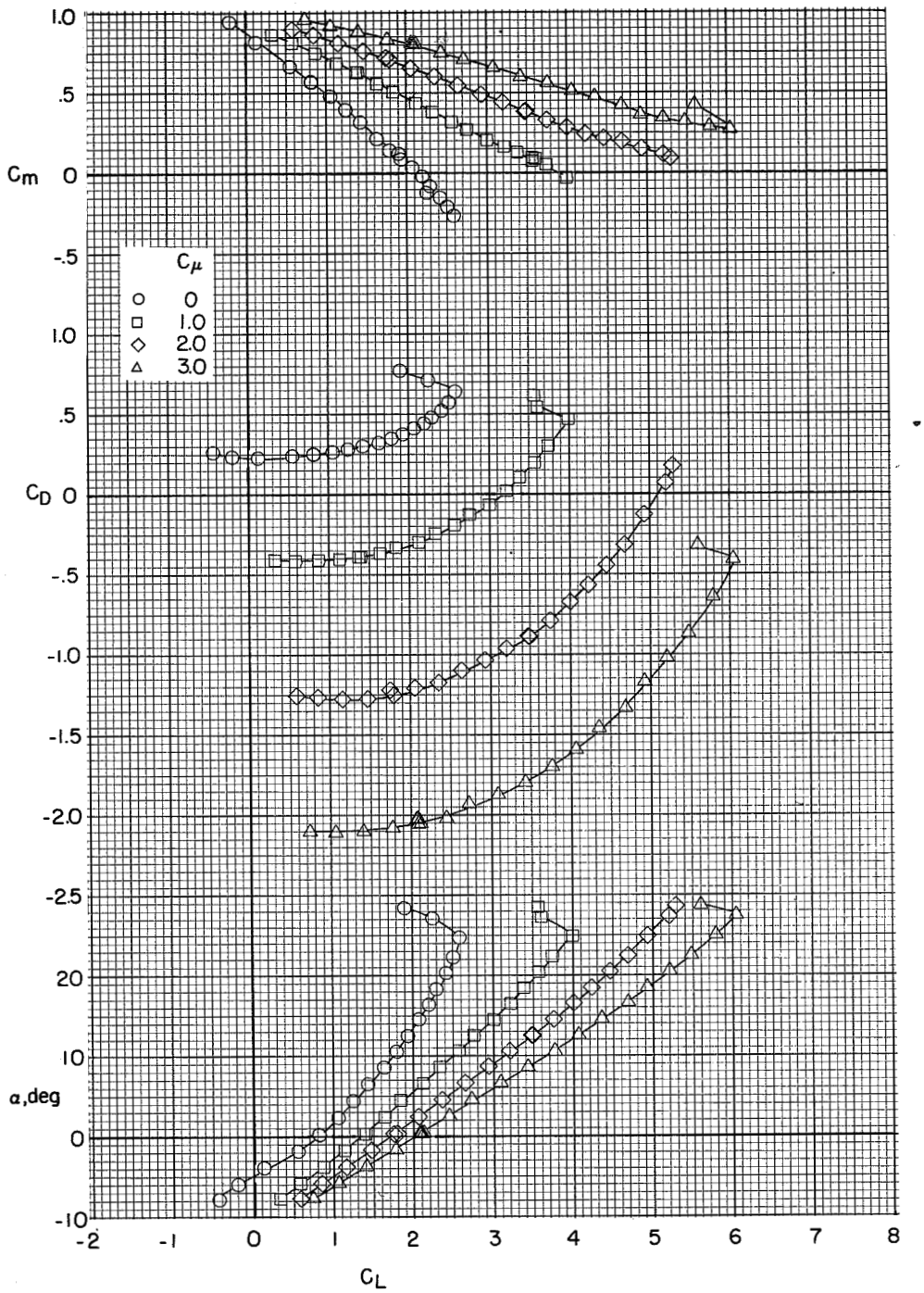

(b) Tail in mid position; $i_t = -10^o$.

Figure 15.- Concluded.

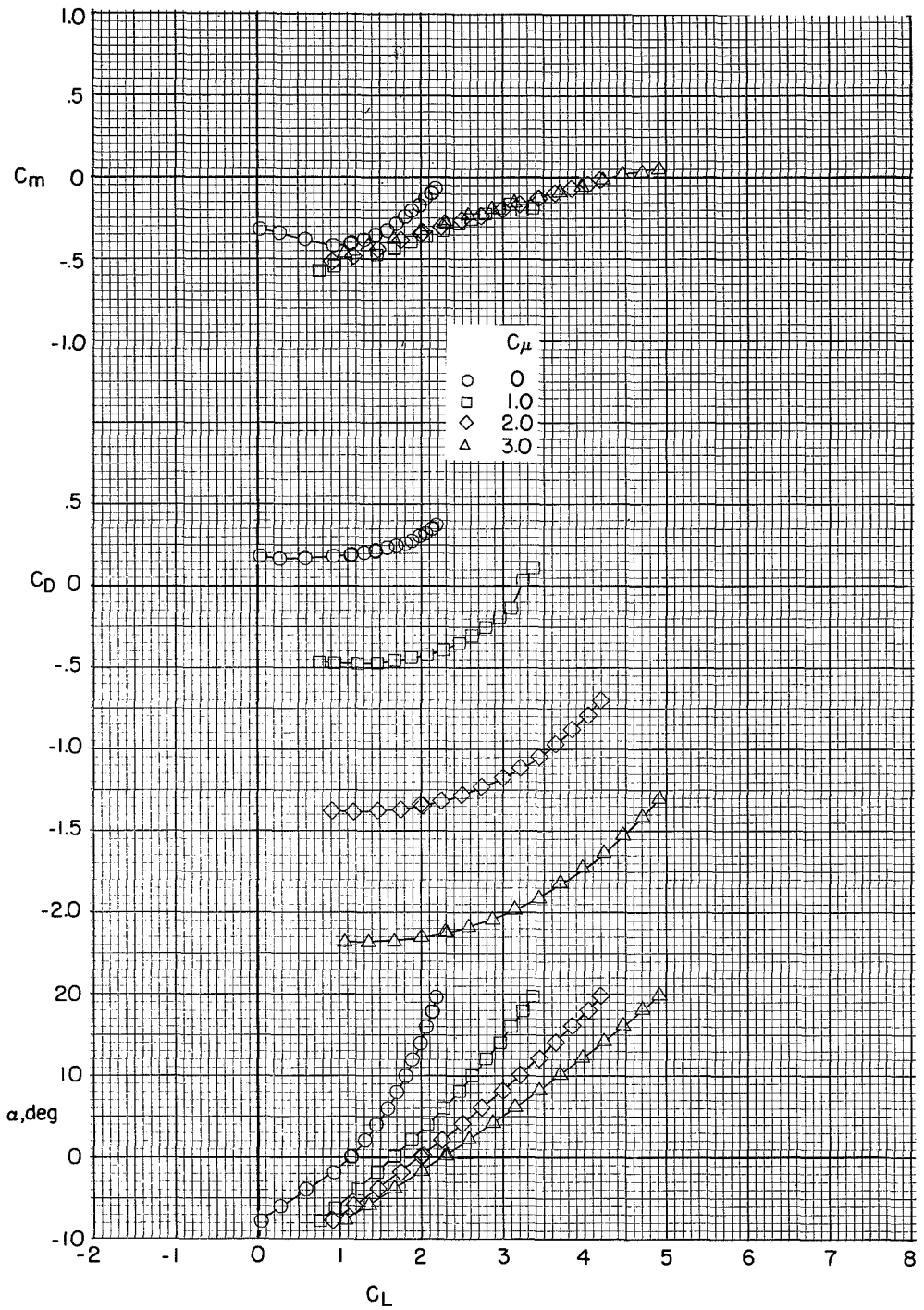

(a) Tail off.

Figure 16.- Longitudinal aerodynamic characteristics of the low-wing configuration in ground effect. h/b = 0.19; $\delta_f = 30^o, 60^o, 0^o$.

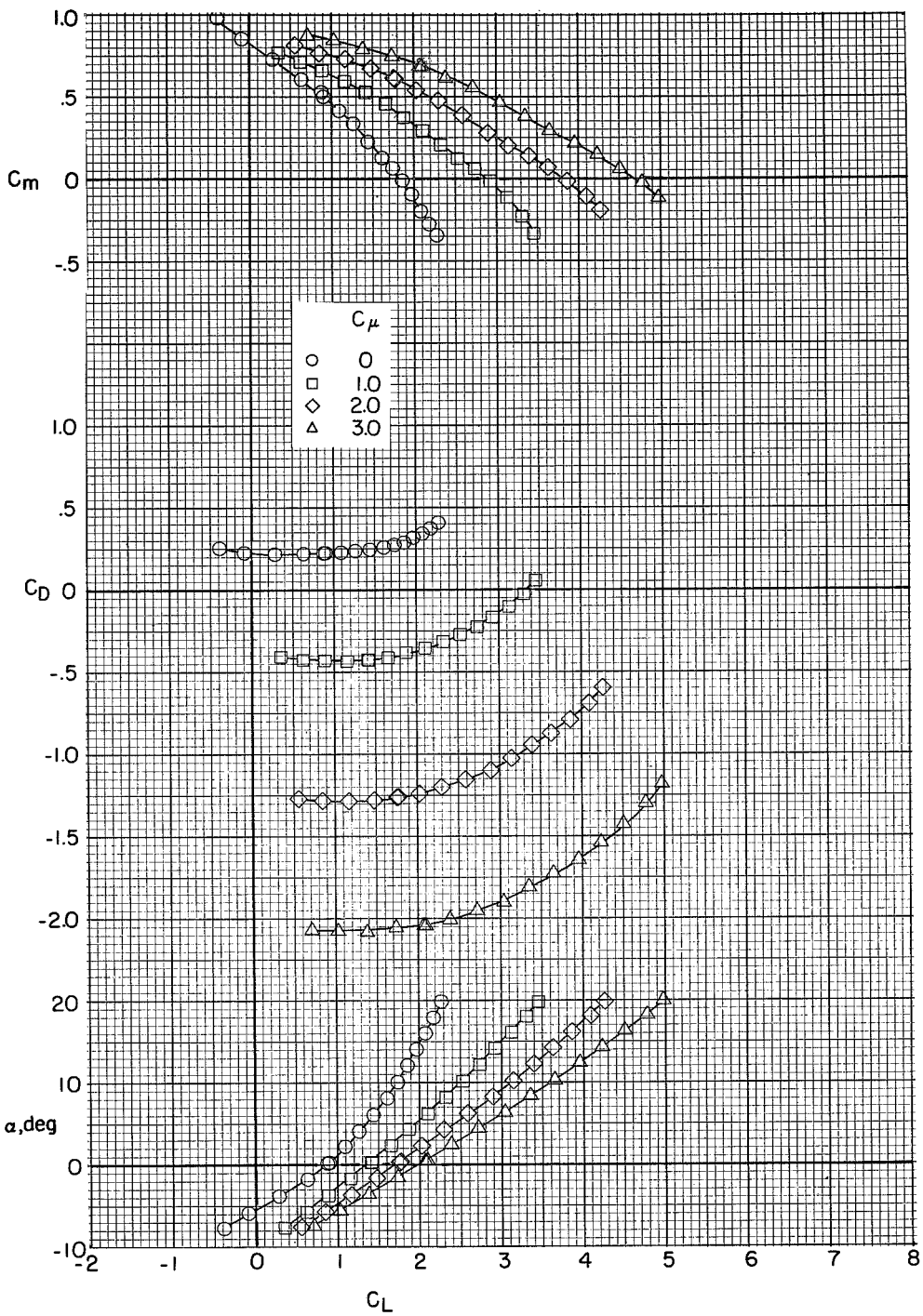

(b) Tail in mid position; $i_t = -10^o$.

Figure 16.- Concluded.

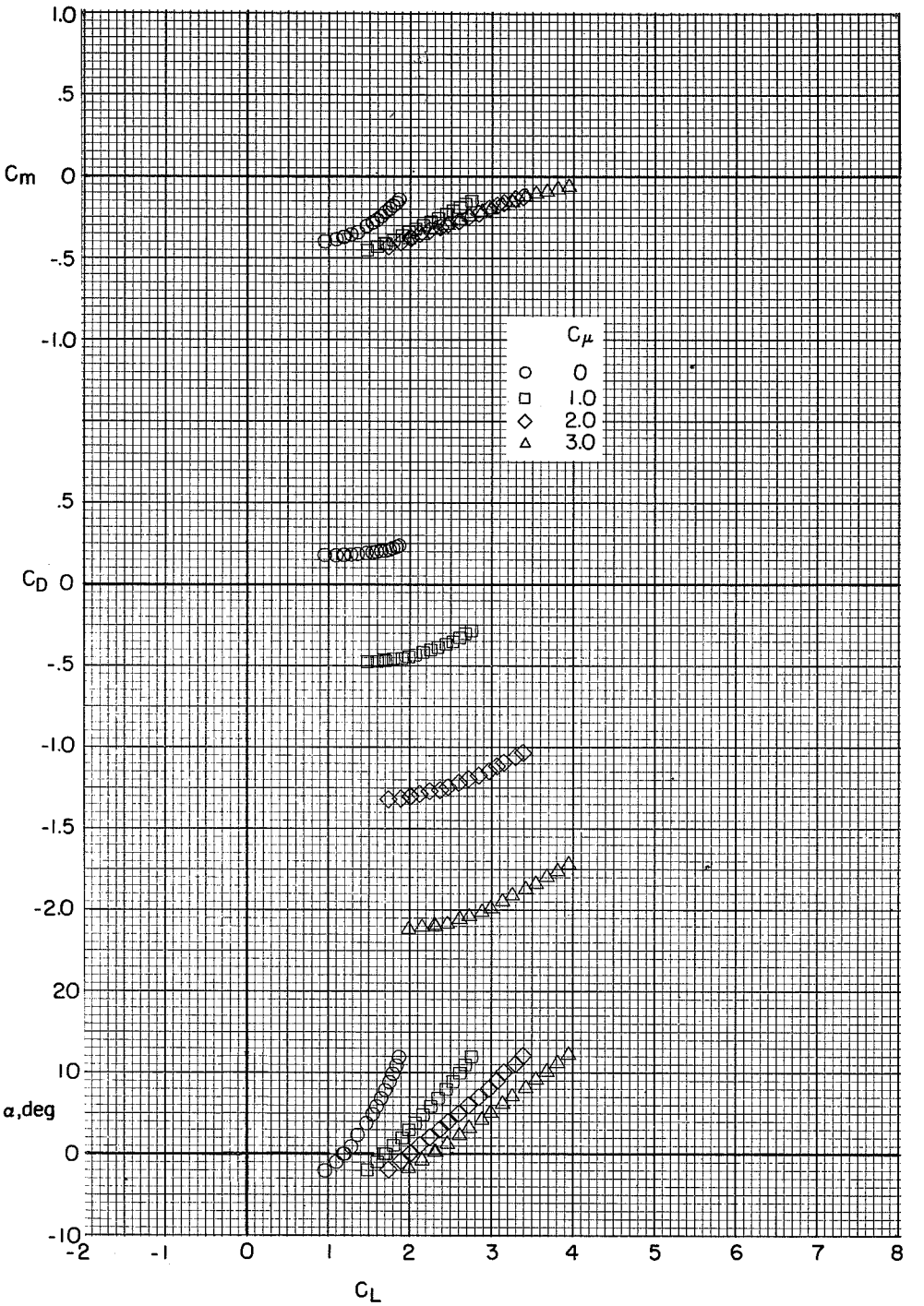

(a) Tail off.

Figure 17.- Longitudinal aerodynamic characteristics of the low-wing configuration in ground effect. $h/b = 0.12$; $\delta_f = 30^o, 60^o, 0^o$.

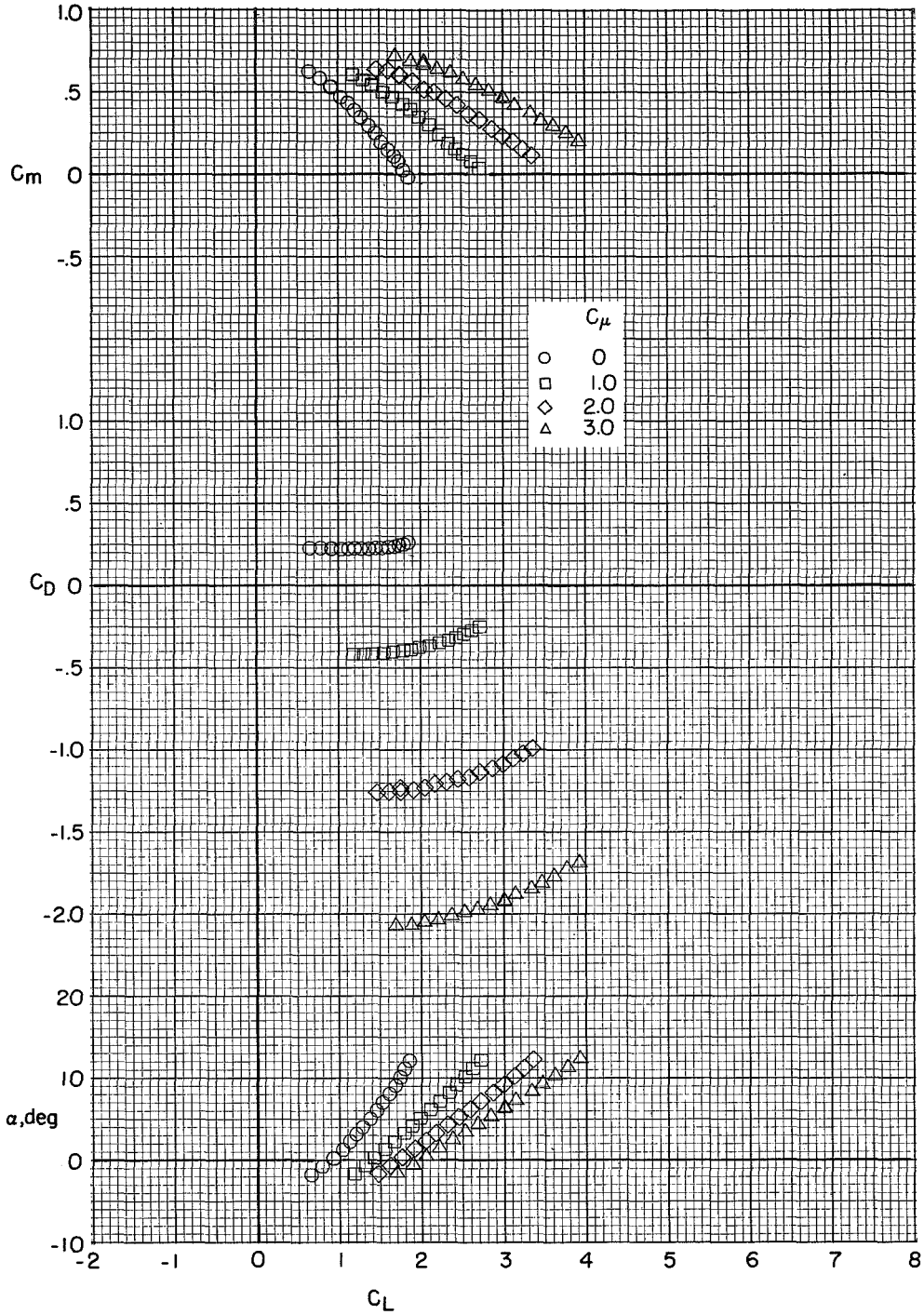

(b) Tail in mid position; $i_t = -10^o$.

Figure 17.- Concluded.

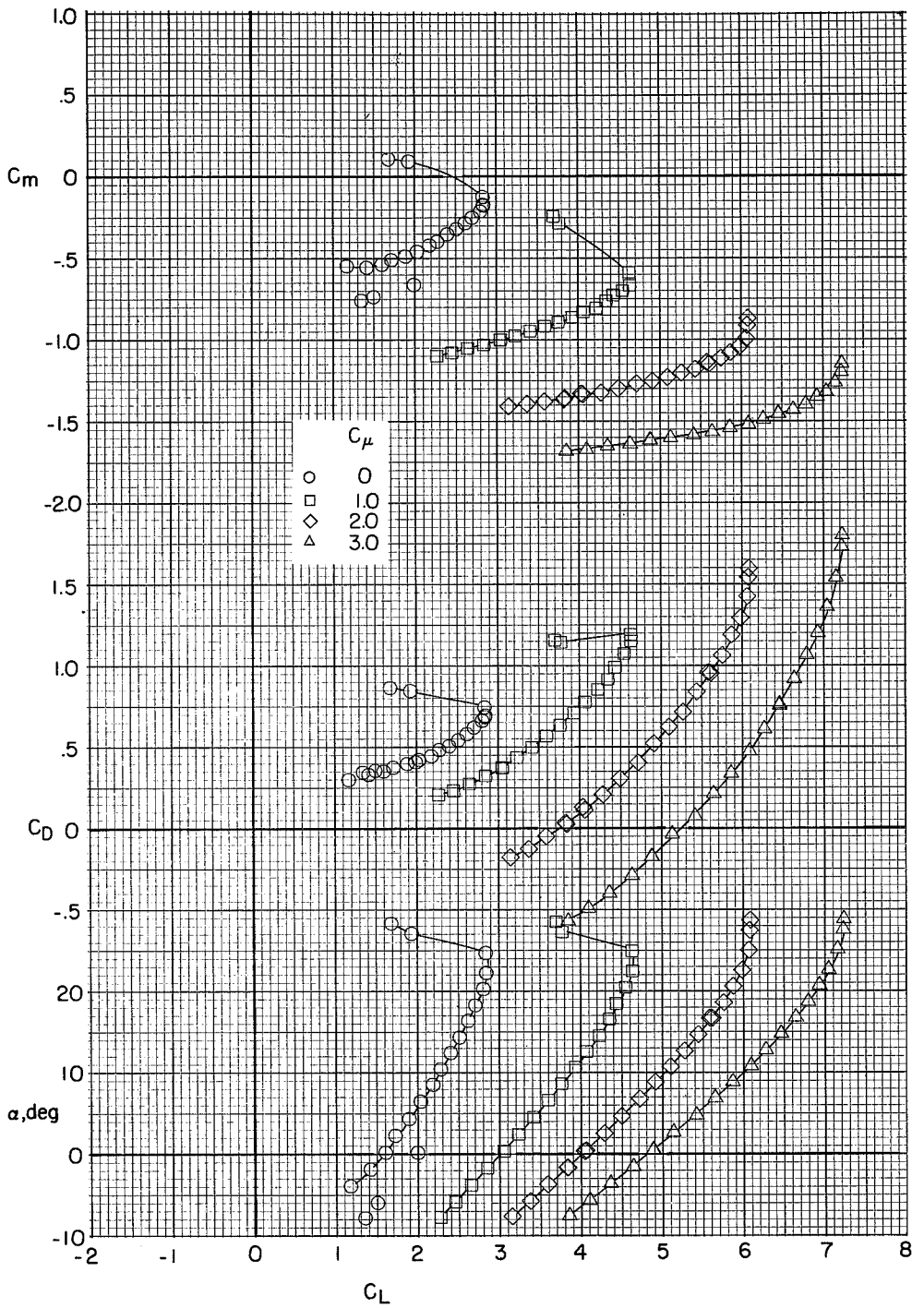

(a) Tail off.

Figure 18.- Longitudinal aerodynamic characteristics of the low-wing configuration out of ground effect. h/b = 1.24; δ_f = 60°, 60°, 0°.

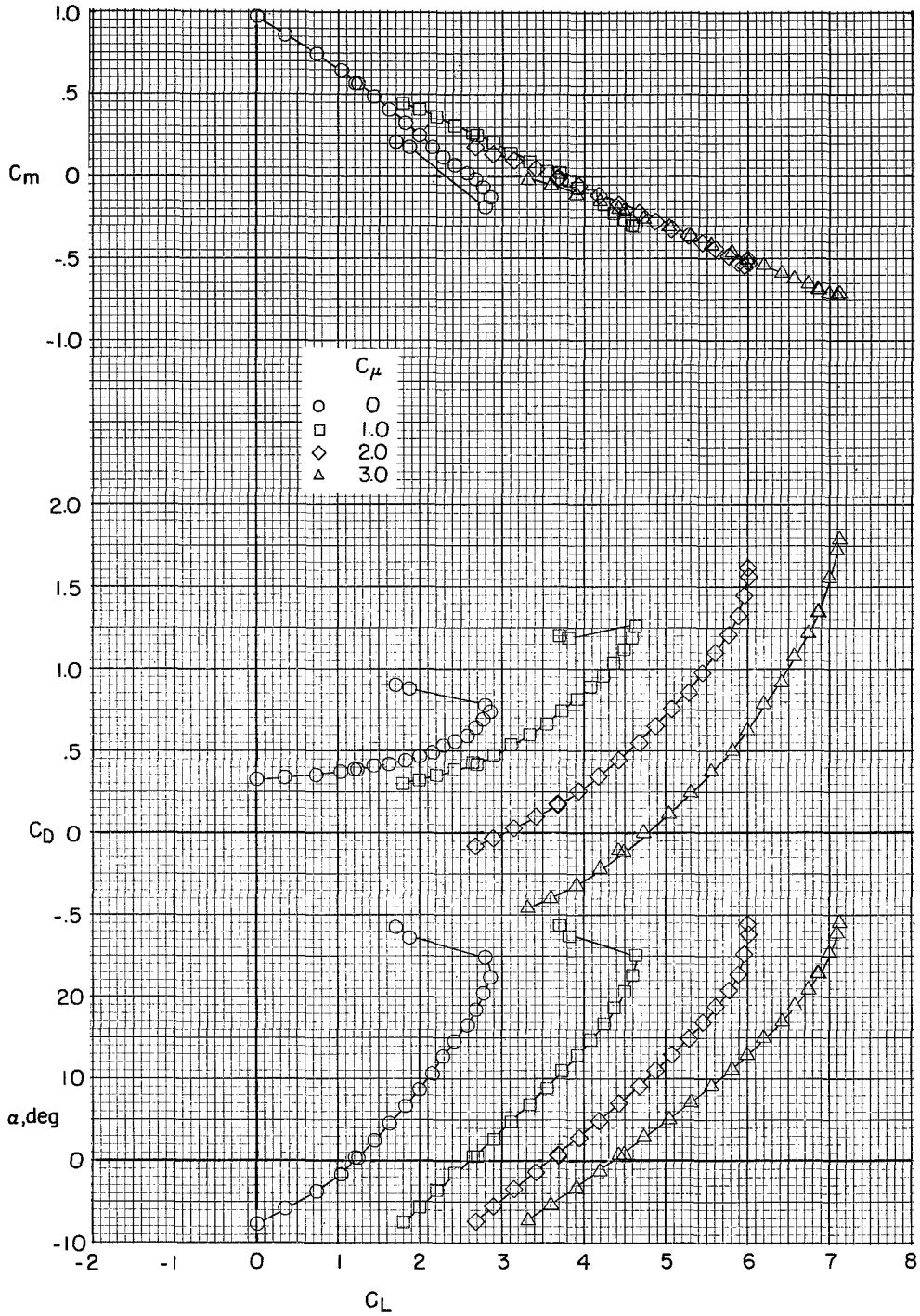

(b) Tail in high position; $i_t = -10^o$.

Figure 18.- Continued.

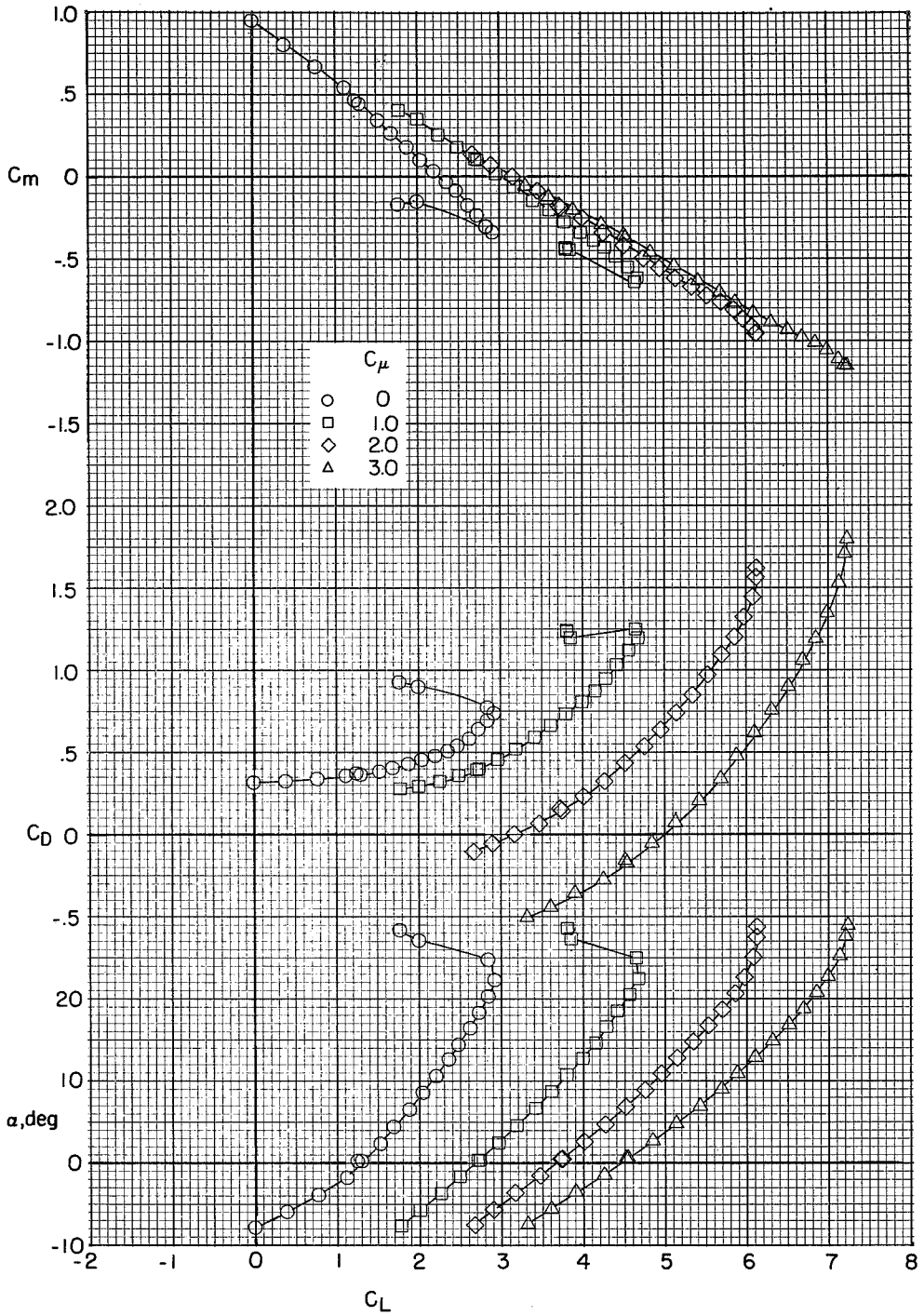

(c) Tail in mid position; $i_t = -10^o$.

Figure 18.- Concluded.

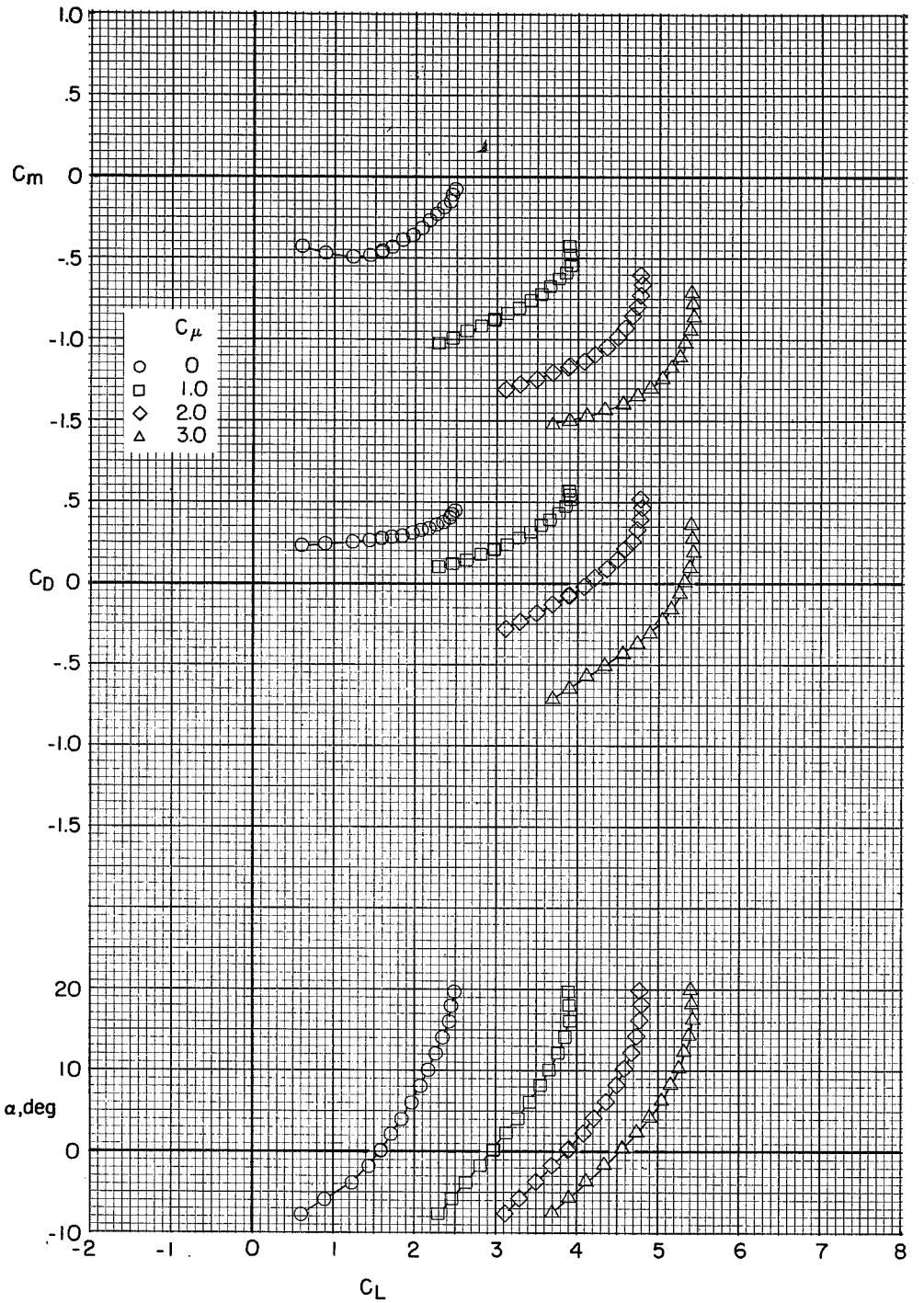

(a) Tail off.

Figure 19.- Longitudinal aerodynamic characteristics of the low-wing configuration in ground effect. h/b = 0.19; $\delta_f = 60^o, 60^o, 0^o$.

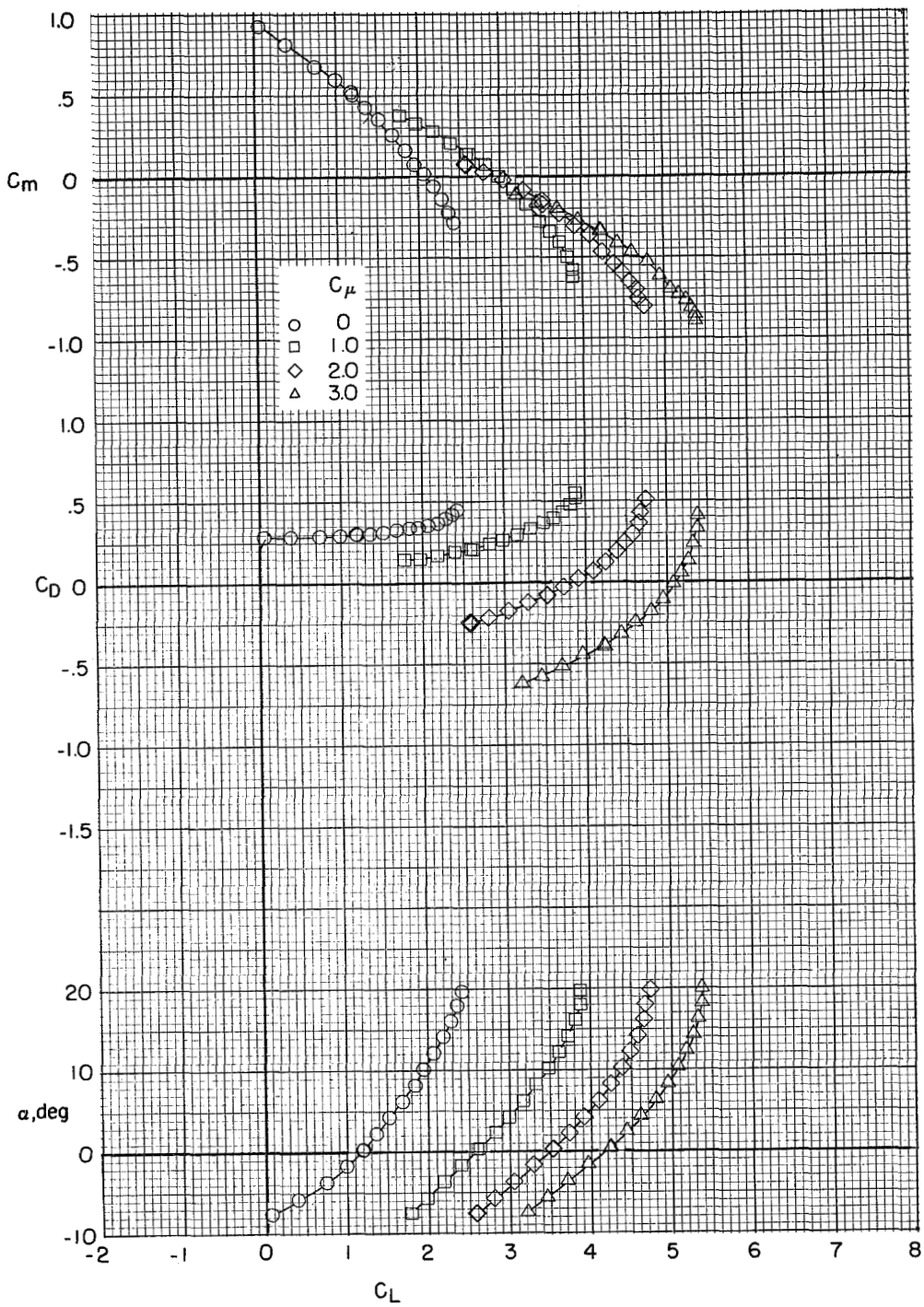

(b) Tail in mid position; $i_t = -10^o$.

Figure 19.- Concluded.

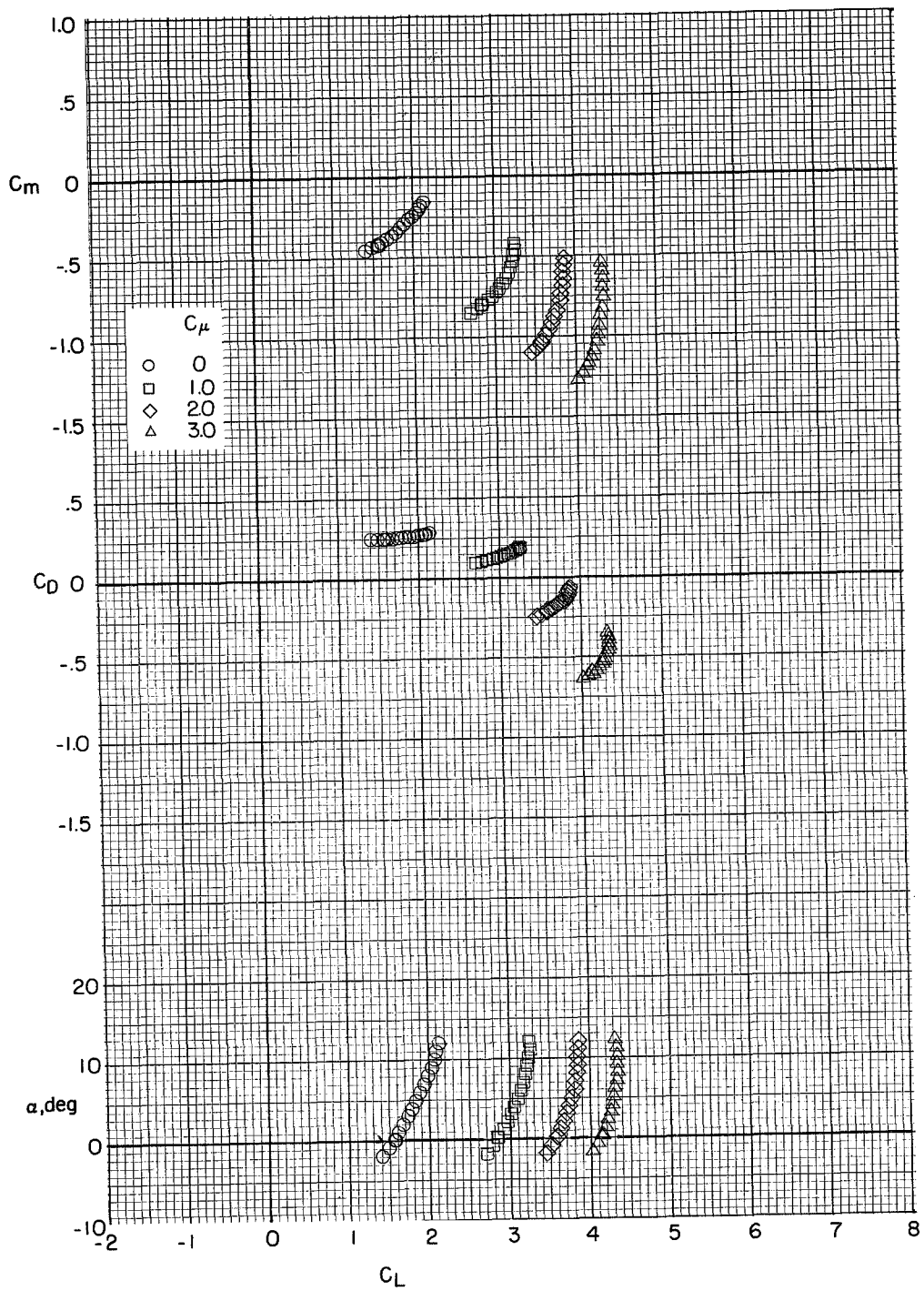

(a) Tail off.

Figure 20.- Longitudinal aerodynamic characteristics of the low-wing configuration in ground effect. h/b = 0.12; $\delta_f = 60^o, 60^o, 0^o$.

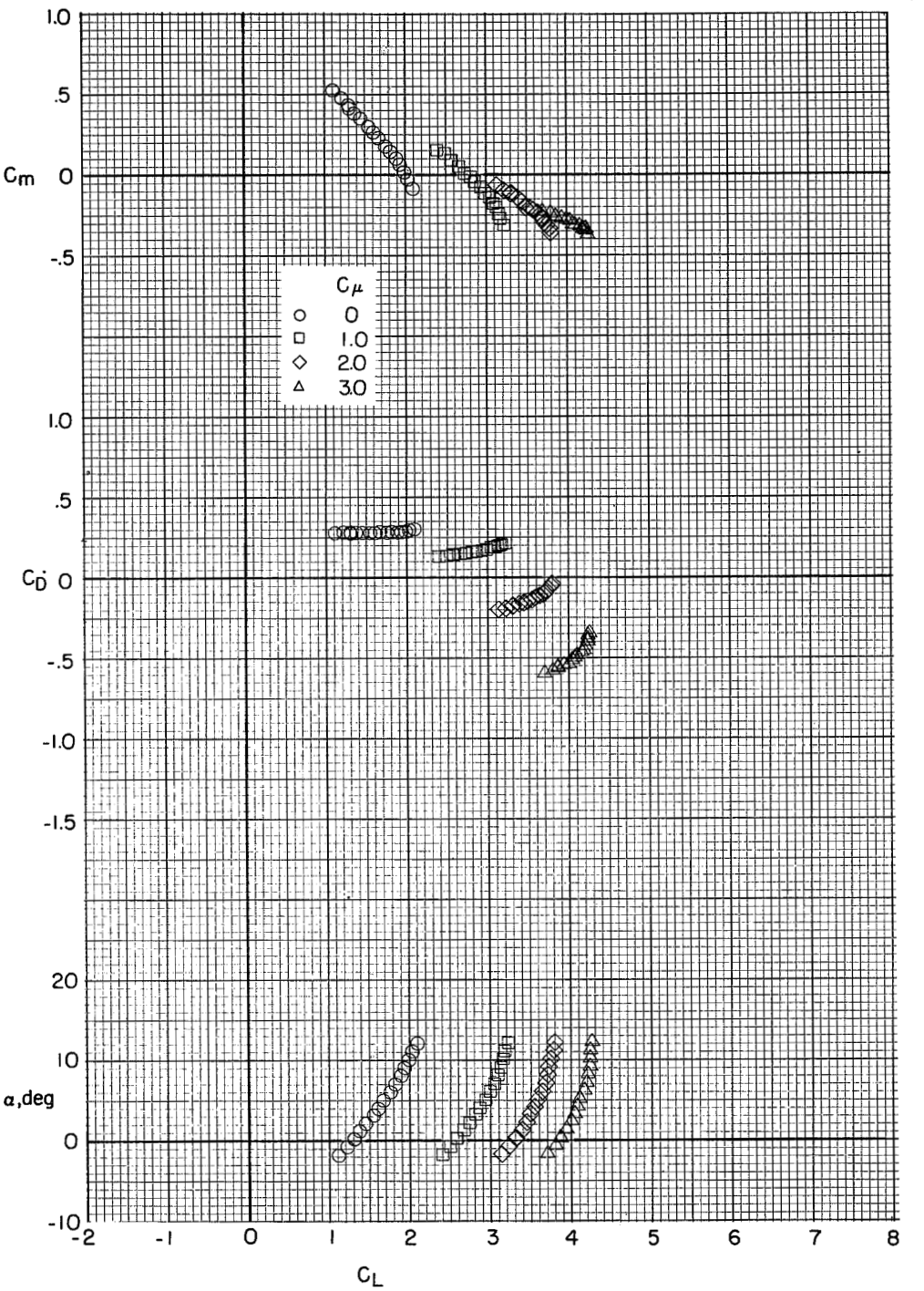

(b) Tail in high position; $i_t = -10^o$.

Figure 20.- Continued.

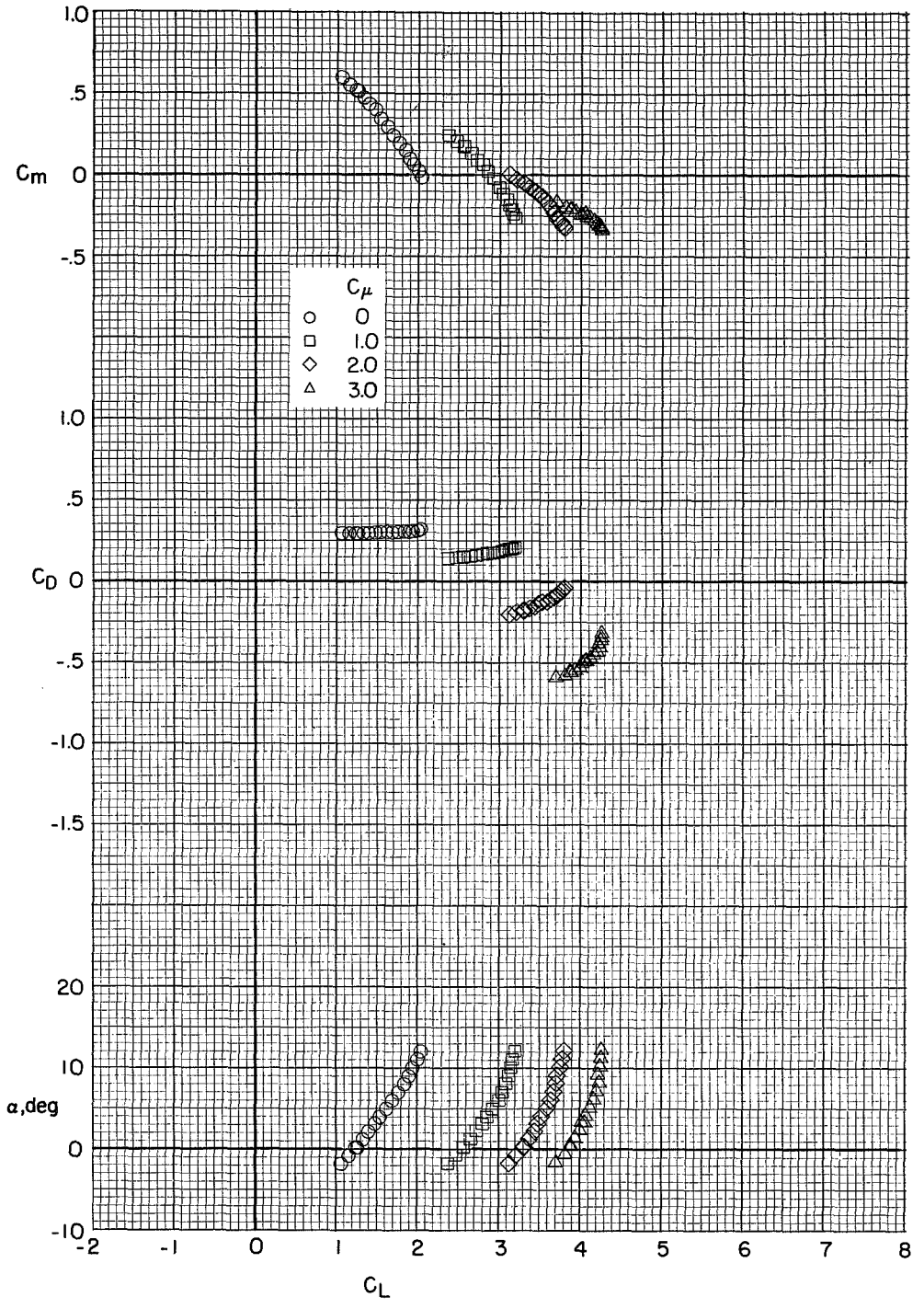

(c) Tail in mid position; $i_t = -10^o$.

Figure 20.- Concluded.

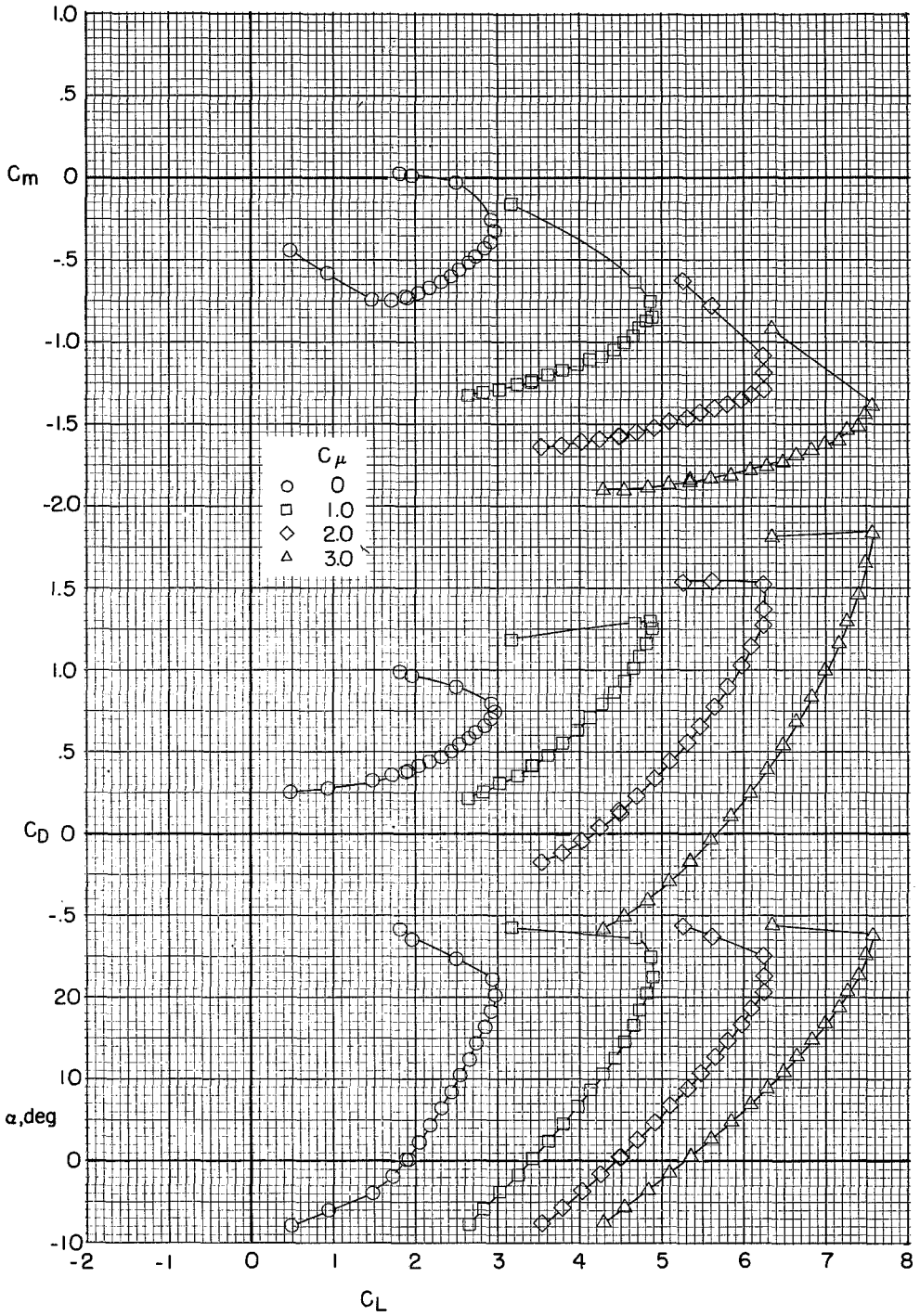

(a) Tail off.

Figure 21.- Longitudinal aerodynamic characteristics of the low-wing configuration out of ground effect. h/b = 1.24; $\delta_f = 60^o, 60^o, 60^o$.

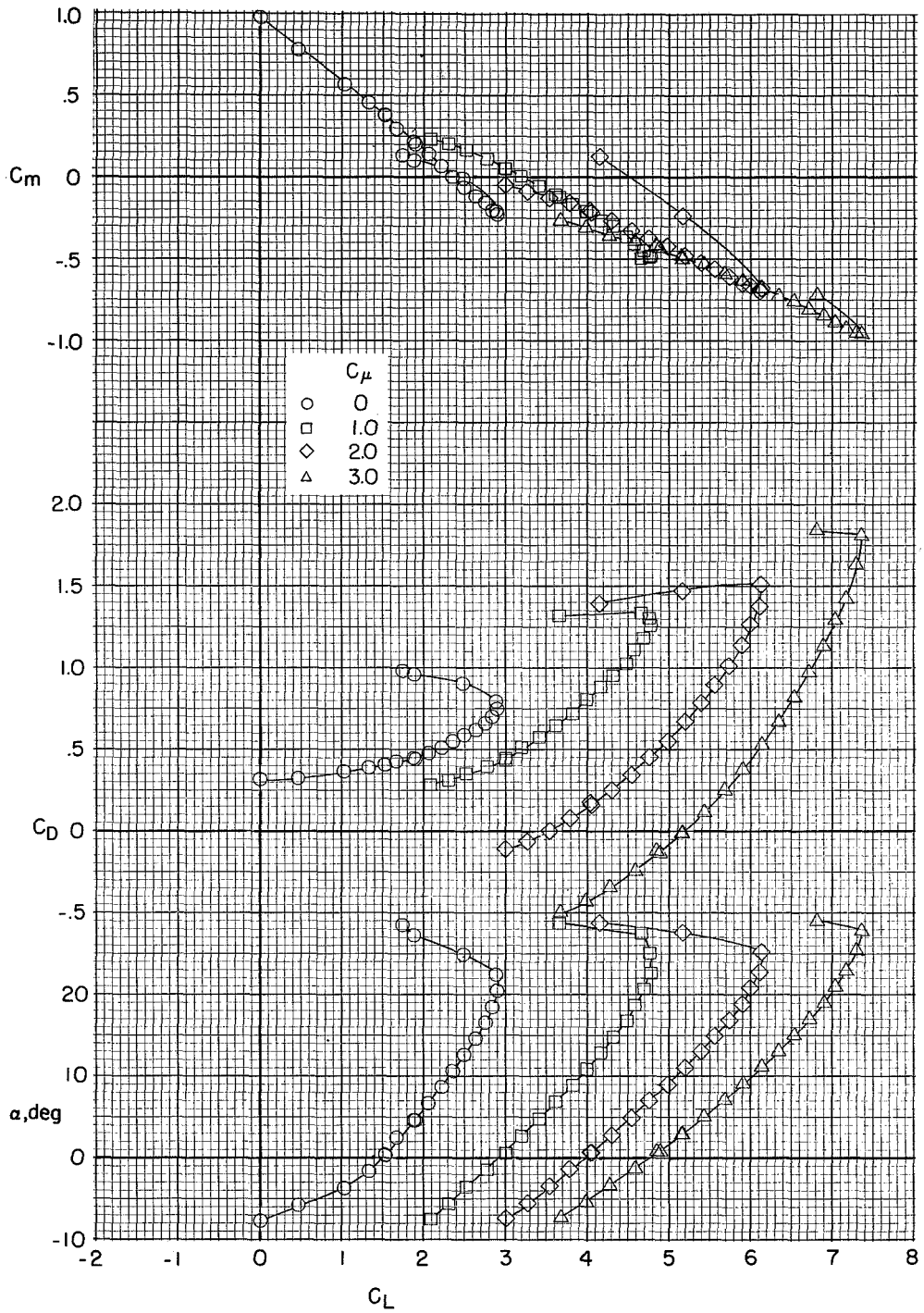

(b) Tail in mid position; $i_t = -10^o$.

Figure 21.- Concluded.

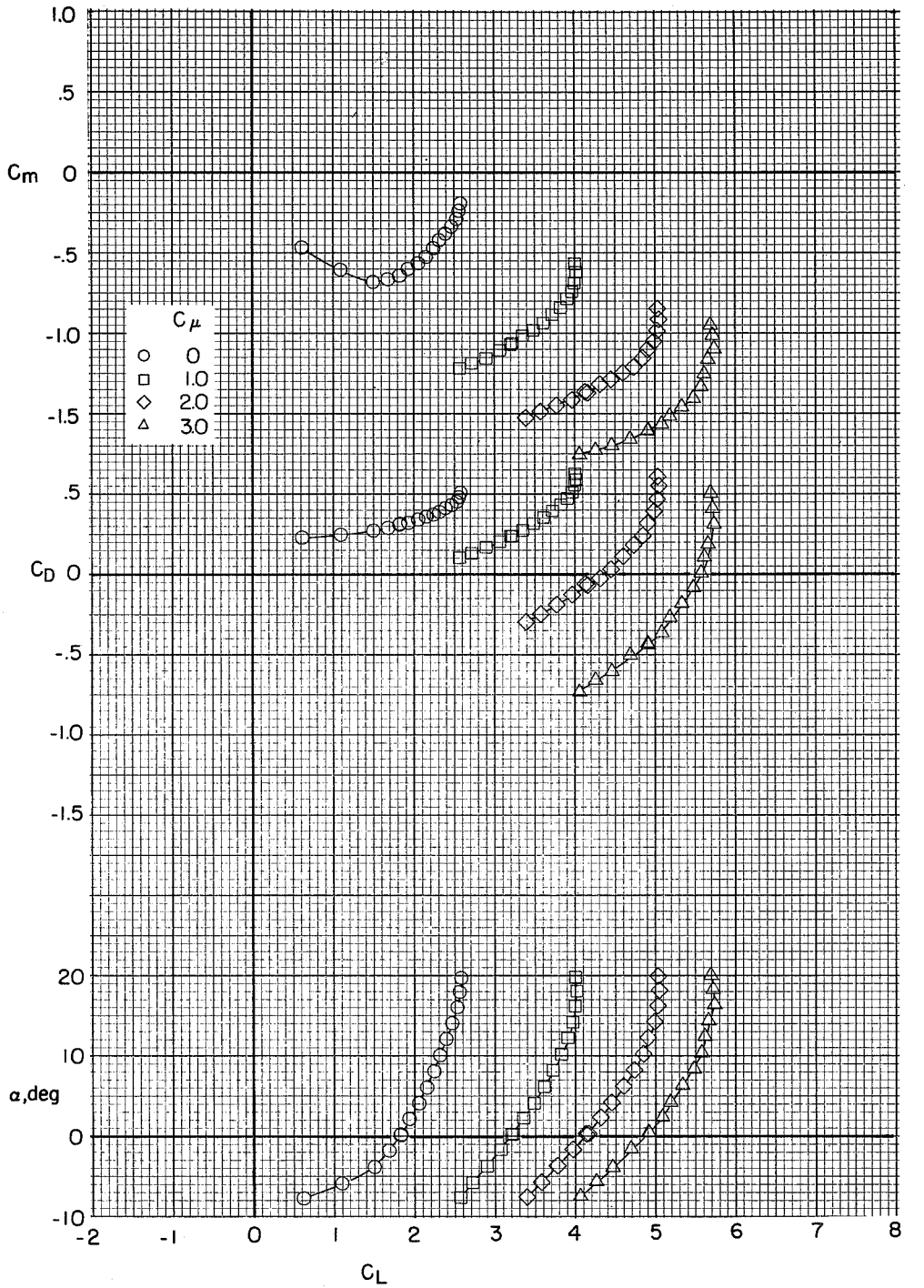

(a) Tail off.

Figure 22.- Longitudinal aerodynamic characteristics of the low-wing configuration in ground effect. h/b = 0.19; $\delta_f = 60^o, 60^o, 60^o$.

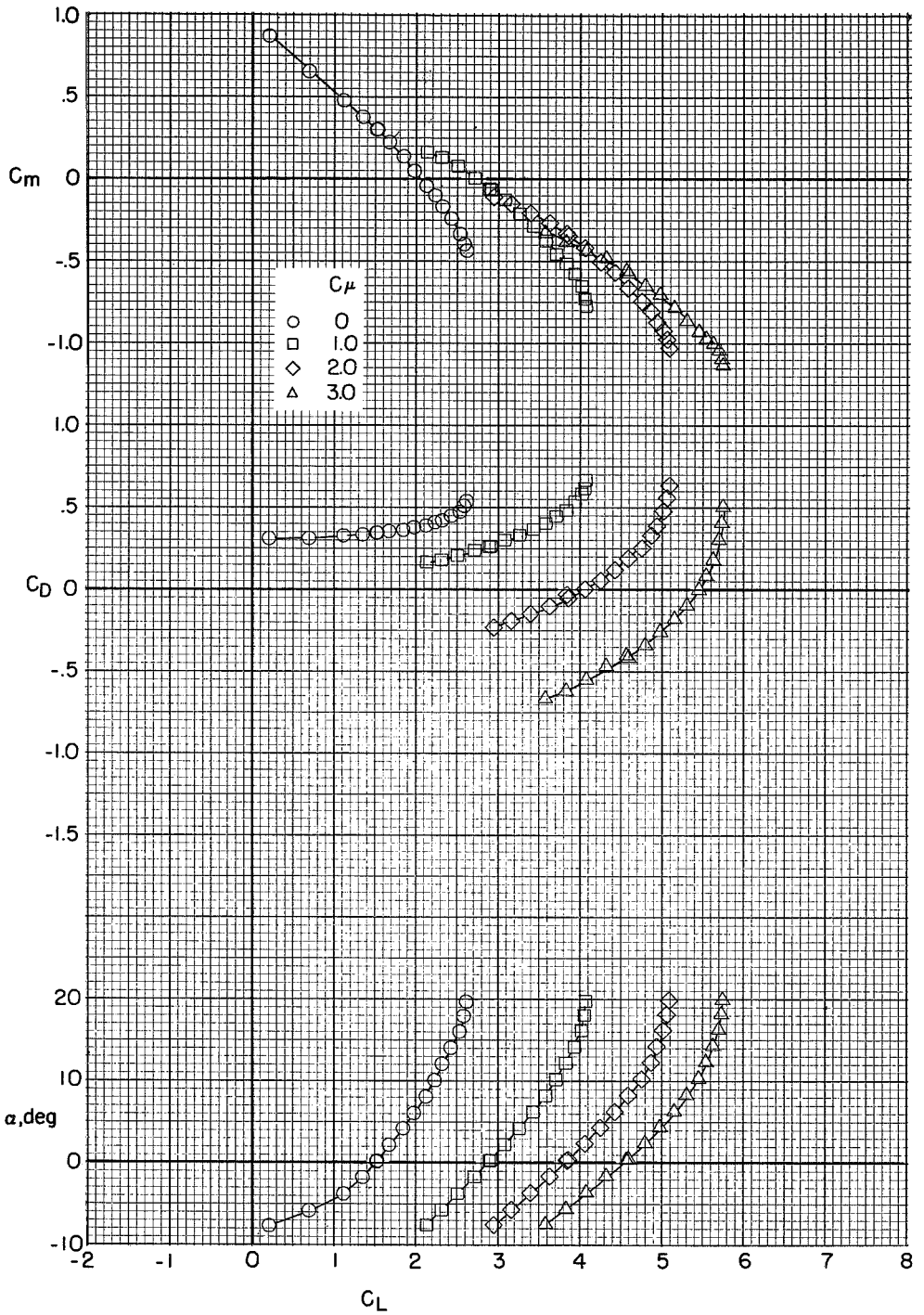

(b) Tail in mid position; $i_t = -10^o$.

Figure 22.- Concluded.

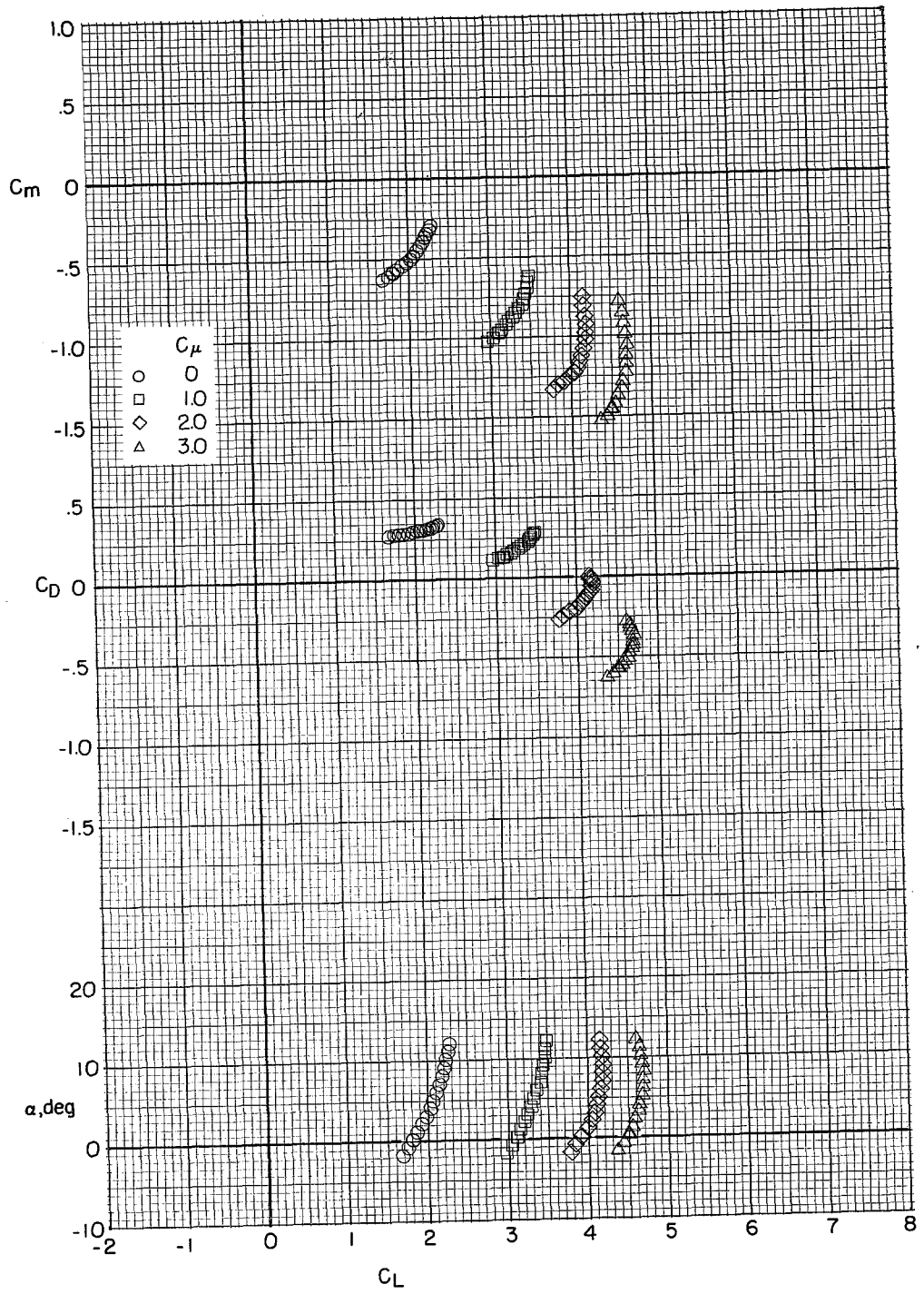

(a) Tail off.

Figure 23.- Longitudinal aerodynamic characteristics of the low-wing configuration in ground effect. h/b = 0.12; $\delta_f = 60^o, 60^o, 60^o$.

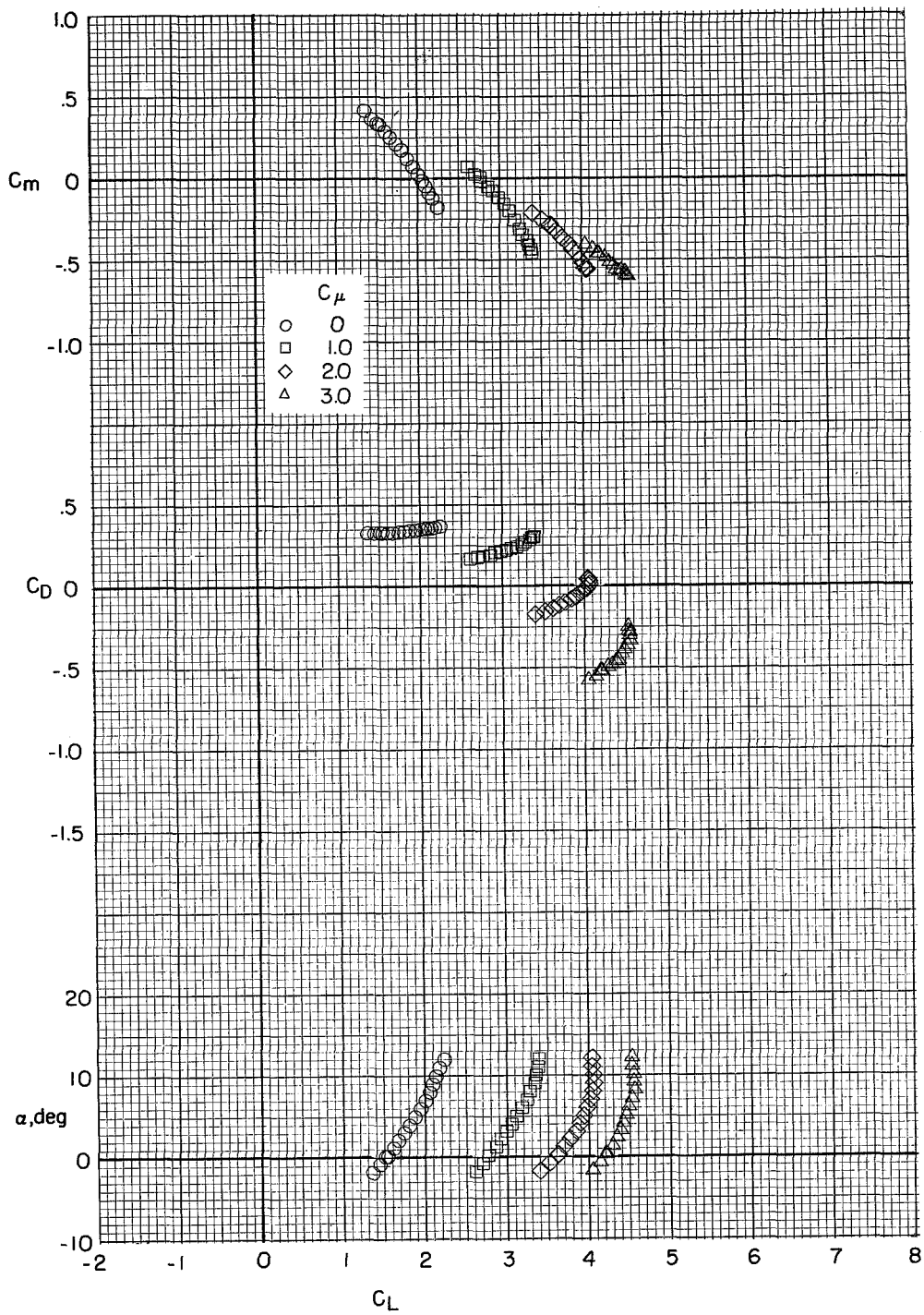

(b) Tail in mid position; $i_t = -10^o$.

Figure 23.- Concluded.

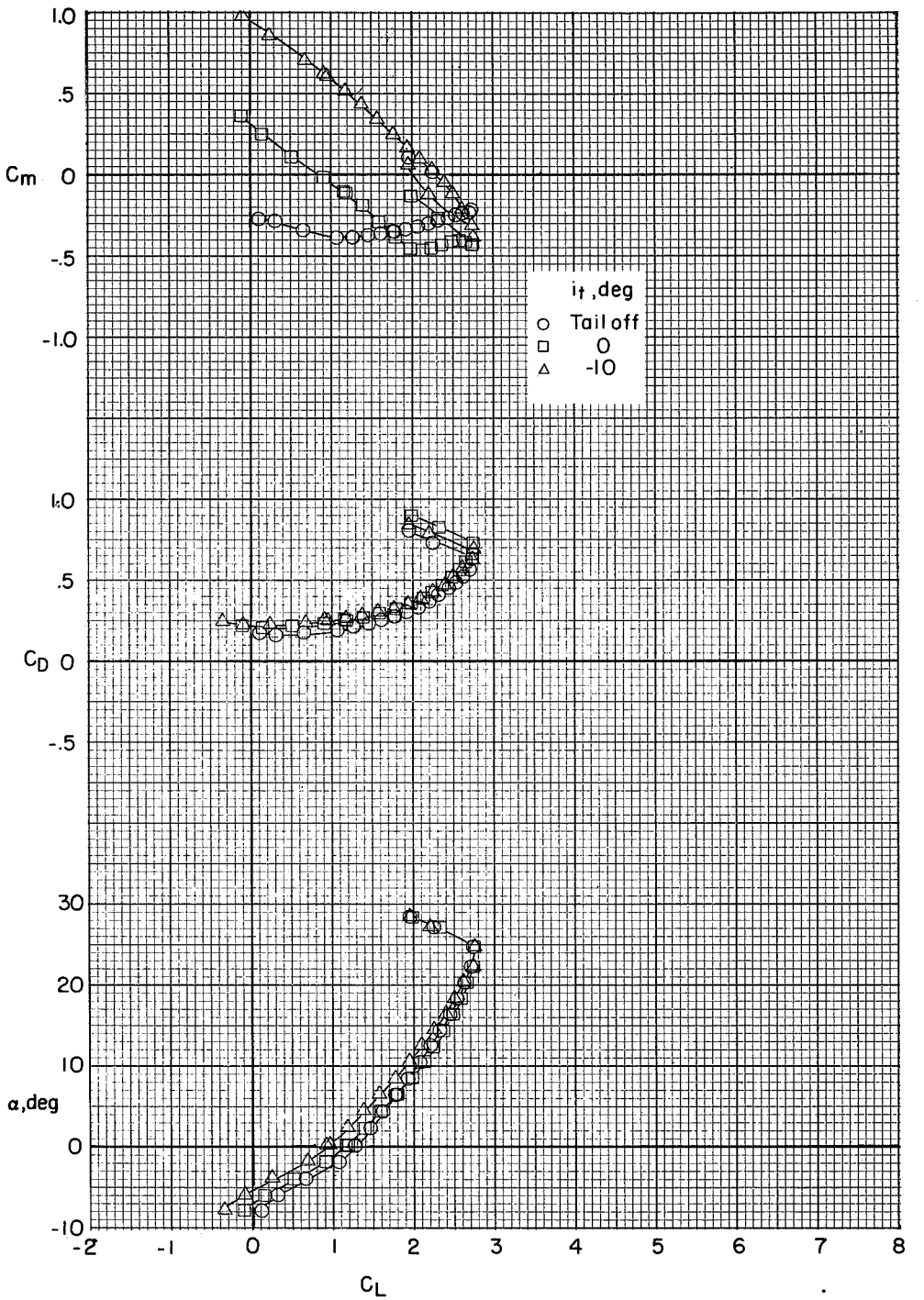

(a) $C_\mu = 0$.

Figure 24.- Effect of high horizontal tail incidence on the longitudinal aerodynamic characteristics of the high-wing configuration out of ground effect. h/b = 1.24; $\delta_f = 30^o, 60^o, 0^o$.

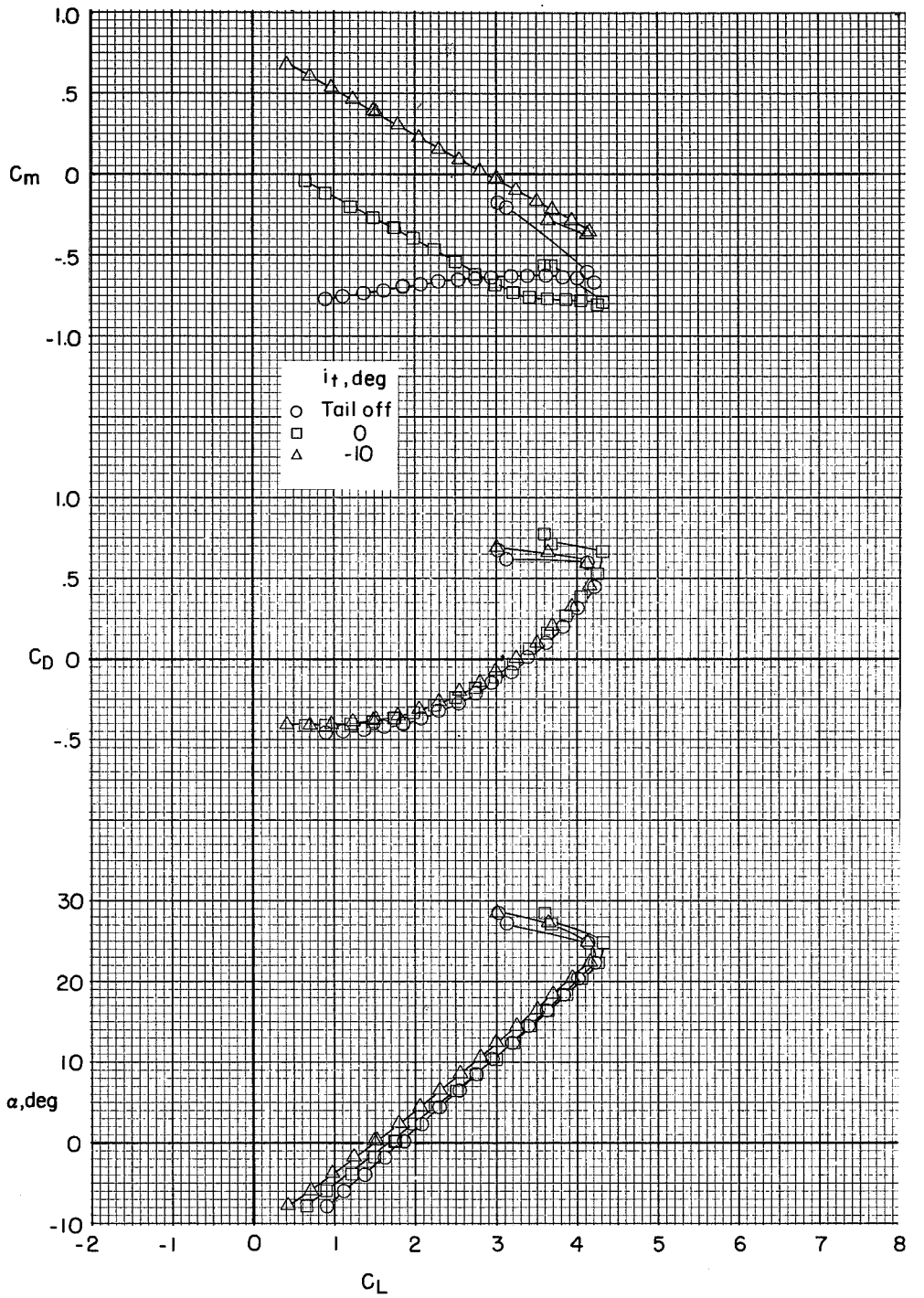

(b) $C_\mu = 1.0$.

Figure 24.- Continued.

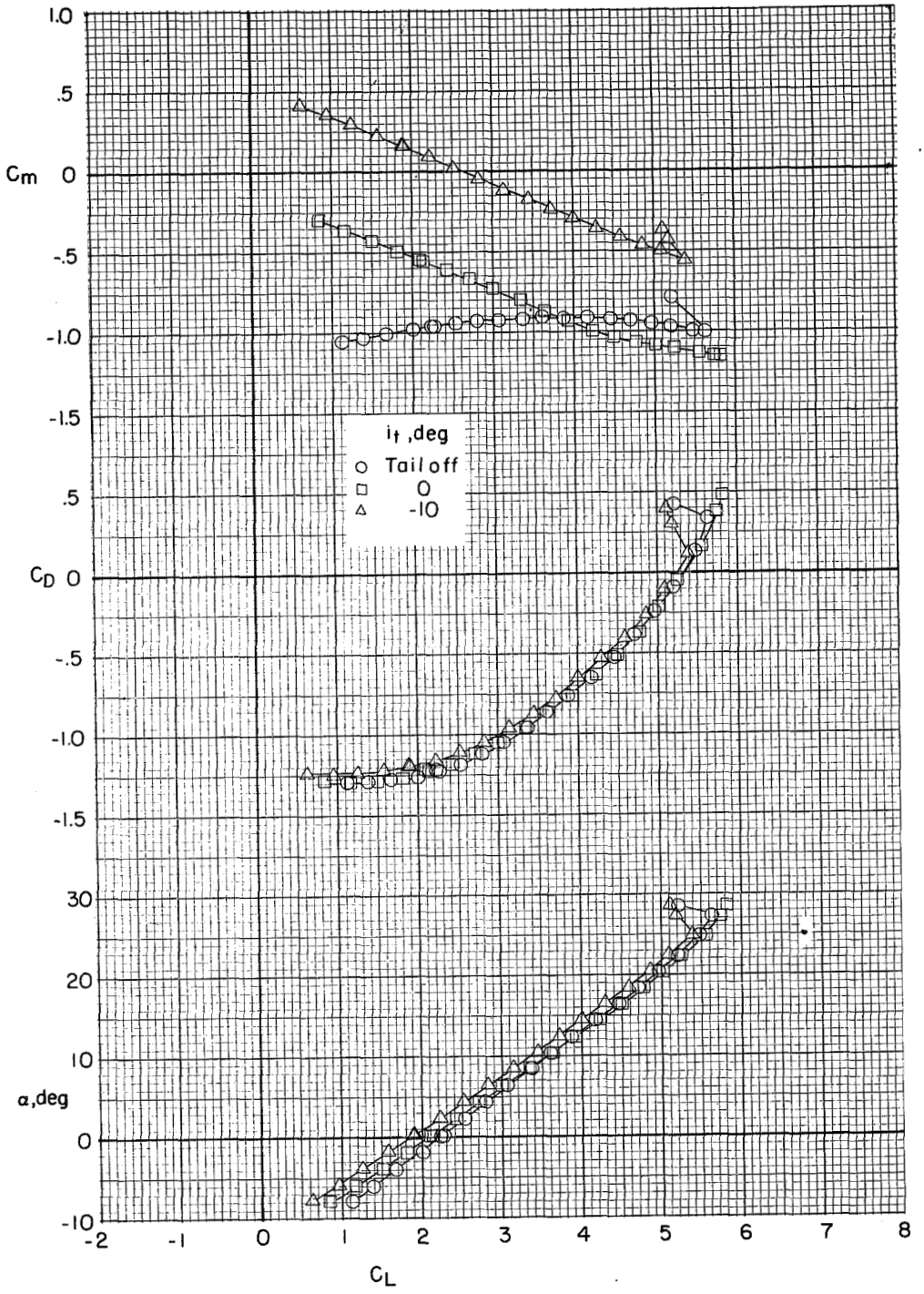

(c) $C_{\mu} = 2.0$.

Figure 24.- Continued.

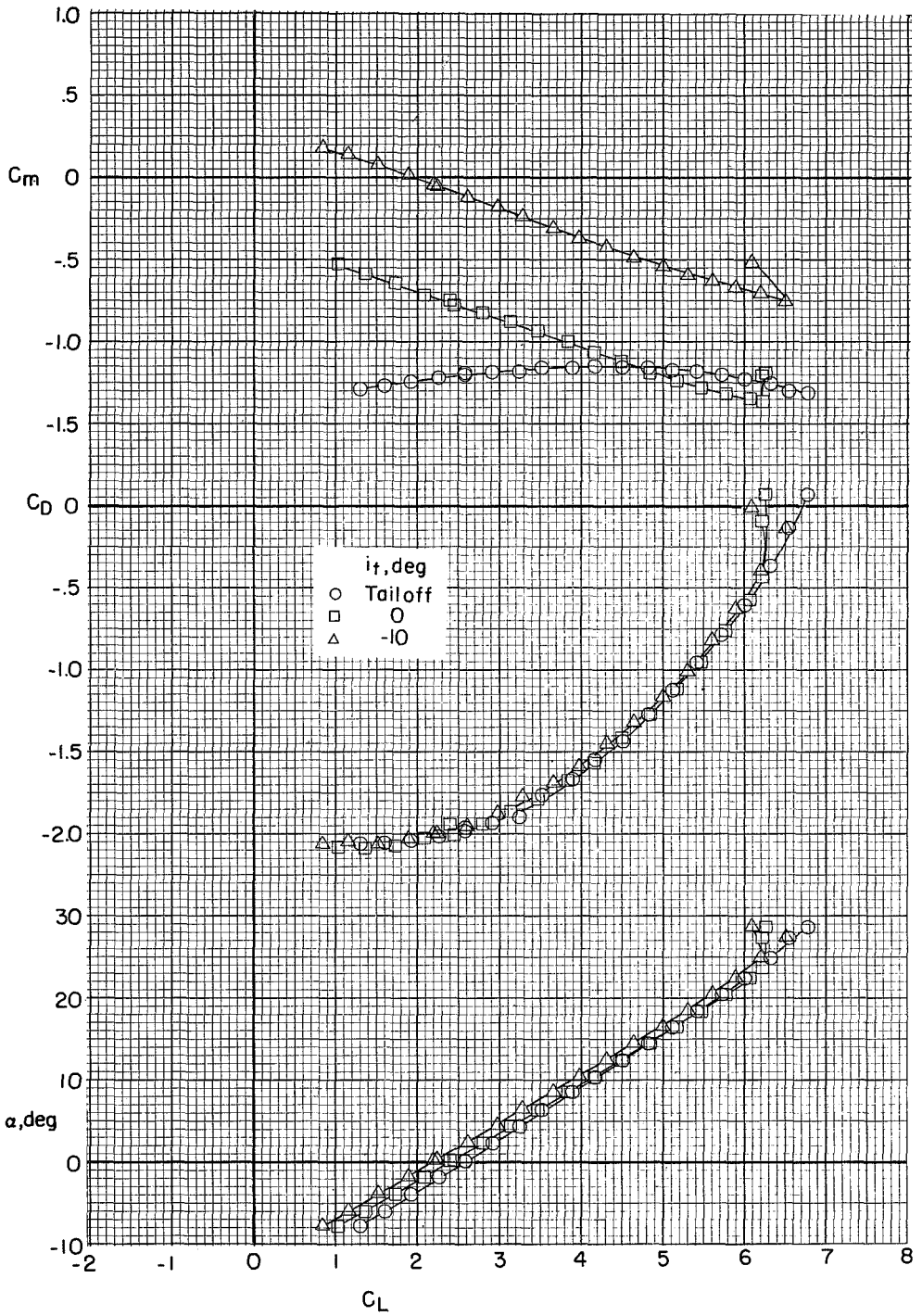

(d) $C_{\mu} = 3.0$.

Figure 24.- Concluded.

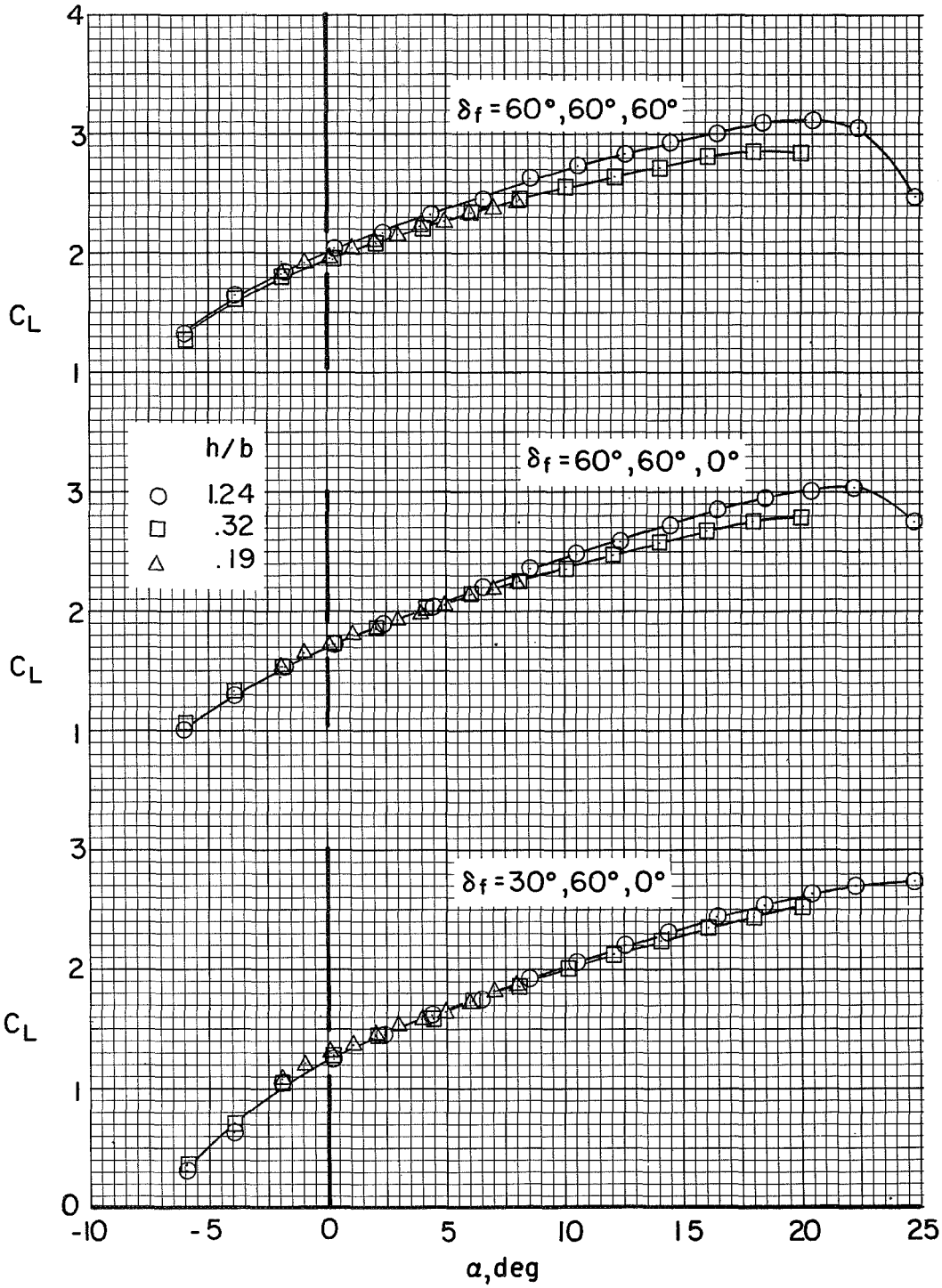

(a) $C_\mu = 0$.

Figure 25.- Effect of ground proximity on the lift characteristics of the high-wing configuration with tail off.

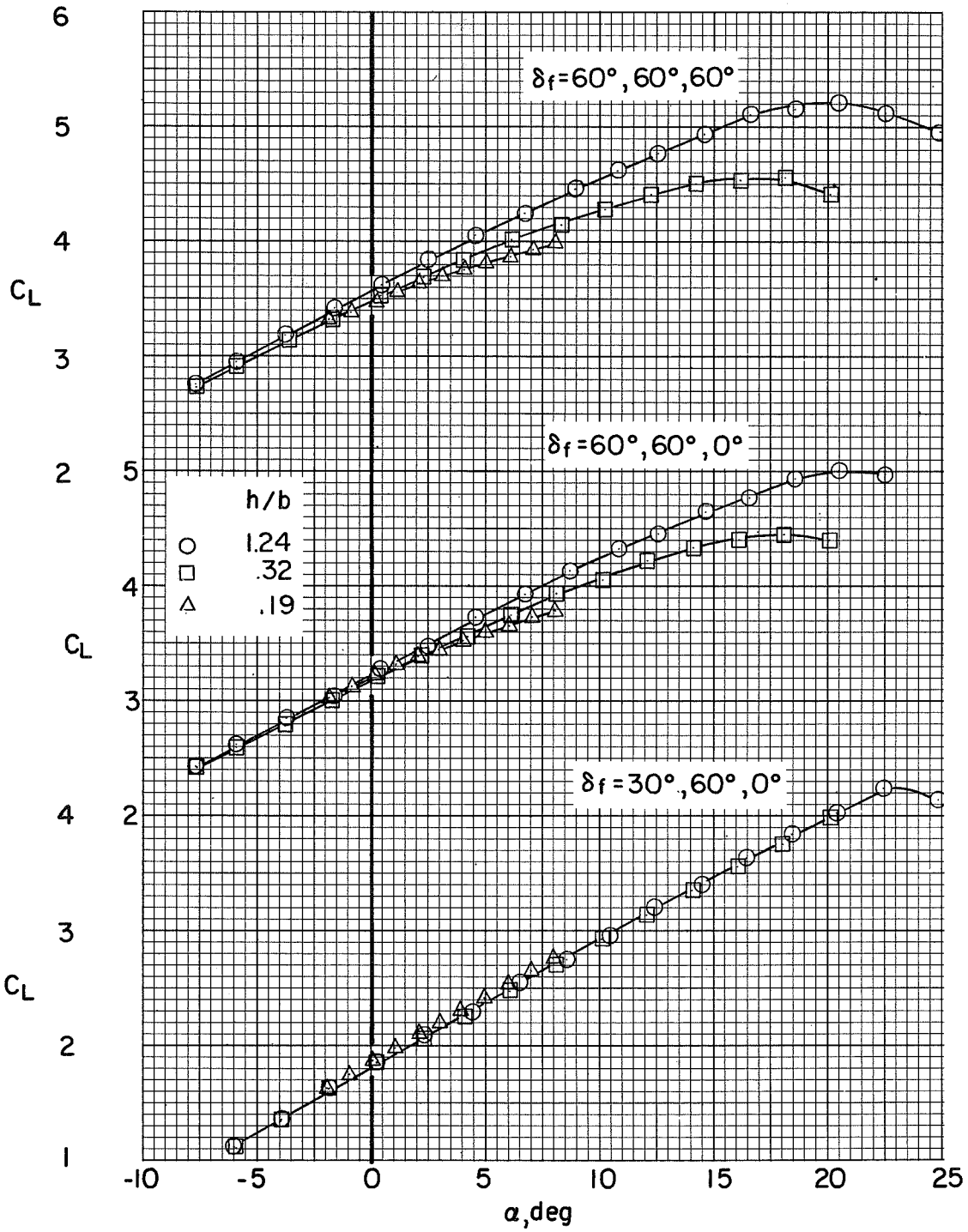

(b) $C_\mu = 1.0$.

Figure 25.- Continued.

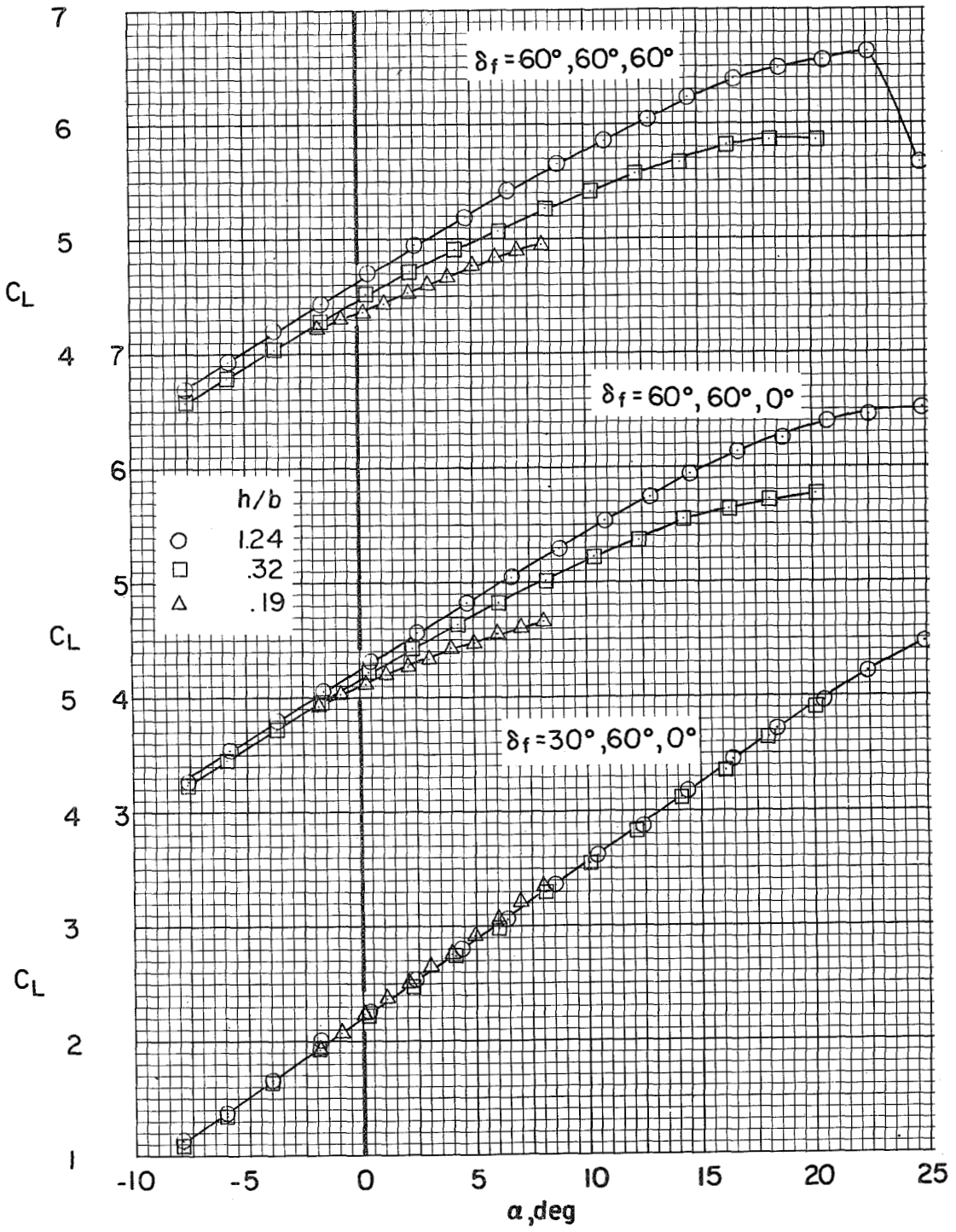

(c) $C_\mu = 2.0$.

Figure 25.- Continued.

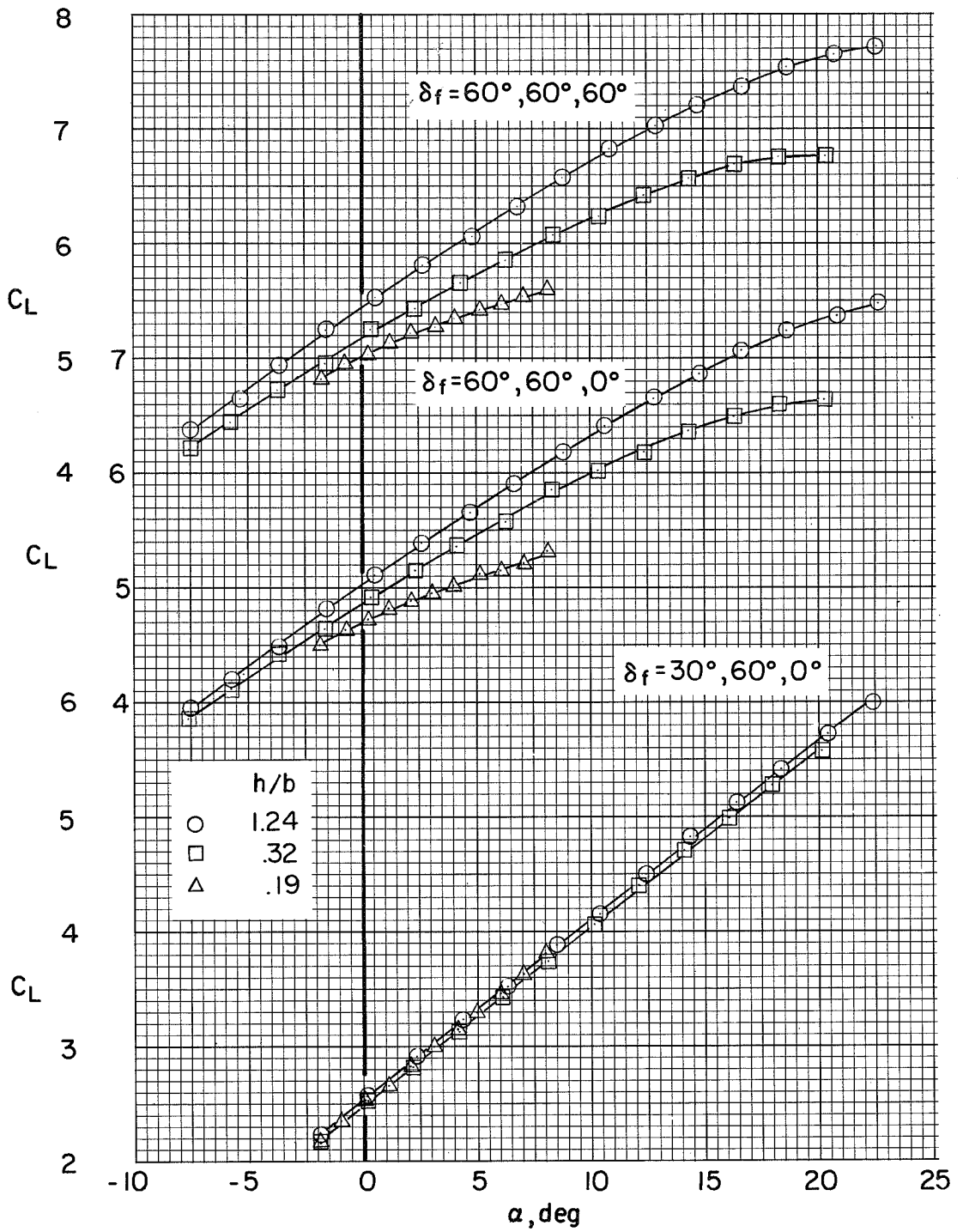

(d) $C_\mu = 3.0$.

Figure 25.- Concluded.

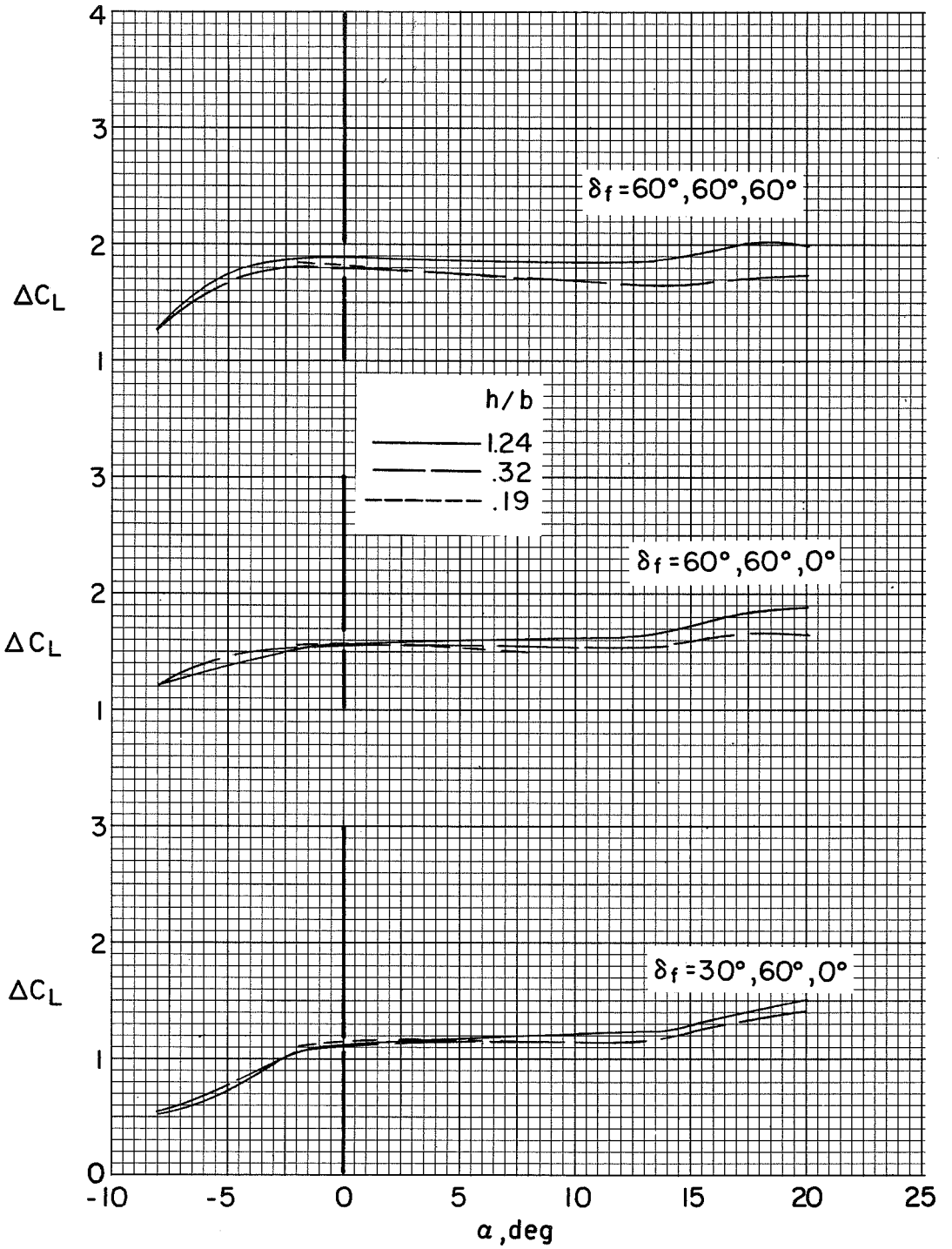

(a) $C_\mu = 0$.

Figure 26.- Incremental lift coefficients produced by flap deflection with the model in and out of ground effect. High wing; tail off.

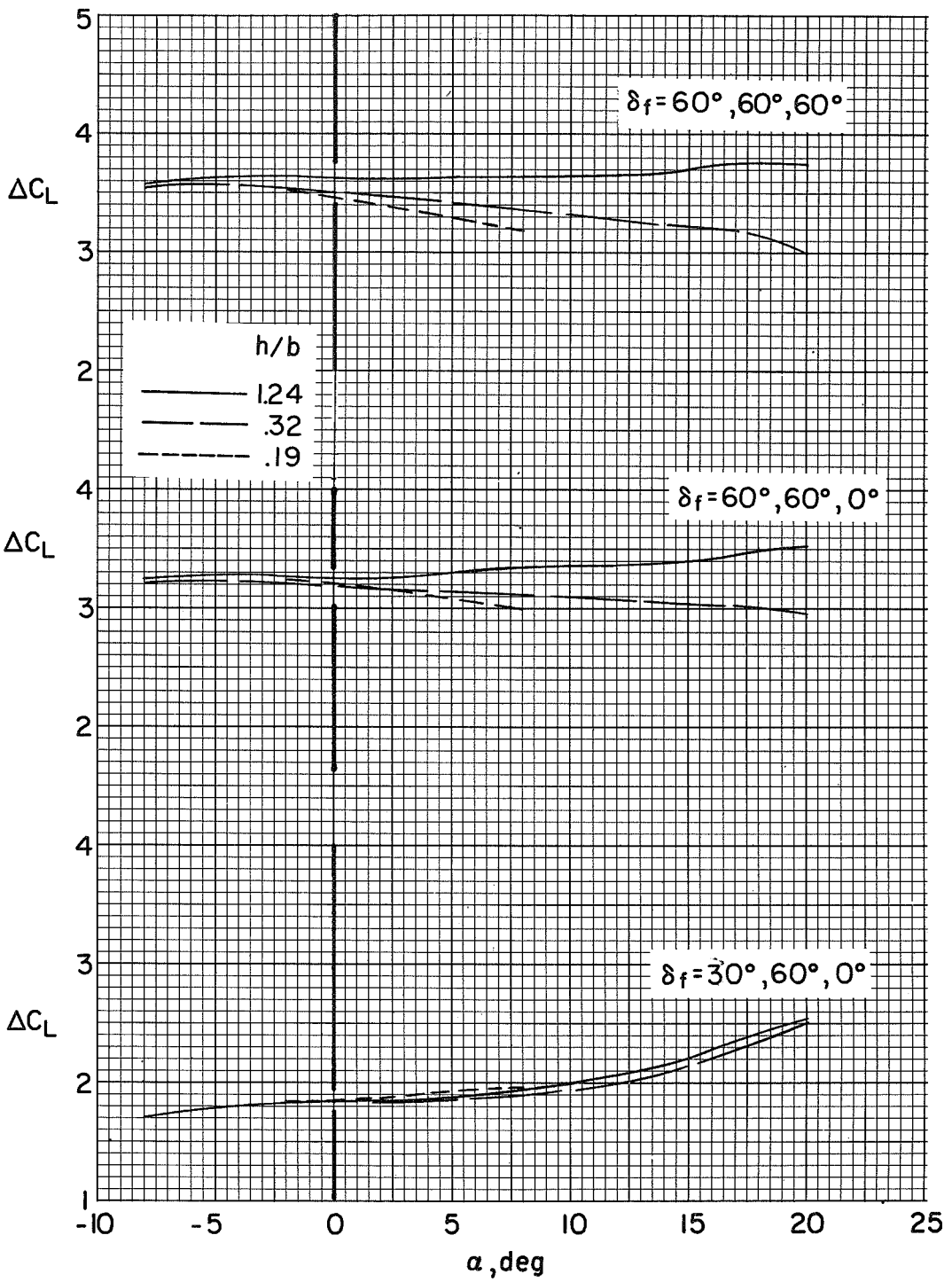

(b) C_μ = 1.0.

Figure 26.- Continued.

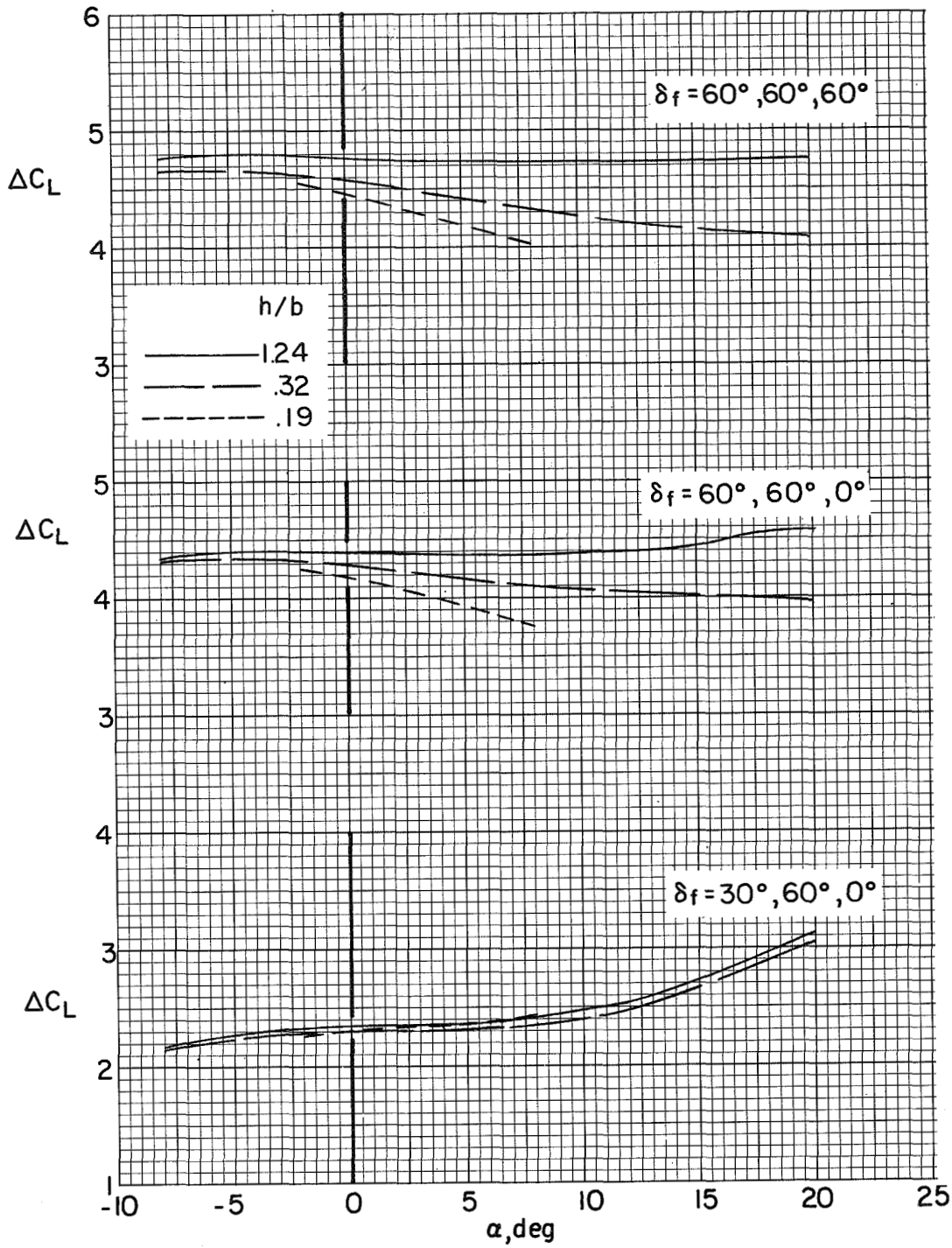

(c) $C_\mu = 2.0$.

Figure 26.- Continued.

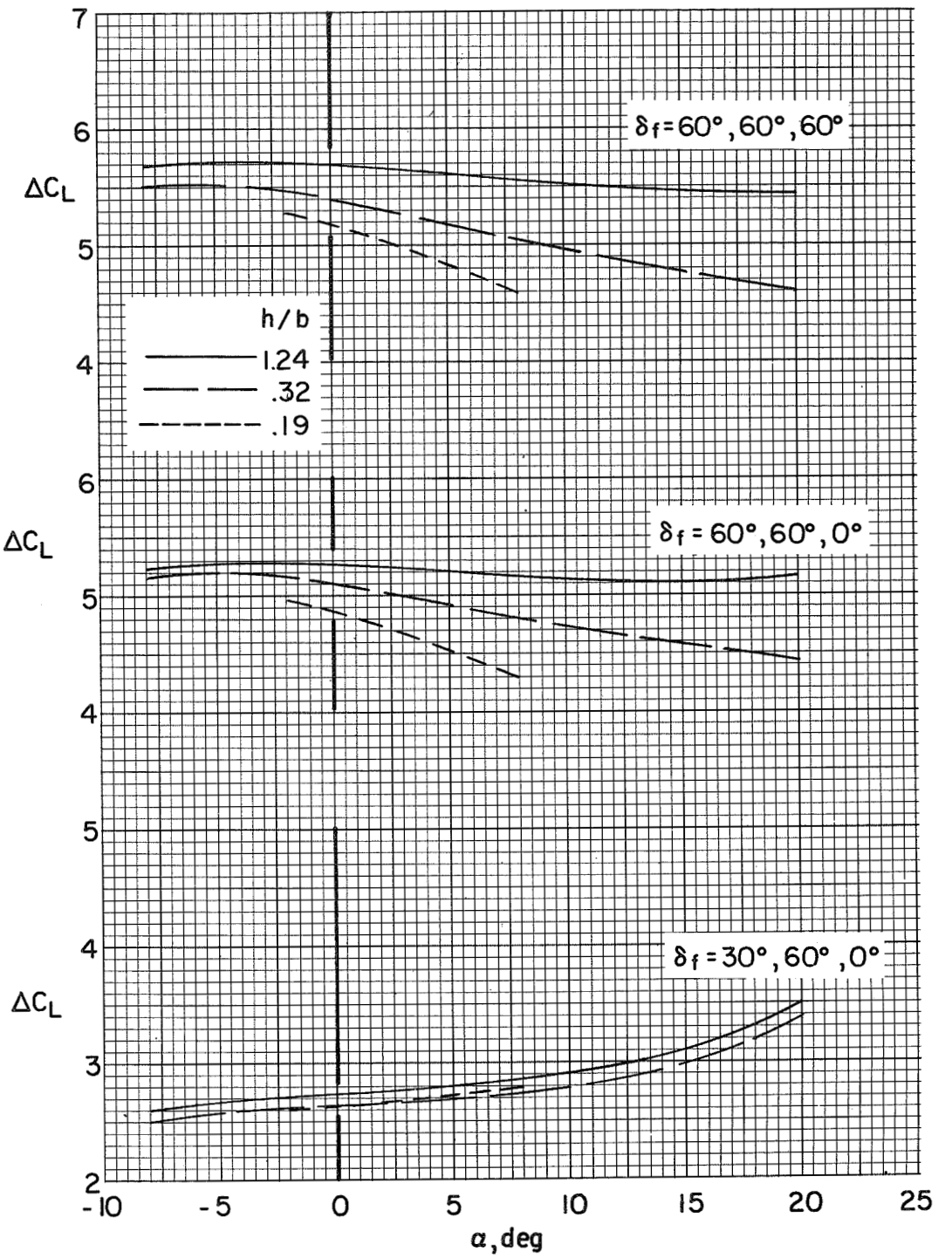

(d) C_μ = 3.0.

Figure 26.- Concluded.

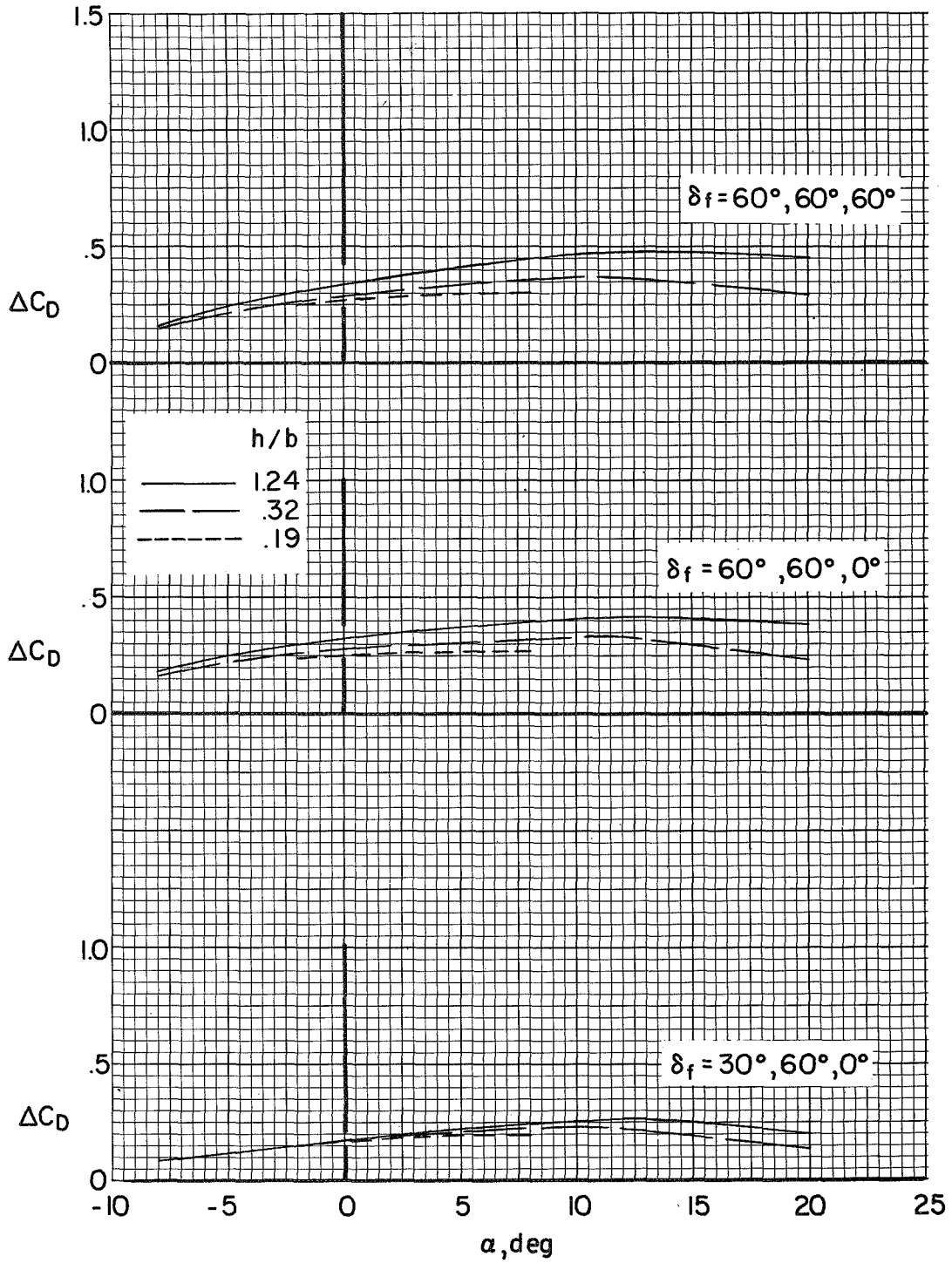

(a) $C_\mu = 0.$

Figure 27.- Incremental drag coefficient produced by flap deflection in and out of ground effect. High wing; tail off.

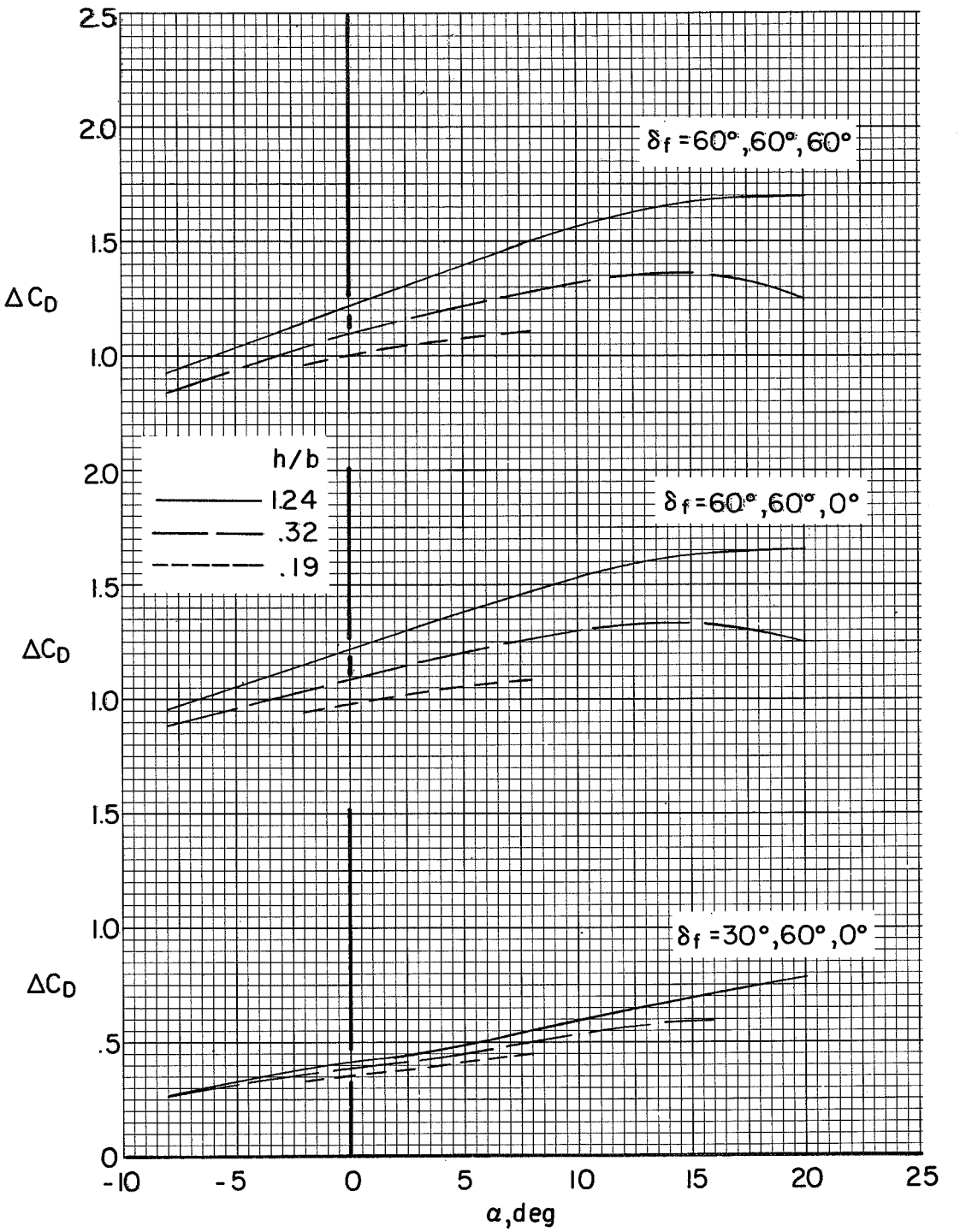

(b) $C_\mu = 1.0$.

Figure 27.- Continued.

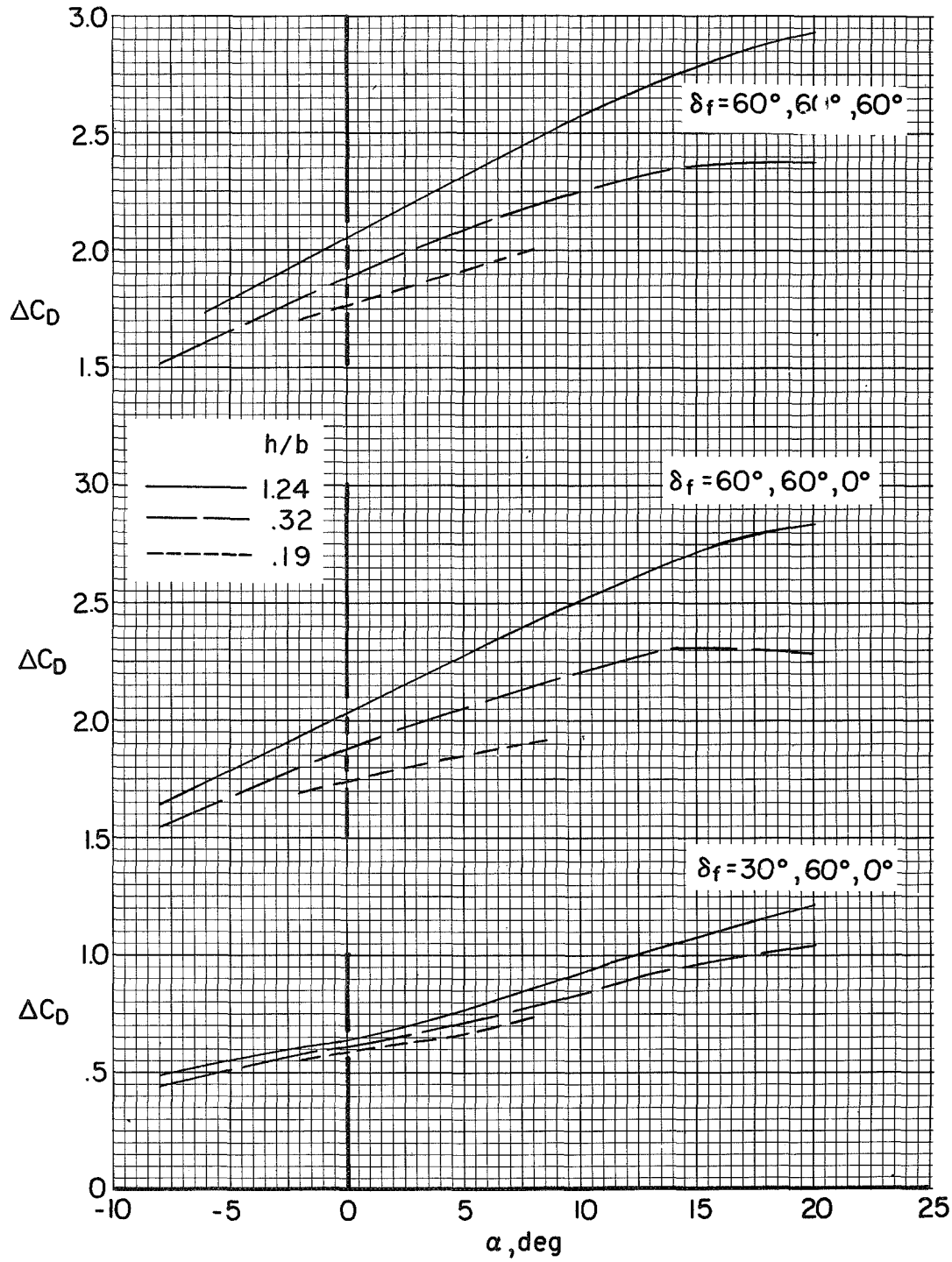

(c) $C_\mu = 2.0$.

Figure 27.- Continued.

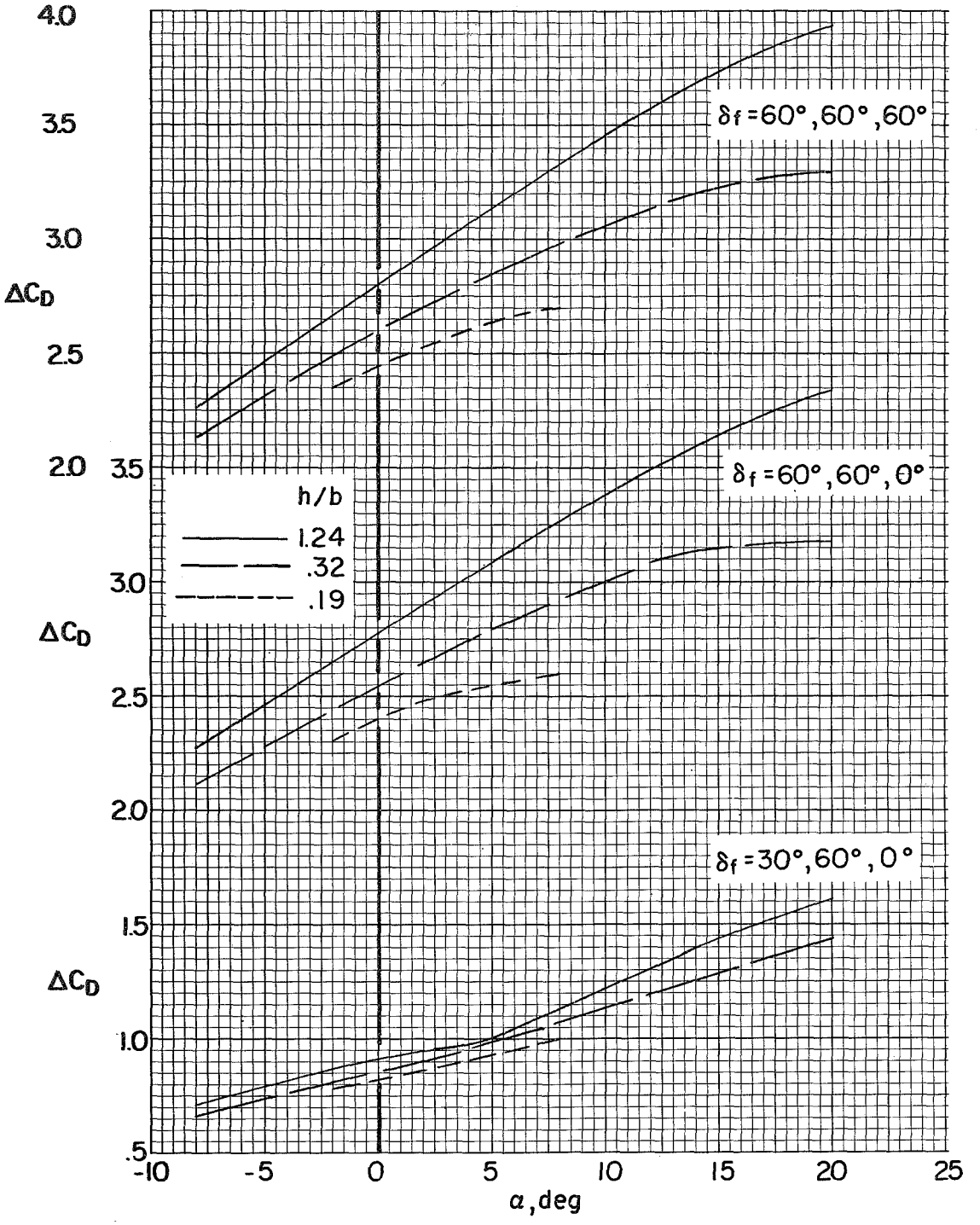

(d) C_μ = 3.0.

Figure 27.- Concluded.

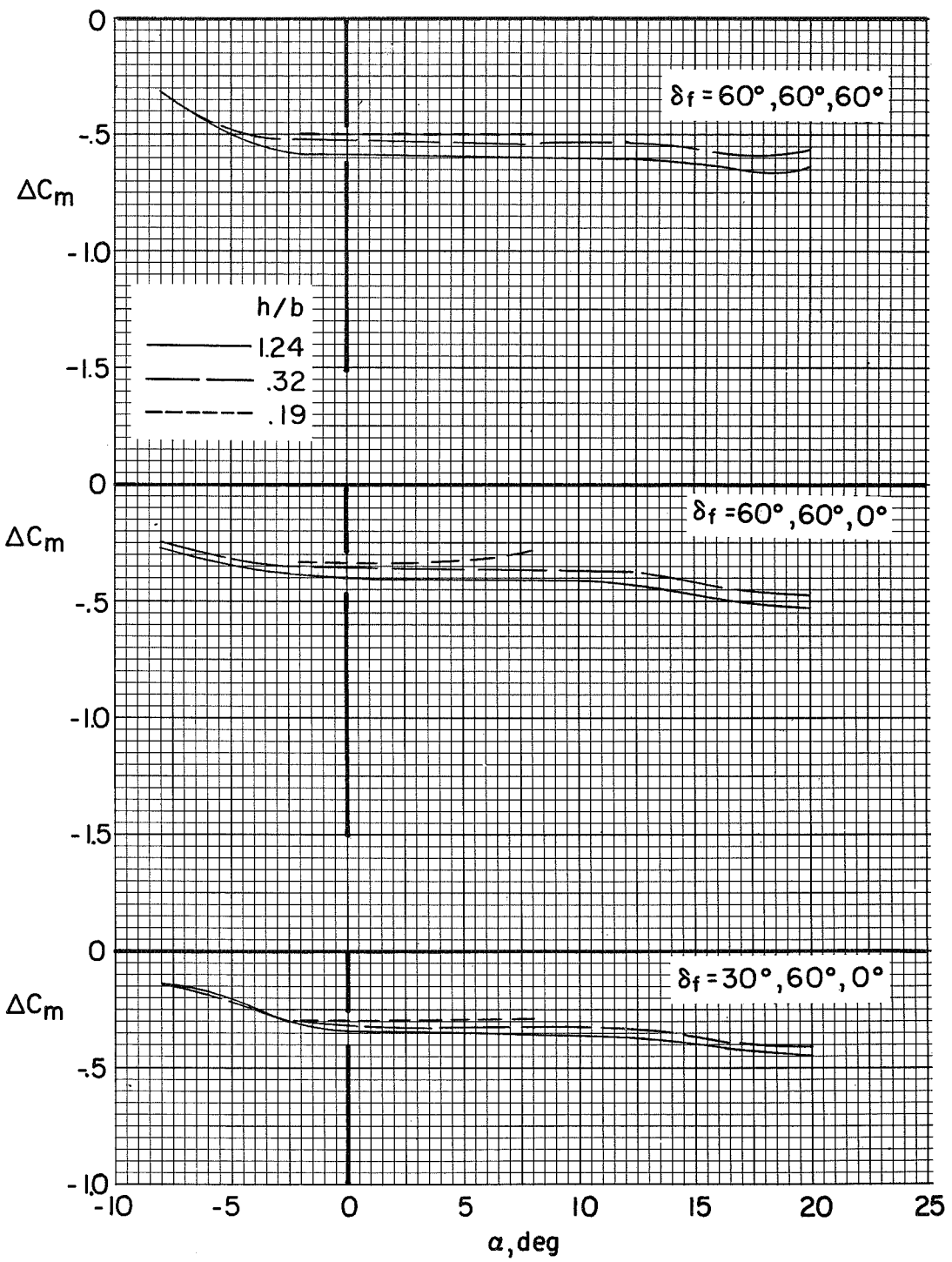

(a) $C_\mu = 0$.

Figure 28.- Incremental pitching-moment coefficients produced by flap deflection in and out of ground effect. High wing; tail off.

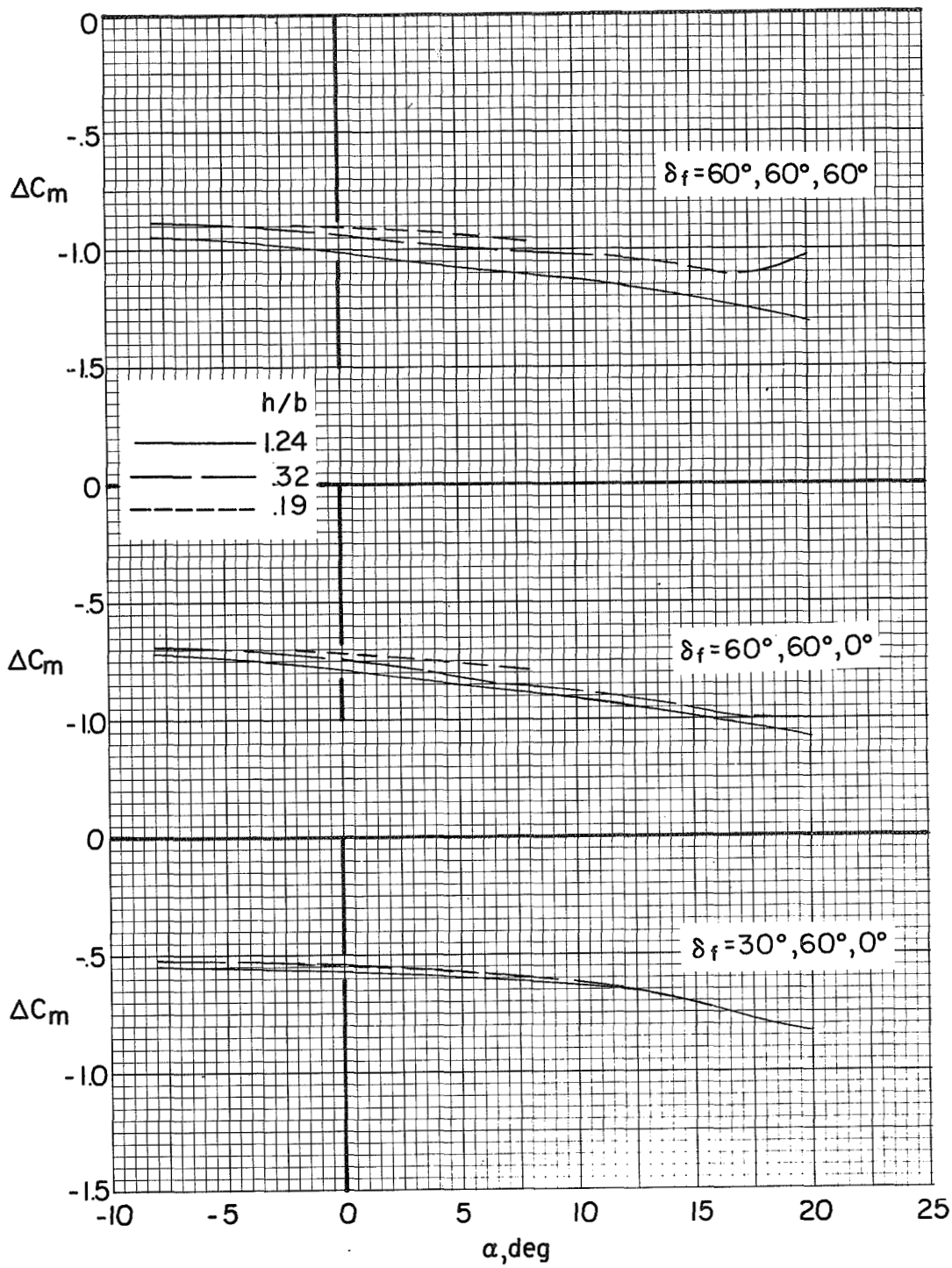

(b) $C_\mu = 1.0$.

Figure 28.- Continued.

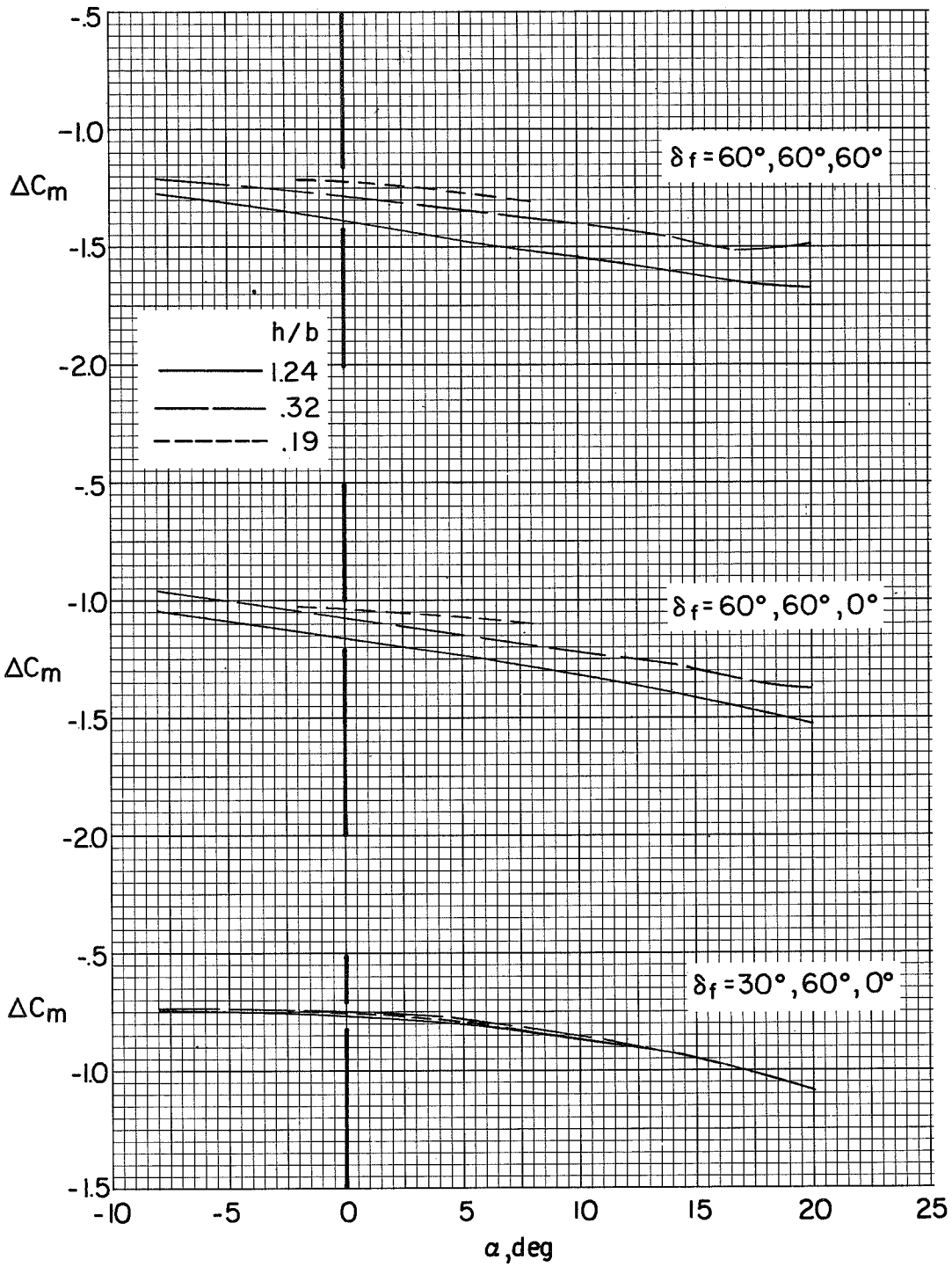

(c) $C_\mu = 2.0$.

Figure 28.- Continued.

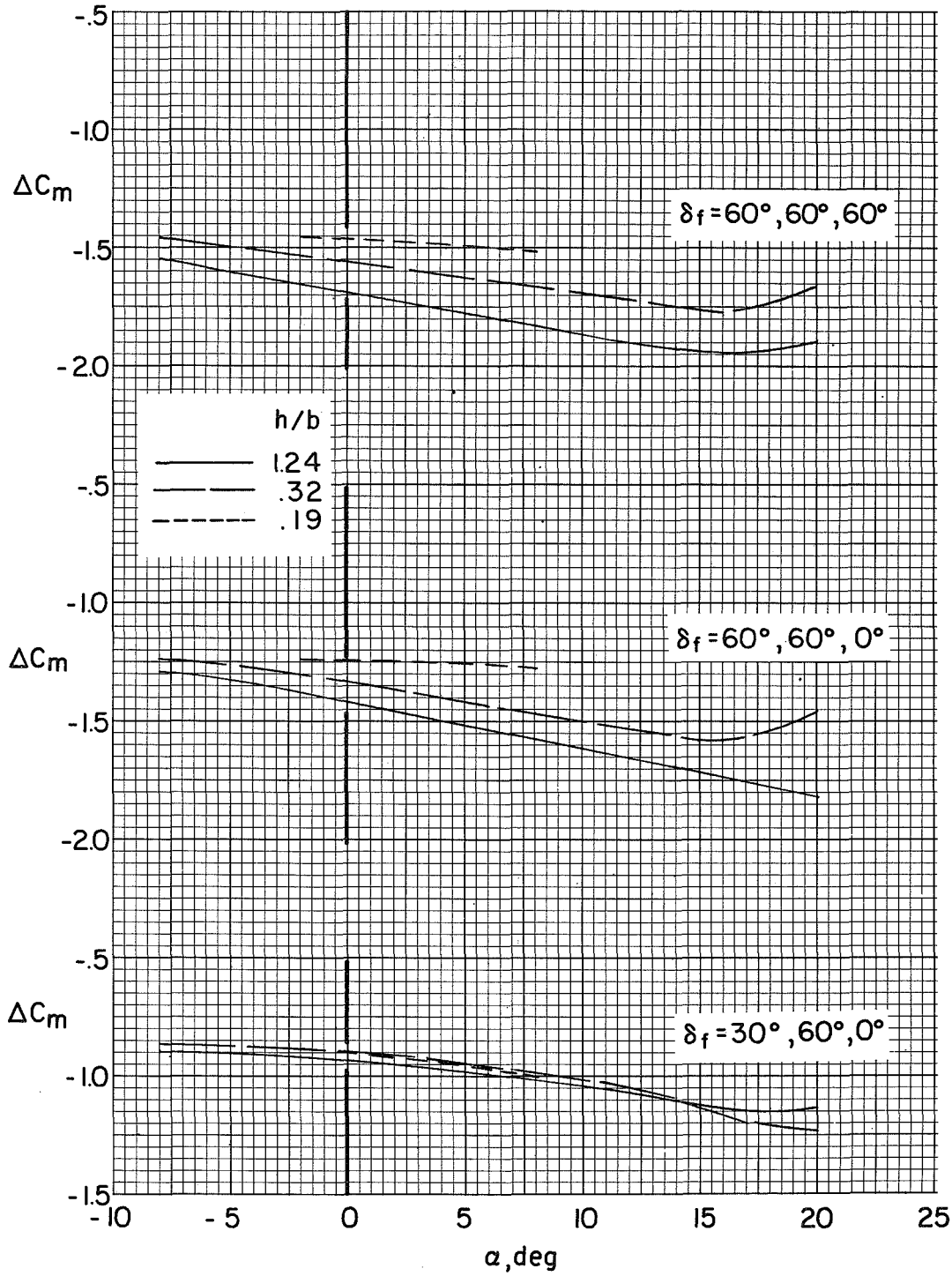

(d) $C_{\mu} = 3.0$.

Figure 28.- Concluded.

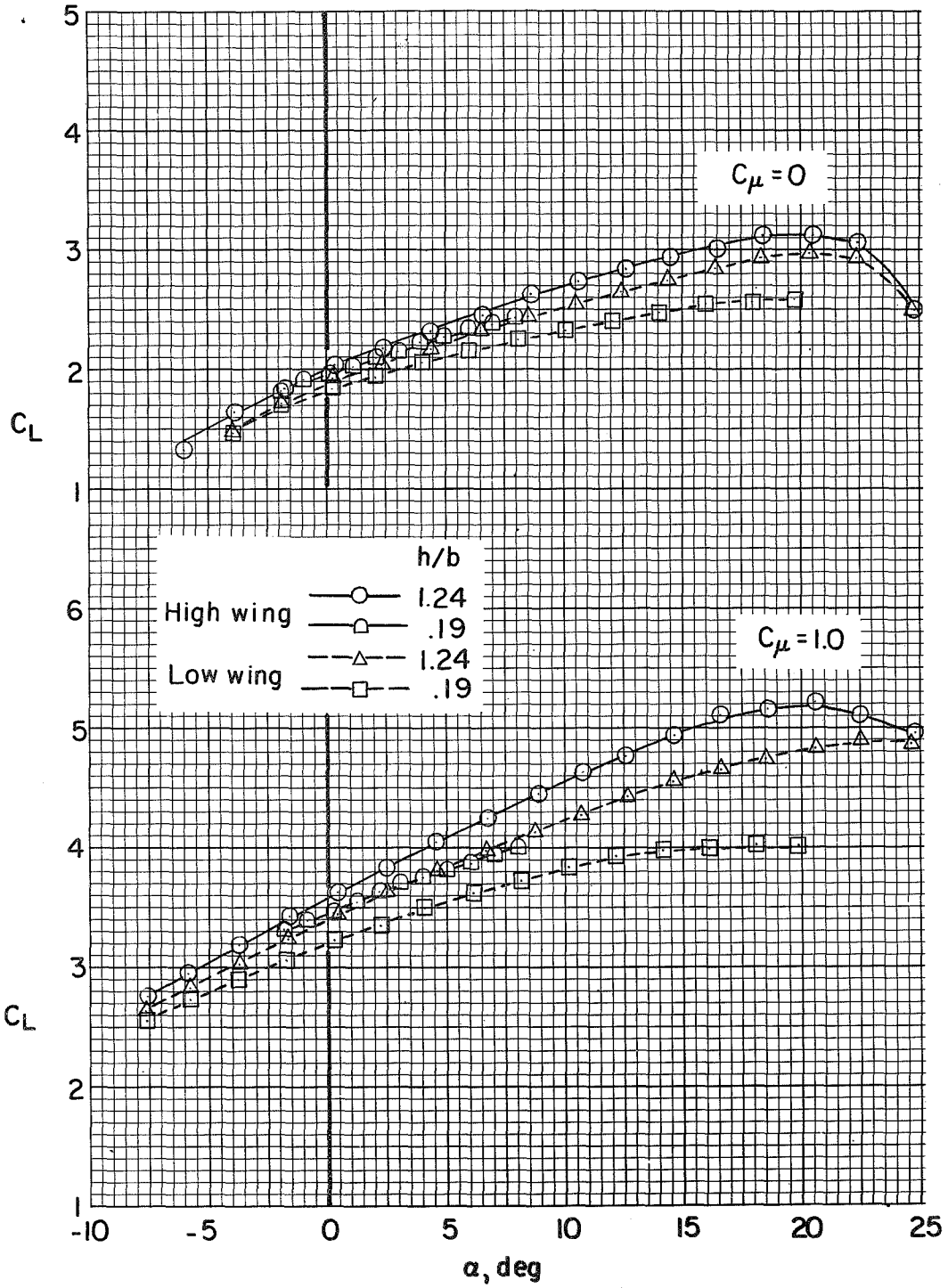

Figure 29.- Comparison of the lift characteristics of the high-wing and the low-wing configurations in and out of ground effect. Tail off; $\delta_f = 60^o, 60^o, 60^o$.

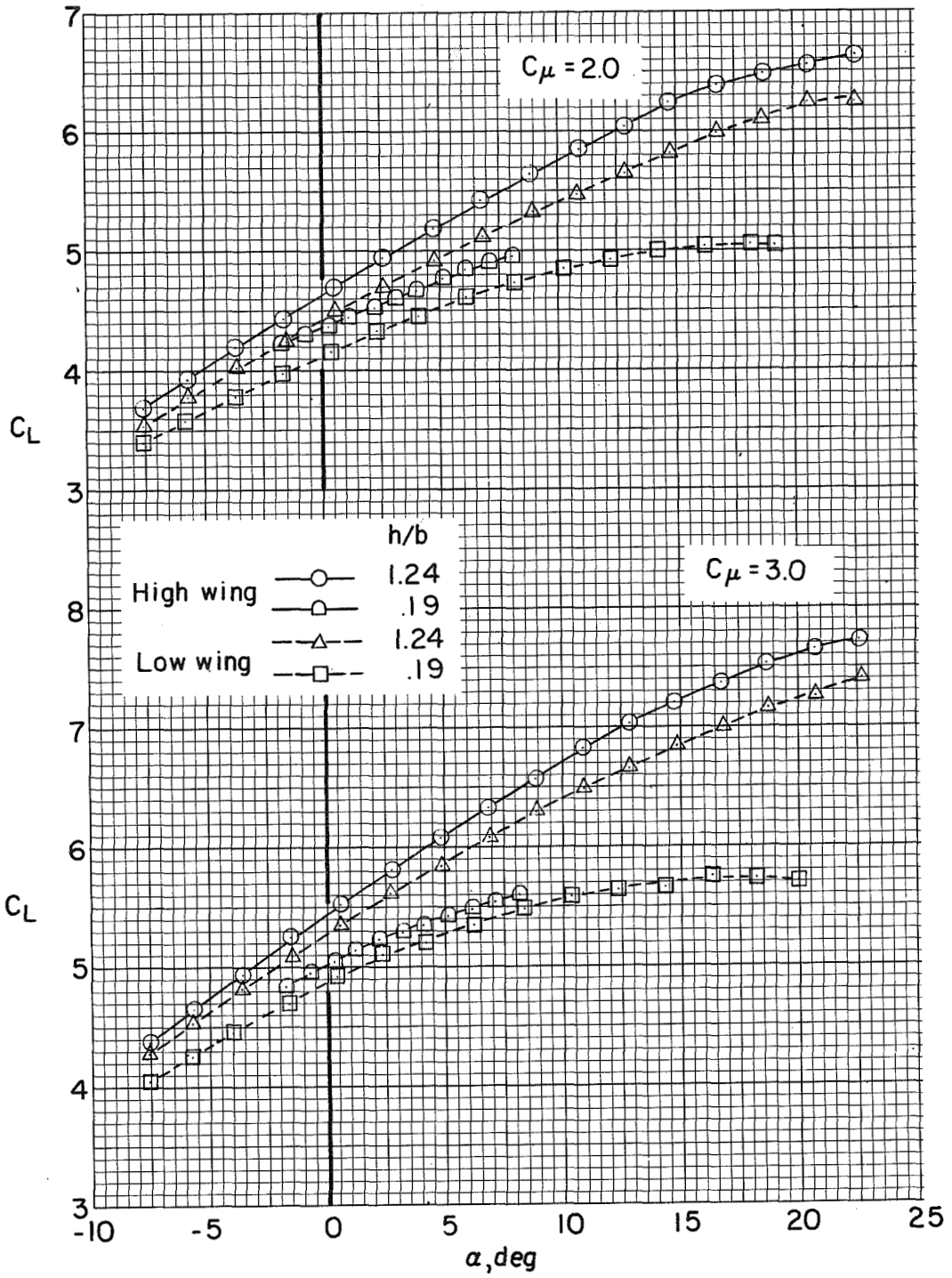

Figure 29.- Concluded.

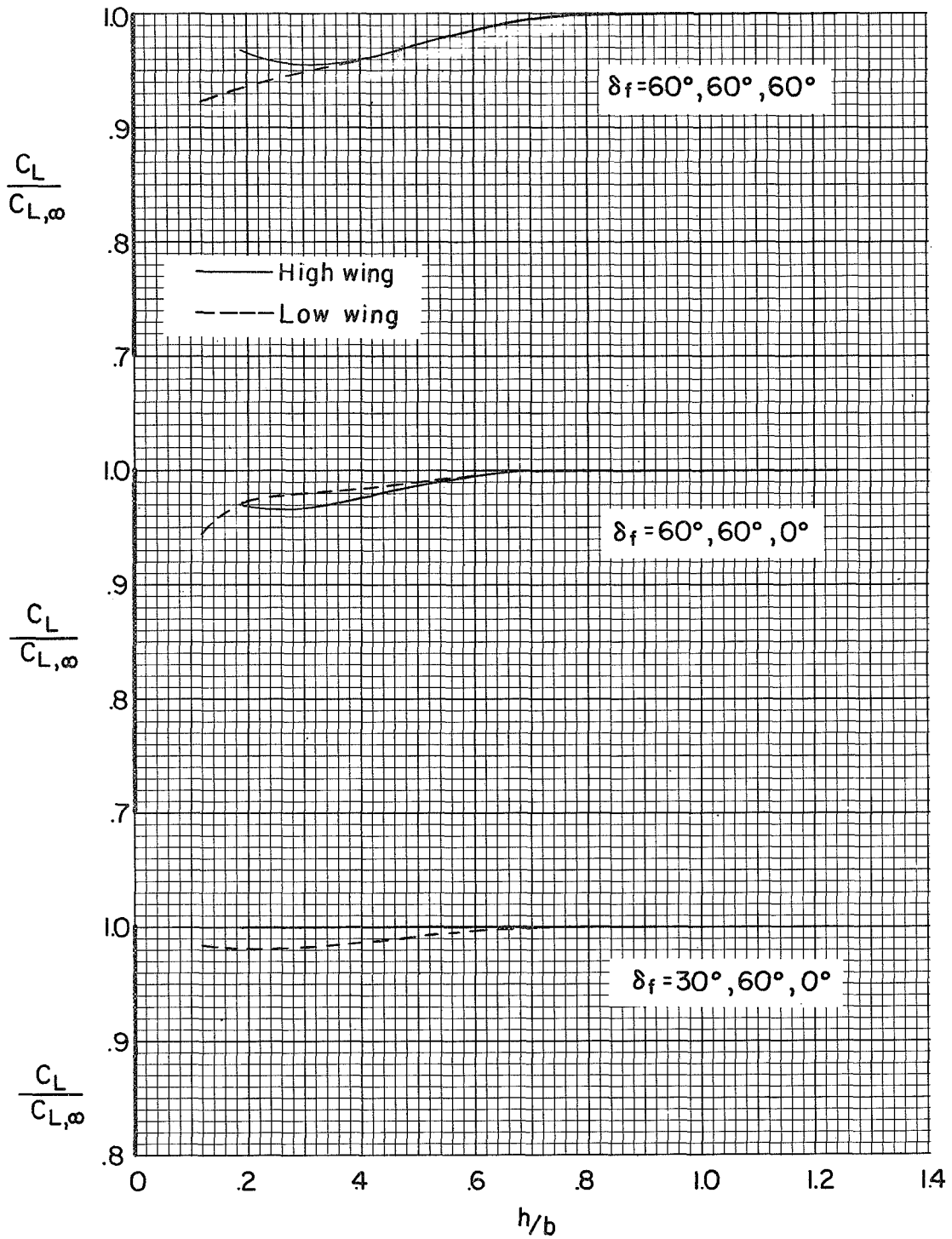

(a) $C_\mu = 0$.

Figure 30.- Effect of ground proximity on the ratio of lift coefficients in ground effect to those out of ground effect. Tail off; $\alpha = 6^o$.

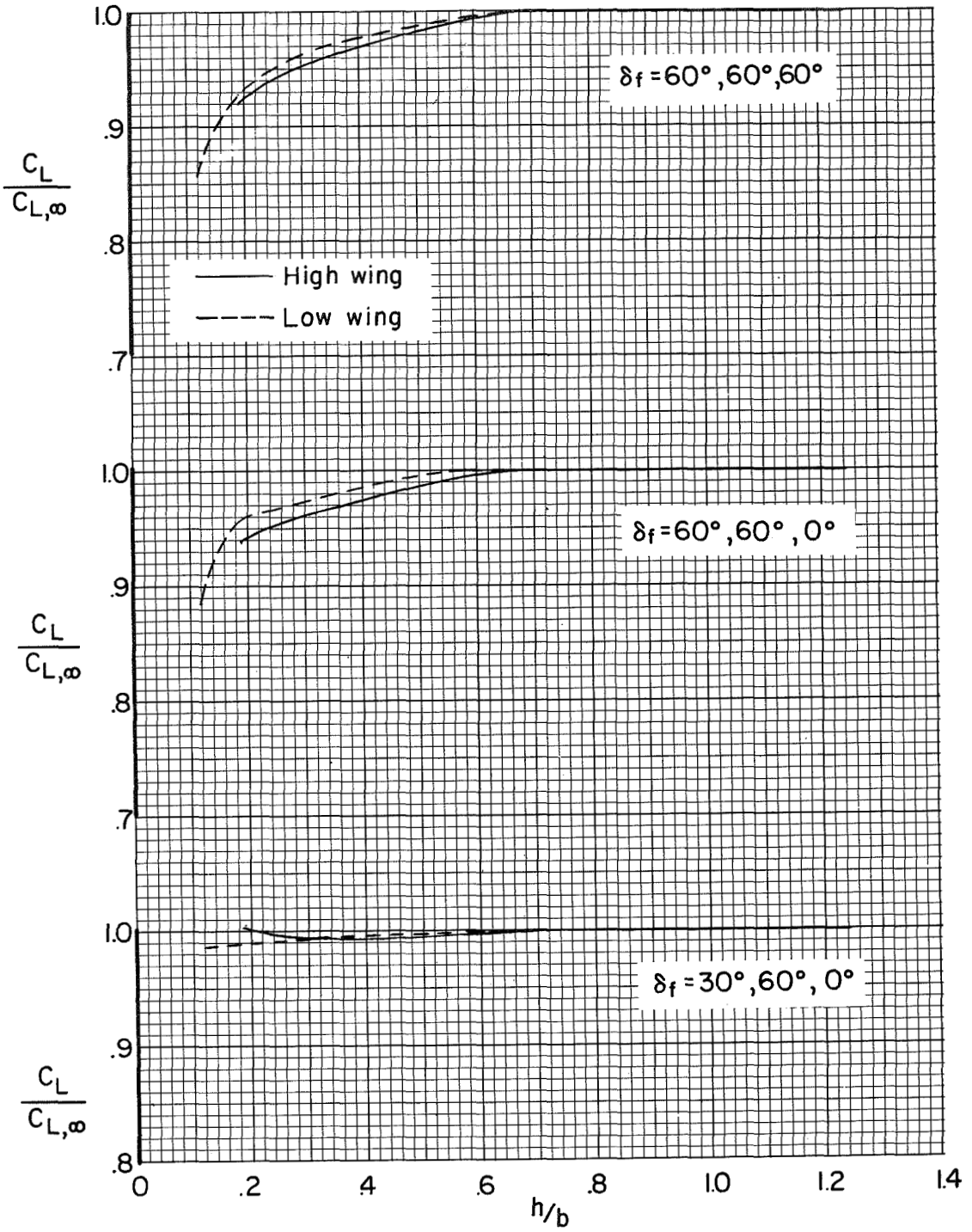

(b) $C_\mu = 1$.

Figure 30.- Continued.

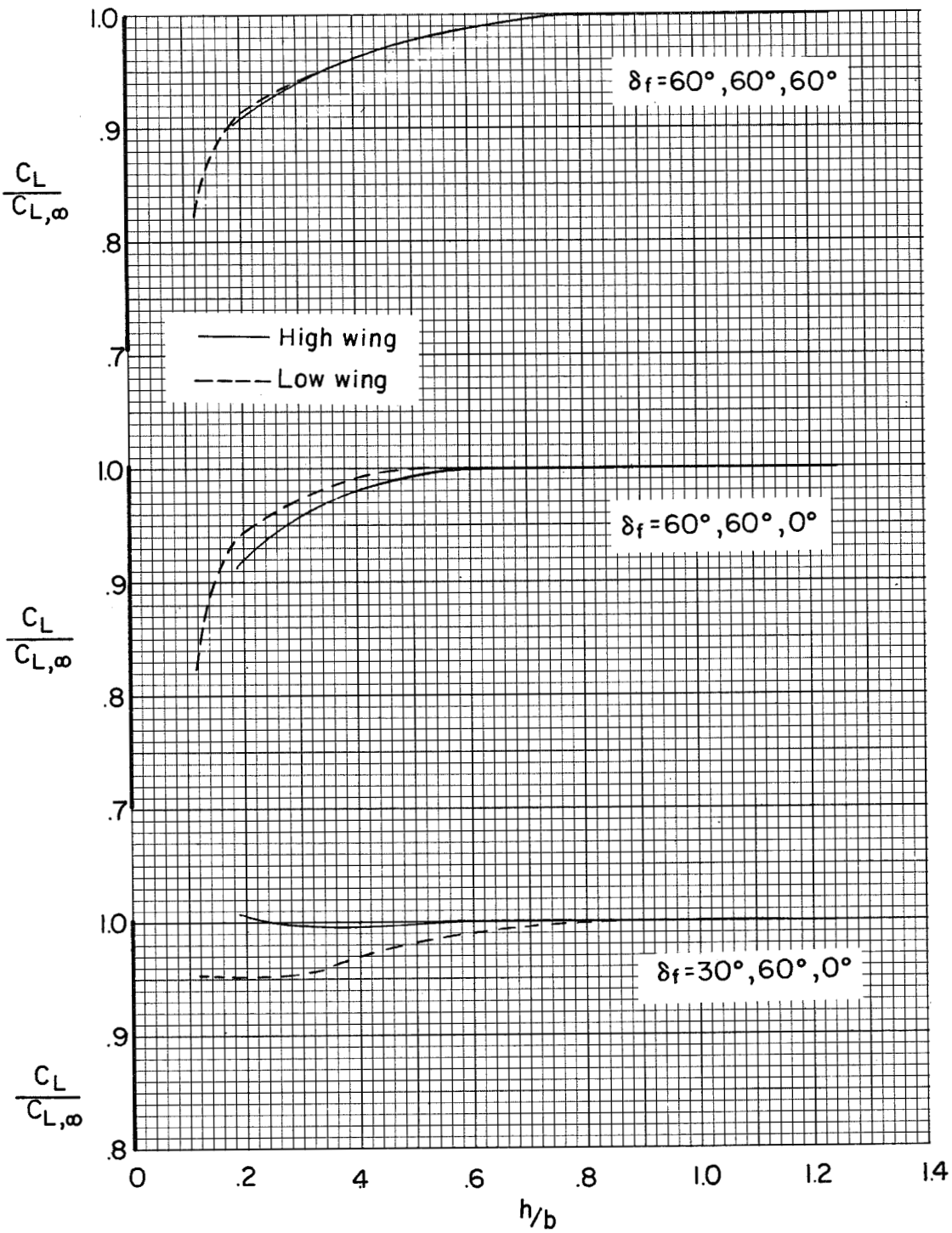

(c) $C_\mu = 2.$

Figure 30.- Continued.

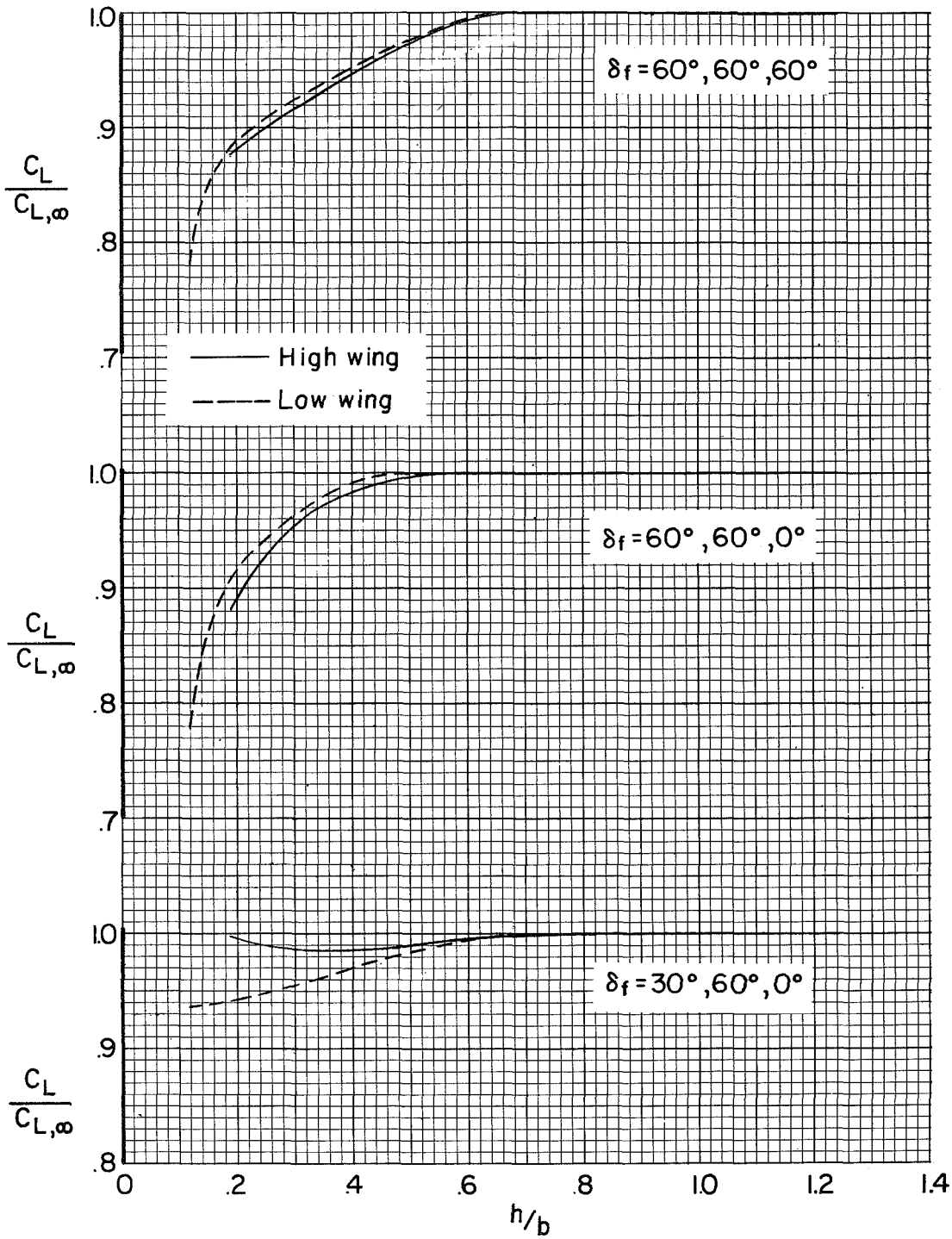

(d) $C_\mu = 3.$

Figure 30.- Concluded.

NASA-Langley, 1970 — 2 L-7546

"The aeronautical and space activities of the United States shall be conducted so as to contribute . . . to the expansion of human knowledge of phenomena in the atmosphere and space. The Administration shall provide for the widest practicable and appropriate dissemination of information concerning its activities and the results thereof."

—NATIONAL AERONAUTICS AND SPACE ACT OF 1958

NASA SCIENTIFIC AND TECHNICAL PUBLICATIONS

TECHNICAL REPORTS: Scientific and technical information considered important, complete, and a lasting contribution to existing knowledge.

TECHNICAL NOTES: Information less broad in scope but nevertheless of importance as a contribution to existing knowledge.

TECHNICAL MEMORANDUMS: Information receiving limited distribution because of preliminary data, security classification, or other reasons.

CONTRACTOR REPORTS: Scientific and technical information generated under a NASA contract or grant and considered an important contribution to existing knowledge.

TECHNICAL TRANSLATIONS: Information published in a foreign language considered to merit NASA distribution in English.

SPECIAL PUBLICATIONS: Information derived from or of value to NASA activities. Publications include conference proceedings, monographs, data compilations, handbooks, sourcebooks, and special bibliographies.

TECHNOLOGY UTILIZATION PUBLICATIONS: Information on technology used by NASA that may be of particular interest in commercial and other non-aerospace applications. Publications include Tech Briefs, Technology Utilization Reports and Notes, and Technology Surveys.

Details on the availability of these publications may be obtained from:

SCIENTIFIC AND TECHNICAL INFORMATION DIVISION

NATIONAL AERONAUTICS AND SPACE ADMINISTRATION

Washington, D.C. 20546